The Potential of Cable Pooling in the Dutch Context

Identifying and Optimizing the Potential of a Shared Grid Connection

Isabel Oosterhagen

Delft University of Technology

TU Delft

The Potential of Cable Pooling in the Dutch Context

Identifying and Optimizing the Potential of a Shared Grid Connection

by

Isabel Oosterhagen

to obtain the degree of Master of Science Sustainable Energy Technology
at the Delft University of Technology,
to be defended publicly on Tuesday November 14, 2023 at 3:00 PM.

Student number:	4567986	
Defense date:	November 14, 2023	
Thesis committee:	Dr. S. Tindemans,	TU Delft, supervisor
	C.G. Kooij,	Vattenfall, supervisor
	Prof. Dr. Ir. O. Isabella	TU Delft, chair
	Dr. Ir. K. Bruninx	TU Delft, committee member

This thesis is confidential and cannot be made public until November 14, 2025.

Cover: Renewable Energy by Public Domain Pictures, 2023

TU Delft

VATTENFALL

Preface

A word of thanks

I want to thank my supervisors Simon and Carel for their constructive feedback and involved guidance throughout this thesis. I have enjoyed working on this topic with both of you. The collaboration has been productive and each of your areas of expertise have been a contribution to this work. Both of you have been able to take the time in your busy schedule to guide me. Thanks a lot!

I want to thank Simon's team within IEPG for the warm welcome and the positive mentality. A special thanks to Kutay and Nanda for helping me with Python. I also want to thank Hesan from PVMD for understanding my train of thinking in a short period of time and giving me advice.

I also want to thank the Solar Development Team in Vattenfall for their warm welcome and the opportunity for me to work autonomously on my project, while also getting to know the organisation. Carel, thank you for finding the right persons for me to talk to outside the team. Annemarie, Oswin, Max, Eric, Levent, Michiel, Jan-Martin, Maud, Ronald, Martijn, Marjolijn, Kai, Dorine, Rik, Til, Nicola and many more, thank you!

Furthermore, Olindo, thank you for the kick-start of this project and chairing my committee. Kenneth, thank you for being my external committee member.

Last of all, I want to thank my family and friends for the continuous support and interest throughout this thesis.

Isabel Oosterhagen
Amsterdam, November 2023

Abstract

Grid congestion, which results from a larger demand for electricity transport than the available transport capacity, is a challenge in the Dutch energy transition. The growing pace of decentralized renewable energy development in less densely populated areas and the electrification of demand leads to congestion, which potentially hinders the connection of new renewable projects to the grid and slows down the energy transition.

Due to the intermittent behaviour of renewable resources, the grid connection capacity is not used to its full capacity at all times. Cable pooling is introduced as a possible solution to congestion, allowing an existing and a new renewable resource to share a grid connection and improving the utlilisation of the current grid infrastructure.

This thesis' main objective is to develop a calculation framework to assist developers to evaluate the economic potential of a cable pooling location by optimizing the Net Present Value ("NPV") of a shared grid connection, considering technical, regulatory, legal, and financial aspects. It aims to provide developers with a tool for making a preliminary decision on whether to continue development for a potential cable pooling location.

The Dutch context is used to identify different grid connecting possibilities, different combinations of wind and solar to form a hybrid farm and different revenue streams. These are used in a methodology to find the optimal installed capacity of the added resource and the impact of on-site storage to one of the hybrid farms. The approach considers the influence of market prices on the technology specific cable pooling business case at an hourly level and accounts for long-term market developments. Other factors accounted for in the tool are the hourly export capacity, defined as the residual space after the export of the existing farm, land size and costs of installation.

A case study of a solar farm oriented to the east-west is used to test the tool and draw conclusions on the potential of cable pooling for this case study. The additions of a wind and solar resource with either south or east-west generation all yield positive NPV values with the highest values seen for the wind addition. Sensitivity tests for technical and economic inputs show that the results are sensitive to weather data and various economic inputs, but the results of this case study are robust. The case study however considers a relatively large grid connection. Generalizing the results by considering a smaller grid connection shows the value of complementary production patterns.

The impact on the cost-benefit framework by adding a battery is considered. The addition of a battery adds value by peak-shifting the produced energy, but not enough to cover the costs of the battery without any subsidy or alternative revenue streams.

In conclusion, cable pooling shows potential for this case study, for different revenue streams and additions. The tool used to obtain the results can be tailored to different case studies and input scenarios and shows the economical attractiveness of a cable pooling location, based on the Dutch context. The Dutch context shows a promising potential for cable pooling as a method to deal with congestion, but not many projects are present yet. Considering different parties sharing one grid connection, coming to an agreement on the terms can form a hurdle. Therefore, the introduction of more transparent cable capacity calculations by DSOs and a separate subsidy for cable pooling projects could help incentivize the development of more cable pooling projects. The impact of developments such as the "Use-it-or-lose-it" on the cable pooling potential should be monitored closely. Other solutions to dealing with congestion, such as using the fault reserves, should not be disregarded.

Contents

Preface i

Abstract ii

1 Introduction 1

2 Cable Pooling and the Dutch Grid 4
- 2.1 Regulatory Context . . . 4
- 2.2 Legal Context . . . 5
- 2.3 Technical Requirements . . . 7
- 2.4 Electricity Markets and Policies . . . 7
  - 2.4.1 Stimulering Duurzame Energie ++ (”SDE++”) . . . 8
  - 2.4.2 Power Purchase Agreements (”PPA”) . . . 10
- 2.5 Future Developments . . . 11
  - 2.5.1 Congestion Management (”CM”) . . . 11
  - 2.5.2 Alternative Transport Rights (”ATR”) . . . 12
  - 2.5.3 Use it or lose it (”UIOLI”) . . . 13
  - 2.5.4 Other . . . 13
- 2.6 Batteries . . . 14
  - 2.6.1 Current Revenue Streams . . . 14
  - 2.6.2 Impact Future Developments . . . 15
- 2.7 Cable Pooling Project Examples . . . 16
- 2.8 Overview . . . 17

3 Problem Definition and Scope 18
- 3.1 Literature Overview . . . 18
  - 3.1.1 Combinations of Renewable Resources in Hybrid Farms . . . 18
  - 3.1.2 Identifying the Potential of Hybrid Farms . . . 19
  - 3.1.3 Optimization of Hybrid Farm Components . . . 19
  - 3.1.4 Optimization of Grid-Connected Hybrid Farms - In Depth Analysis . . . 25
- 3.2 Possible Contributions to Research . . . 28
- 3.3 Decision problem . . . 28

4 Methodology 30
- 4.1 Hybrid Farm Optimization Problem Formulation . . . 30
- 4.2 Hybrid Farm with Battery Optimization Problem Formulation . . . 36
- 4.3 Installed Power Density . . . 40
- 4.4 Weather and Losses Factor (”WLF”) . . . 45
- 4.5 Cable Capacity and Electrical Components . . . 48
  - 4.5.1 Cable Capacity . . . 48
  - 4.5.2 Electrical Components . . . 48
- 4.6 Performance Indicators . . . 49
- 4.7 Assumptions and Simplifications . . . 49

5 Case study 52
- 5.1 Case Study Description . . . 52
- 5.2 Case Study Inputs . . . 52
  - 5.2.1 Weather and EPEX Data Input . . . 52
  - 5.2.2 Economic Input . . . 57
  - 5.2.3 Yield and Losses Inputs . . . 61
- 5.3 Battery . . . 66

6 Results and discussion **68**
6.1 Base Case Inputs . . . 68
6.1.1 Weather data . . . 68
6.1.2 Output of Existing Farm and Cable Capacity . . . 69
6.1.3 Weather and Losses Factors . . . 71
6.2 Base Case Hybrid Farm Optimization Results . . . 75
6.3 Sensitivities . . . 90
6.3.1 Technical inputs . . . 90
6.3.2 Economic Sensitivity . . . 96
6.3.3 Generalization . . . 100
6.4 Hybrid farm including Battery Optimization Results . . . 104

7 Conclusions and Recommendations **110**

A Output of added farms **121**

B Battery Behaviour **125**

1 Introduction

The Netherlands has committed to transforming its energy system from conventional fossil-based sources to renewable alternatives in their ambitions to mitigate climate change, reduce greenhouse emissions and secure a sustainable future. The first milestone on the path towards a sustainable future is the aim of reducing the carbon emissions by at least 55% and preferably 60% before 2030 as formulated in the latest coalition agreement (Rijksoverheid, 2023). Therefore, carbon emitting, centralized, fossil fueled power plants are being replaced by renewable, decentralized power production by mostly wind and solar farms.

This transition to a renewable energy system bears its challenges. One example is matching the weather dependent, intermittent renewable supply to demand. Furthermore, the adaption of the existing energy infrastructure is critical. Grid congestion is a prominent issue in the Netherlands (RVO, 2023b). Congestion means that there is no free capacity on either electricity distribution substations or cables, in the medium or high voltage network (Royal HaskoningDNV, 2021) and the demand for transport of electricity is larger than the transport capacity of the grid (RVO, 2023b). Congestion can occur for both feeding to the grid and extracting from the grid.

The capacity of the distribution grid traditionally depends on population density. The renewable energy generation is often located in less densely populated areas with low priced land, where the grid is thus less robust. The growing decentralized renewable generation connecting to the grid at rural locations puts strain on the grid infrastructure and requires reinforcements of the grid infrastructure by system operators (Andergie, 2023; Netbeheer Nederland, 2019; TenneT, 2022). Next to reinforcements, the Dutch grid infrastructure also needs replacements of existing grid infrastructure and expansions of the 220-380 kV grid (TenneT, 2022). The required replacements and expansions combined with reinforcements of the congested parts of the grid, is a large challenge for system operators. The pace of the reinforcements does not keep up with the pace of the growth of renewable generation. The expectation is therefore that the grid overload will increase in the coming years, even though TenneT plans to invest over 10 billion euros in the coming ten years (Andergie, 2023; TenneT, 2022).

System operators award grid connection capacity in the Netherlands to parties that request it whenever the project meets the basic requirements and there is room for the size of the requested grid connection. With the current congestion status, it is becoming increasingly challenging to obtain the right to connect to and use the grid. Developers of renewable energy are forced to deviate to grid connection points positioned further away, inducing high costs and putting strain on the business case of the renewable project, or cannot connect a new project to the grid at all. This could be considered a challenge in the energy transition in the Netherlands, since the development of new renewable energy farms and reaching the set targets is slowed down (Andergie, 2023; Rabobank, 2023), since the reinforcements might take five up to ten years (Jongsma, Van Cappellen, et al., 2021).

Grid-connected renewable generation sites often have grid connections sized to the peak capacity of the farm. This peak capacity is however only produced a limited amount of time. This can be ex-

plained using the capacity factors of solar and onshore wind in the Netherlands. The capacity factor shows the actual yearly output of a farm compared to its theoretical maximum. For onshore wind in the Netherlands this was 23% (IEA-Wind, 2021; Klimaatfeiten, 2020) and for solar energy it is roughly 10% (Klimaatfeiten, 2020), indicating that the grid connections are not used to the full capacity at all times. One could therefore state that the grid is contractually or statistically congested, implying that all contracted grid connections added up, lead to a congested grid, since the system operators are legally bound to have this space available at all times. The *risk* of congestion determines the problem and the consequent connecting constraints. This means that there might be more space on the grid than currently assumed, but grid operators currently are not allowed to take this into account when awarding grid connecting capacity.

Cable pooling is mentioned as a solution to this contracted congestion, by using the free space on a grid connection. Cable pooling indicates that a (existing) renewable resource shares its grid connection with a (new) renewable resource and the combined output is delivered to the grid. Cable pooling shows great potential in the Netherlands. According to Netbeheer Nederland (2020) and Hier Opgewekt (2021), two up to four GW extra solar energy could be realised by combining complementary resources solar and wind at grid connections. It is considered a way of more efficiently using the current grid infrastructure. According to these studies, the joint output of a cable pooling solar and wind farm could increase the capacity factor to almost 40%. In congested areas this could lead to more grid connected capacity, even with no grid reinforcements. Therefore, developers are not forced to wait for the grid reinforcements and the pace of development does not need to be slowed down (Netbeheer Nederland, 2020). The average lead time of development can be decreased to one and a half years (Hier Opgewekt, 2021).

In short, cable pooling could provide new development locations in congested areas and use the existing and future grid infrastructure more efficiently. Cable pooling is however a versatile challenge, dealing with regulatory, legal, technical and financial parameters. The potential of cable pooling in the Netherlands is large, but the operation can be complicated. This research therefore aims to create a calculation framework for developers with a potential cable pooling location to make a preliminary analysis of the economical potential of the location, which can be used as a decision tool on whether or not to continue the cable pooling development there.

This has led to the following main research question: ***How to identify and optimize the potential of a renewable resource sharing a grid connection with an existing renewable resource in the Netherlands?*** which will be answered by the use of the following sub-questions:

- *SQ: How does the Dutch context shape the grid connecting possibilities and limitations currently and in the near future?*
- *SQ : What are the possible cable pooling scenarios and corresponding cost aspects and revenue streams?*
- *SQ : How to determine the optimal size and corresponding revenues of the added farm of a case study considering costs, size of land and cable capacity?*
- *SQ : How does the presence of on-site storage affect the cost-benefit framework?*
- *SQ : What are the most important sensitivities?*

The aim is to create a methodology that quickly shows the economical attractiveness of a potential cable pooling location to a developer, taking into account technical and regulatory limitations and possibilities. This requires a techno-economical analysis of the potential cable pooling location, taking into account the Dutch context. The research is conducted in collaboration between the TU Delft and Vattenfall, one of the largest energy suppliers in the Netherlands.

To explore the technical and regulatory grid connecting limitations and possibilities currently and in the near future, the Dutch context will be used in chapter 2. The Dutch context will also be used to draft the possible hybrid farm combinations and corresponding the conceptual revenue streams and cost images. The Dutch grid context and an analysis of the literature field lay the foundation of the problem definition used to find the optimal size of the added renewable resource in chapter 3. The methodology

to solve the problem will be introduced in chapter 4, with the approaches used to model the resources, revenues and costs. The model will be tested using data from a case study provided by Vattenfall, which is introduced in chapter 5. The results of the case study are discussed and a sensitivity analysis is performed in chapter 6.

2

Cable Pooling and the Dutch Grid

The topic of this research is focused on cable pooling in the Dutch grid context. This chapter discusses the regulatory and legal context for cable pooling projects in the Netherlands, as well as technical requirements, with the focus on the grid connecting possibilities. The Dutch context for cable pooling is also shaped by the different revenue streams based on the Dutch electricity market. Furthermore, possible future developments on other grid connecting possibilities for renewable resources in congested areas and cable pooling projects are discussed.

2.1. Regulatory Context

This section deals with the Dutch regulatory context by generally explaining the Dutch grid structure and different actors and their responsibilities in the regulatory framework. The procedure of obtaining a grid connection in the Netherlands are generally discussed and the influences of congestion on this procedure are further introduced.

The Dutch grid is divided into a transmission grid for transportation of the power at high voltage (110-380 kV), and a distribution grid for distribution of the power at low voltage (0,4 kV) to supply households' demand. These voltage levels are connected by intermediate (25-50 kV) and medium voltage levels (10-20 kV), both part of the distribution grid. Transformers are used to change voltage levels. Traditionally, large generators respond to demand from large- of small-scale consumers, ramping up or down when demand is high or low.

In the Netherlands, the energy system has been restructured in 1998 by effect of the *Elektriciteitswet 1998* (Electricity Law of 1998) which mandated the separation of the production, trade and delivery of energy from the management of the grid. A national grid operator was created, the transmission system operator (”TSO”), executed by the state-owned company TenneT. The TSO is responsible for transmission over the high voltage grid (110-380 kV) and balancing the grid using a variety of resources. Different distribution system operators (”DSO's”) are since then responsible for the distribution over the medium and low voltage grid (0.4 kV - 50 kV). The responsibility of the DSO's is divided into different regions for different operators. This division and the tasks of the system operators are defined by the Electricity Law. The Electricity Law of 1998 also describes the requirements to connect to the grid in multiple *netcodes* (grid codes).

The adherence to the law and grid codes is overseen by the *Autoriteit Consumenten & Markt* (”ACM”), or Authority for Consumers and Markets, who monitors the functioning of market and of the TSO and DSOs, to ensure efficient and honest practice. The ACM is authorized to change these grid codes, for example when industry associations or other parties request an amendment. ACM assesses these requests and decides on the execution of the requested amendments. In 2019 the grid code, tariff code and metering code have been updated based on new European Regulations for Generation (”RfG”), imposing new technical requirements for generating units. The aim was to create uniformity in the European Union in terms of security of supply, the energy transition and grid safety (Entso-E, 2023;

van Gastel and de Jonge Baas, 2019). All farms built after the RfG came into force are to comply with the new code.

If a renewable resource wishes to connect to the grid, a request is made at the DSO or TSO, depending on the capacity and voltage of the connection. Awarding the grid connecting capacity works on a first-come-first-served basis in the Netherlands. If there is enough space on the grid and the resource complies with the Electricity Law, the grid operators award grid connection capacity using an *aansluit- en transportovereenkomst* (”ATO”), translating to connecting and transporting terms, to the first party applying for it. The terms of the ATO are based on the grid codes and dictate, amongst others, the voltage, current, frequency and power quality boundaries for the asset to be connected.

Once an ATO is awarded by the DSO or TSO, the party connecting to the grid is always allowed to use their grid connection at the full capacity, as specified in the ATO. The connection point, or primary allocation point (”PAP”) receives a unique Europese Artikel Nummering (”EAN”) code as is required for every connection point to the grid. The different quality and quantity indicators are measured at the PAP by a metering responsible party (”MRP”), of which there are eleven active in the Netherlands.

Applying for a new grid connection is becoming increasingly difficult in congested areas (RVO, 2023b). Therefore, there is a growing need for alternative connecting possibilities. One alternative is a renewable resource cable pooling with an existing renewable farm by connecting to an existing grid connection (Firan, 2023; Hezelaer Energy, 2019). Sharing a grid connection for solar orientated to the south and wind energy could increase the capacity factor at the PAP from 23% for wind and 10% for solar to 35-42% combined (Netbeheer Nederland, 2020). Grid operators expect 2 GWp up to 4 GWp extra solar energy to be able to connect to the grid using cable pooling with the current infrastructure (Hier Opgewekt, 2021; Netbeheer Nederland, 2020).

Another promising alternative is the usage of the fault reserves, the so-called emergency lanes of the grid (ACM, 2022d; Hezelaer Energy, 2019; Jongsma, Van Cappellen, et al., 2021). All medium- en and high-voltage networks in the Netherlands are built redundantly to prevent system outages in case of malfunction or maintenance. This principle is called N-1 (Hezelaer Energy, 2019). To use the current grid infrastructure more efficiently, these fault reserves could be used to connect renewable generation to the grid (ACM, 2022d; Hezelaer Energy, 2019; Jongsma, Van Cappellen, et al., 2021). In case the reserve is needed due to maintenance or faults, the production will need to be curtailed. Since 2021, system operators are allowed to use the reserves as transport capacity for renewable generation (ACM, 2022d). In 2023, ACM formalised a method to reimburse the parties using this redundant line in case of a fault (ACM, 2022b), allowing the roll-out of this measure. Using this measure, Enexis and Liander expect extra solar capacity of 1 GWp up to 3 GWp to be able to be connected to their distribution network respectively (Energiesamen, 2022). The use of the fault reserves is however not used in this research, since the ability to allow this lies with the ACM and the system operators, not with the parties developing the renewable energy.

2.2. Legal Context

This section discusses the legal characteristics and requirements of cable pooling within the current context, divided into three different options. It also mentions available tools to guide the cable pooling development process.

In 2018, an amendment of the Electricity Law allowed *Meerdere Leveranciers Onder Een Aansluiting* (”MLOEA”), translating to multiple suppliers at one connection. At the PAP, one or more Secondary Allocation Points (”SAP”) can be requested at the DSO or TSO to which a second resource can be connected (Zwager, 2020). Similar to the PAP, the SAP will have a unique EAN-code. MLOEA enables the connected allocation points to have different suppliers of energy as part of one ATO. One requirement for a MLOEA, is that the generating assets must be in one real estate object and be part of one legal entity, with the exception of large wind farms covering multiple real estate objects (Zwager, 2020). In 2020, a bill passed the ”Eerste Kamer” in the Netherlands changing The Electricity Law. It allowed solar and wind generation resources in close proximity to be considered as one real estate object and

one generating unit, in case that a request for sharing the grid connection was applied jointly (Tweede Kamer, 2020; Zwager, 2020). Therefore, two generating units belonging to two different owners and built on two different pieces of land sharing one grid connection, are still eligible for a MLOEA (Netbeheer Nederland, 2020).

Currently, cable pooling is defined as a maximum of two generating renewable resources such as solar and wind sharing one grid connection (Tweede Kamer, 2020). Different cable pooling combinations within the current legal structure are therefore: solar and wind, wind and wind and solar and solar combined (Netbeheer Nederland, 2020). The solar generation could have every orientation, yielding different generation patterns, which is a degree of freedom. Energy conversion or storage installations are not part of the current cable pooling definition.

Cable pooling can be achieved in three ways in the current framework.

- **Behind-the-meter (”BTM”)** The simplest way is one legal entity combining different generating sources behind the PAP on one real estate object. This concept is BTM, all energy enters the grid at the PAP and is measured by the MRP as a combined power output (Netbeheer Nederland, 2020). If the different generating resources are complementary, the output of one EAN-object is more stable and can become less intermittent. Internal energy measurements can be performed to divide the energy outputs and profits.
- **SAP** With the other two options, the power output of the farms is measured separately by effect of a SAP. The ATO remains valid at the PAP, so those agreements still hold when adding a SAP (Netbeheer Nederland, 2020; Zwager, 2020).
  - One method of applying for a SAP is to have two different legal entities on two real estate objects in proximity to each other sharing one PAP and ATO. Legally, the PAP still belongs to the existing renewable resource. The added resource therefore has no rights to the PAP and access to the grid in case of bankruptcy of that party.
  - In the other construction one legal entity consisting of the two connected parties can be created (Zwager, 2020). To achieve this, negotiations to divide the capacity and costs of construction and maintenance are necessary, which may be time consuming. This does however ensure the right to use the PAP when one of the parties goes bankrupt.

  The difference between the first and second SAP construction is purely legal, technically it can be considered similar as in both cases the power can be exported over the PAP and is measured and sold separately by effect of the SAP. The output of both generating units must be measured by the same MRP.

When cable pooling, the grid connection capacity needs to be divided amongst the two renewable resources. An approach to divide the capacity could be to prioritize the output of one generating resource over the other. This could be used for example if one party has secured the grid connection and has sized the generating resource accordingly, and another party wishes to add a generating resource to that grid connection. The generating resource belonging to the party that has secured the grid connection, can export the produced electricity at all times, given the export capacity. The added generating resource could use the free space on the cable. Another approach could be to negotiate on the share of the grid connection capacity to be used by each party. Both approaches can be used for parties co-developing a grid connection or a party joining a secured grid connection, either with an active farm or a farm in development.

A guide for the negotiations and arrangements has been developed, the *cable-pooling concept agreement* (EnergyStorageNL, 2021). The aim of the concept agreement is to optimally use the capacity available at the grid connection point for electricity exchange and saving expenses by allowing the new renewable resource to use the existing grid connection (EnergyStorageNL, 2021). The concept agreement is used after having secured a SAP and separate EAN code. The concept agreement deals with the following topics: planning, permissions, definition of the mutual installation, cost divisions of construction and grid usage, meters and metering responsibility, program responsibility, operations and maintenance (”O&M”), curtailment, decommissioning and other financial and legal agreements (EnergyStorageNL, 2021). The concept agreement is drafted for two generating resources, as imposed by

the legal context. A more general step-by-step approach to cable pooling is created by Firan (Firan, 2023) and can be used as a guideline to cable pooling in the Netherlands.

2.3. Technical Requirements

The sections above describe the regulatory and legal framework and available tools for cable pooling, which show a solid basis for cable pooling in the Netherlands. To realize a cable pooling project, technical requirements for cable pooling need to be considered as well. This section discusses these requirements.

The request for sharing the grid connection and for the application of the SAP has to be submitted to the system operator in question. Two cases can be considered: a case with an ATO sized to a generating resource to which an extra generating resource wishes to be added, or a case where a joined ATO is requested for two generating resources. The generation profiles influence the degradation of grid infrastructure. Since DSO's and TSO are responsible for the security of supply and the infrastructure of the grid, it is important to discuss the addition of a renewable resource in an early stage of the negotiations.

In the first case, where the grid connection has already been formalized in an ATO based on the generation profile of the original generating resource, the generation profile at the PAP changes by adding another renewable resource by means of a SAP. The grid connection is sized for the existing farm. The system operator determines to what extent the grid infrastructure can be used when a new resource is added to it. The system operators can deny the request for a SAP or limit the existing grid connection capacity as a result of degradation calculations, based on the expected combined output of the two resources. If the SAP is denied, the only option left is to share the grid by use of BTM construction in which case the new and existing generating resource share the PAP and EAN-code and the output is measured by the MRP jointly. In the second case, where a joined ATO with two generating resources with a separate EAN-code each is requested, the joined output of the two farms are used to determine the grid connection capacity.

Apart from considering to what extent the the grid can be used, there needs to be room physically to host the new farm. The physical addition of a renewable resource on an existing grid connection can be done in two ways. One way is adding a new client field in the transformer substation. This is only possible if there is ample space in the substation to build this new client field. The other option is to connect the new farm to the existing cable entering the client field at the substation. The connection could be made by use of electronic circuit connectors or by physically splitting the cable in an agreed ratio. Technically, all options result in an energy export constraint for the generation. The options only have financial implications, since one option might be more costly than the other.

Since the power is still required to stay within the bounds defined in the ATO valid at the PAP, the combined output needs to be measured and controlled by steering the generating sources, requiring extra metering and control components in a cable pooling project.

2.4. Electricity Markets and Policies

So far, the regulatory, legal and technical background in the Netherlands are used to identify the different grid connecting possibilities in congested areas and the possible cable pooling combinations. This section discusses the different electricity markets active in the Netherlands, focusing on the markets where generated electricity is sold and other income sources, such as subsidies or long-term power purchase agreements ("PPA") to identify the relevant revenue steams.

In the Netherlands, there are three different markets to trade generated or consumed electricity on: The Day Ahead Market, the Imbalance Market and the Intraday Market:

1. **Day Ahead Market**
   The Day Ahead Market ("DAM"), or Spot market, is the market used for bids from suppliers and off-takers one day before delivery at 12:00. The bids are submitted via the APX/EPEX stock-exchange (Spotmarkt, 2023). The bids are made based on estimations of hourly consumption or

production for the day after (Jongsma, Van Cappellen, et al., 2021). The bids are ordered using a bid ladder where capacity in MWh and price in euro's offered and demanded are matched. The consumption price point where the offered capacity matches the demanded capacity, determines the price of electricity for all users (Jongsma, Van Cappellen, et al., 2021). The price depends on supply and demand: high supply and low demand result in low prices, while low supply and high demand result in high prices.

Due to the intermittency of renewable production, where the generation does not necessarily match the demand, the price pattern becomes more volatile. This volatility leads to less value for renewable generation on the DAM, given that with high renewable penetration, the prices can become low at times of high wind or solar production. Therefore, at times of high production of these renewable resources, the value of the produced energy is low. During a weekend in April 2022, the prices dropped below zero for thirteen hours due to high renewable generation and low demand, even reaching the lowest point so far: -222 EUR/MWh (Bloomberg, 2022).

The price volatility has increased with 180% between 2011 and 2019 with an increase of solar and wind generation in the energy mix from 24 to 50% in the same time frame (BCG, 2023). With the planned increase in renewable generation, one can expect a further increase in the volatility and extreme price peaks and valleys too (BCG, 2023).

2. **Imbalance Market**
   Balance Responsible Parties ("BRP") are responsible for matching supply and demand. The BRPs are energy suppliers or large consumer or producers (Jongsma, Van Cappellen, et al., 2021). If the expected consumption and production deviates from the actual value, TenneT solves this imbalance by scaling production or consumption up or down, by allowing parties to submit bids for the imbalance capacity for a certain price (Jongsma, Van Cappellen, et al., 2021).

   BRPs pay for the imbalance in their portfolio against this imbalance price. Since the less predictable renewable generation can create an imbalance, BRPs with an increasing number of renewable farms are faced with increasing imbalance costs.

3. **Intraday Market**
   The Intraday Market runs from the closure of the DAM to 15 minutes before delivery and it is based on individual trades. To reduce the imbalance costs, BRPs bid on the intraday market to try and solve the imbalance 15 minutes before it occurs and therefore limiting the imbalance costs (Jongsma, Van Cappellen, et al., 2021).

Renewable generation trades electricity on the EPEX spot market, or the DAM, to generate revenue. To stimulate the development of renewable energy and improving the business cases a subsidy scheme, SDE++ (RVO, 2023c), has been introduced. Another emerging method to improve the business case of renewable energy is by use of long-term power contracts. Both are discussed in the next sections.

2.4.1. Stimulering Duurzame Energie ++ ("SDE++")

To stimulate the development of renewable generation in the Netherlands, the subsidy SDE++ was introduced in 2020, as successor to SDE and SDE+. This subsidy makes up for the unprofitable part of the business case of renewable energy which often have high capital expenditure ("CAPEX") (RVO, 2023a). The subsidy ensures to cover the cost price of the technology by yearly payments during 15 years of the total lifetime of the farm. This creates a more secure business case for renewable energy and stimulates the development thereof.

The principle of the SDE++ subsidy is shown in Figure 2.1. On the y-axis it shows the different values in EUR/kWh and on the x-axis the number of years the subsidy is active. For each technology, a number of full-load-hours ("FLH") is determined, indicating the number of hours that the technology produces at its maximum capacity in one year. The FLH, combined with the installed capacity, give an indication of the production of a certain resource each year.

A party requesting for subsidy makes a calculation based on cost analysis, the predetermined FLH and the subsidy duration, to find the height of the subsidy in EUR/kWh or EUR/MWh required to cover the costs of the installed capacity of the technology. This value is the *Basis bedrag* (”BB”) in EUR/kWh or EUR/MWh, shown in dark blue. The lower this BB bid, the higher the chance the party receives subsidy. The cheapest solutions receive the subsidy, encouraging cost-effective solutions. Using a bid ladder, the BB is based on the highest bid still eligible for the subsidy, determining a clearing price which holds for all bidders that bid lower.

Each year, a projection of the average market price of the upcoming year is made by *Planbureau voor de Leefomgeving* (”PBL”). Apart from the expected average market price, PBL also considers shaping- and imbalance costs of a certain technology. The shaping costs are based on the generation pattern of that technology and how it matches the demand. Solar energy for example does not match demand well. The imbalance costs are based on the imbalance caused by the generation type. Higher shaping and impact costs, cause the market value to decrease.

The expected average price, corrected by the shape- and imbalance costs, indicates the expected average price in EUR/kWh or EUR/MWh of that specific technology and is called the *Marktvergoeding* (”MV”), shown in green. Three scenarios can be distinguished.

1. If the expected MV is lower than the required BB to cover the costs, the difference is paid using the subsidy in EUR/kWh or EUR/MWh, as seen in year six until 14.
2. If the expected MV is higher than the BB, no subsidy is awarded, as seen in year one to five and 14 and 15.
3. If the expected MV drops below a certain value, the *Basisenergieprijs* (”BEB”), shown in light blue, the awarded subsidy is capped. This occurs in year nine and ten. Only the difference between the BB and BEB is awarded as subsidy.

The *Correctiebedrag* (”CB”) shown in red in the figure, follows the trajectory of the MV, except for years when the MV drops below the BEB (year nine and ten).

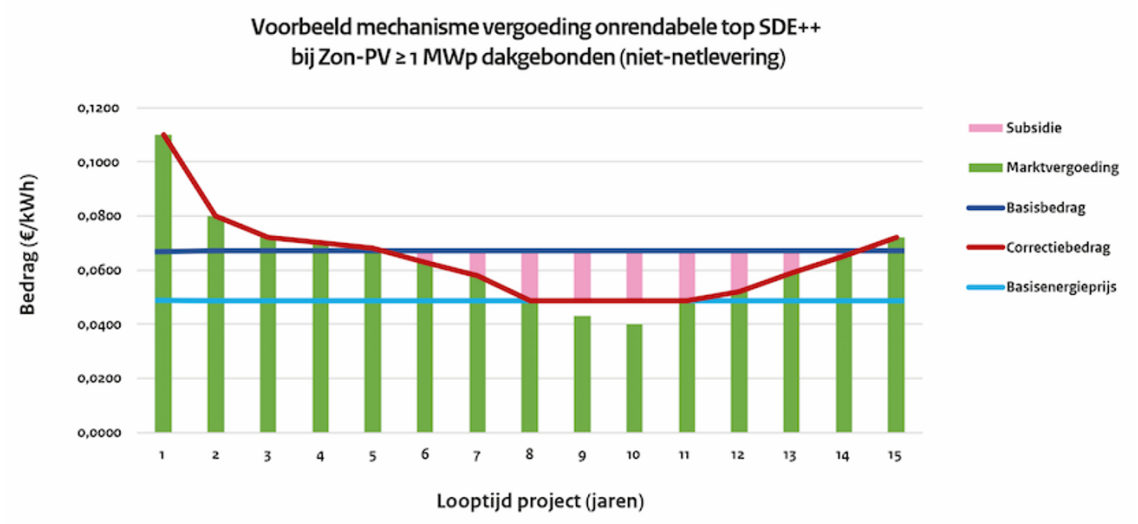

Figure 2.1: Example mechanism subsidy unprofitable top SDE++ for solar PV $\geq$ 1 MW_p (RVO, 2023a)

The mechanism can be summarized using Equation 2.1 and Equation 2.2. In Equation 2.1 and Equation 2.2, $SDE(t)$ represents the height of price the subsidy awarded in year t.

$$SDE(t) = \begin{cases} 0 & \text{if } MV(t) > BB \\ BB - CB(t) = BB - MV(t) & \text{if } MV(t) < BB \\ BB - CB(t) = BB - BEB & \text{if } MV(t) < BEB \end{cases} \tag{2.1}$$

In Equation 2.2, subsidy(t) represents the height of the total subsidy awarded in year t, using the technology specific FLH and the installed capacity.

$$\text{subsidy}(t) = SDE(t) \cdot FLH \cdot P_{\text{installed}} \tag{2.2}$$

Based on the technology dependent BB and BEB, the size of the farm in MW, the technology dependent FLH and the expected MV by PBL, the expected subsidy sum of that year is paid upfront. After the year ends, the PBL makes a new calculations and corrects the subsidy awarded. If the subsidy received was too high, the party needs to pay back the difference. However, if the subsidy was too low, extra subsidy is awarded.

The SDE++ prescribes some requirements for parties wishing to receive this subsidy. In the SDE++ of 2022 (RVO, 2022), solar farms for example may only size their inverters such that the maximum output of the farm is at 50% of the peak capacity, to improve the capacity factor of the farm. For wind energy, a distinction in the height of the subsidy is made between the locations of the turbine. The location of the turbine and the corresponding wind speeds determine the generation yield and influence the BB.

Since the costs of the renewable generation are expected to go down in the coming years, the SDE++ is expected to only be required until 2025, after which the subsidy will cease to exist (Jongsma, van Cappellen, et al., 2021).

2.4.2. Power Purchase Agreements ("PPA")

To secure a long-term income and with the expected phasing out of the SDE++, developers are gaining an interest in long-term contracts or Power Purchase Agreements (”PPA”) (Financiering Zonnepanelendelen, n.d.; Next-Kraftwerke, n.d.). PPAs are purchase agreements for power between two parties, mostly electricity producers and consumers, with predefined quantities of electricity to be delivered and negotiated price. It is often a virtual or synthetic agreement, where the flow of physical power and money are decoupled.

The produced and consumed energy is added to a portfolio of a Balancing Responsible Party (”BRP”). A BRP can be large consumers or electricity suppliers who are responsible for balancing their portfolio. The BRP on the producing side adds the production to their balancing portfolio and trades this electricity on for example the spot market. The BRP on the consumer side buys the power with the same profile as the produced power on the market.

There are variable ways to make long-term arrangements in terms of energy delivery and price. A method to secure a long-term arrangement in terms of price, is to take care of the difference between the price on the market compared to the agreed price in the PPA. This can be done by use of a Contract for Difference (”CfD”). The price the producing partner receives will be topped to the pre-agreed price by the consuming partner, to secure the price. This mechanism is visualized in Figure 2.2.

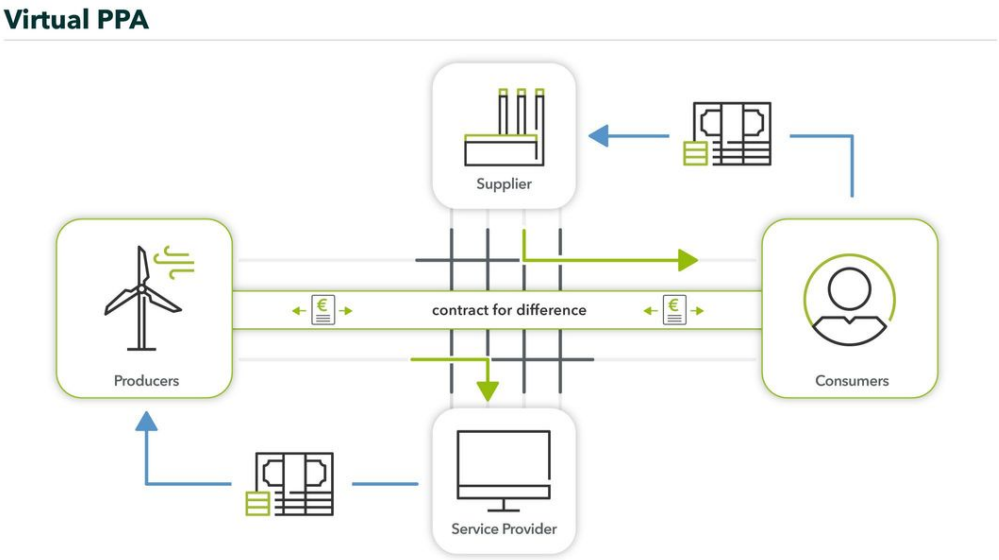

Figure 2.2: Virtual or synthetic PPA (Next-Kraftwerke, n.d.)

Regardless of the shape or form, PPAs with arrangements on price reduce the risk of fluctuating market prices, since the received price or paid costs for energy are constant throughout the duration of the PPA.

2.5. Future Developments

The past sections described the current situation, but with the large-scale roll-out of renewable energy sources, different challenges arise and changes to the system are required. Solutions to congestion are widely researched in the Netherlands and both ACM and industry associations are considering new ways to deal with the issues of the current grid layout. Multiple measures to reduce or prevent congestion and improve the functioning of the energy system are being explored in the Netherlands either now or in the near future. This section describes the future developments, both in terms of upcoming law amendments possibly influencing the Dutch context for cable pooling and future outlooks. An overview of the different mechanisms in be found in Table 2.1.

Table 2.1: Overview of Different Possible Future Measures and Their Status

Measures	Initiator	Status	In Effect
Congestion Management	ACM	Approved and currently in development	Q3 2023
Alternative Transport Rights	ACM	Orientation	TBD
Use it or Lose it	ACM	Orientation	TBD
Law Amendment	Government	Approved by Tweede Kamer, needs to pass Eerste Kamer	TBD
First Come First Serve	ACM	Definite decision to be published	TBD
Battery at Solar Farm	Government	Part of proposed mechanisms to reduce emissions before 2025	TBD

2.5.1. Congestion Management ("CM")

The branch organisation of system operators, *Netbeheer Nederland*, struggles with congested regions and has proposed an amendment to the Electricity Law. A region is defined congested when the predicted demand for transport capacity in a region is higher than the actual capacity. In these congested region, congestion management tries to steer the demand of transport capacity by using price mechanisms and market forces. This is realised using four mechanisms (GOPACS, 2023), all linked to trading platform GOPACS:

1. **Voluntary redispatch**
   Using redispatch, the demand of transport capacity can be reduced during the peak hours. The

reduction is realised by working with a bidding structure during these peak time slots. Parties connected to the bidding system in a congested region can respond to the bidding openings by placing a buy order on the GOPACS trading platform. This buy order is combined with a sell order by a party outside the congested area to still match supply and demand.

2. ***Biedplichtscontract***
   This *Biedplichtscontract* is a contract obliging parties, called Congestion Service Parties (”CSP”), to make redispatch bids. This obligation and corresponding returns are part of the ATO, creating more security for both system operator and transport demanding parties. The bids are coupled to the Intraday Market.
3. ***Capaciteitsbeperkend contract met afroep*** or ***zonder afroep***
   Both of these contracts are capacity limiting contracts which are activated when the system operator expects congestion. *Met afroep* means on-demand: on the day before the expected congestion, the parties with this contract are requested to limit their transport capacity for a fixed time-block on the day after. The contract contains pre-agreed conditions and reduced tariffs in case of limited capacity. *Zonder afroep* means that the contract contains pre-agreed conditions and tariffs for limiting capacity at specific time periods.

In 2022, ACM published their decision on the proposition of the branch organisation of the system operators for new laws concerning the lack of transport capacity and congestion management. From approximately Q3 in 2023, the congestion management will be in effect and must be executed by all system operators (ACM, 2022a; Jongsma, van Cappellen, et al., 2021).

ACM analysed the investment plans by the system operators and has concluded that the congestion will be actual for at least five to 10 years. ACM considers this measure a method to reduce the impact of congestion while awaiting the grid reinforcements, by using the existing grid infrastructure more efficiently (ACM, 2022a).

The proposed grid connection alternatives such as the obligating contracts or capacity limiting contracts are most suitable for flexible generating resources or consumers or other flexible assets such as batteries, and not for renewable generation.

2.5.2. Alternative Transport Rights ("ATR")

Traditionally, the grid-connected party is always entitled to using the full size of their contracted grid capacity. When awarding new ATOs to potential projects, this right is taken into account, limiting the available grid capacity even if during certain time periods there is still space available (ACM, 2022c, 2022e, 2023c). Therefore, another solution to the grid-connection limitations due to congestion under investigation are alternative or flexible transport rights. Alternative transport rights are transport rights that are not, or not completely, fixed. These alternative rights give the system operators the possibility to connect more generation on the grid, only allowing them to use this free space, for example by use of a Non-Firm ATO (“NFA”).

At times when there is space on the grid, the grid operator can fill this free space by allocating transmission capacity to a connected party (ACM, 2022c). Important to note is that the available excess space is divided over all parties, meaning that the security of transport decreases with more parties using flexible or variable transmission rights. The proposed benefits for large consumers are a reduction in grid-tariffs.

In summary, a party does not have any rights to transport, but is allowed to transport when system operator allows it (off-peak hours) against a reduced grid tariff for consumers, with the contracted fee per connected unit capacity put to zero. In the daily planning process of the system operator, the system operator informs the connected party with an NFA before the closing of the day-ahead market at which times and to what extent transmission is permitted. When the system operator has published this, the transmission rights for the specified moment and for the size of the specified capacities will be regarded as ’fixed’. Flexibility is needed, which is why it will probably be most suitable for storage. Using these flexible transport rights, ACM sees a possibility for batteries to become active in congested areas and relieve congestion.

ACM has recently (September 2023) published the proposed changes in the grid codes based on a NFA (ACM, 2023c) with a six week response term. The NFA may be used in congested or imminent congested areas, meaning congestion will start to play a role within 12 months. No specifics on the time blocks are presented yet.

2.5.3. Use it or lose it ("UIOLI")

Use it or lose it ("UIOLI") is a proposed mechanism by ACM (ACM, 2022c, 2023d) where part of the transport capacity contracted by a customer is taken back by the system operator if that customer does not use it for a specific period. This capacity is then released to other customers via the system operator. UIOLI therefore ultimately forms an incentive for customers to critically assess their capacity needs and not to reserve capacity that they do not need. If the peak of the connection is reached once, the UIOLI principle does not hold and the full grid connection size remains available to the customer.

The UIOLI could cause that oversized grid connections at renewable farms become less present. UIOLI has been approved by ACM (ACM, 2023d), allowing system operators to reduce the grid connection size to the historical maximum peak capacity after discussing this with the connected party. The connected party can always keep the oversized connection in case expansions are in the pipeline and require the full capacity within two years.

The formalized grid code amendment will be published and enforced towards the end of 2023. ACM will monitor the effects of UIOLI closely, given the possible impact of the measure.

2.5.4. Other

Currently, cable pooling is defined in the Electricity Law as generating sources in close proximity sharing one grid connection. The generating sources may be located on different real estate objects, with a maximum of two real estate objects. In February 2023, a law amendment (Tweede Kamer, 2023) has been proposed to expand this to four objects. Furthermore, an extension in the type of sources that are allowed to cable pool has been proposed. Currently, only generating sources, such as solar and wind generation, are allowed to cable pool. This amendment aims to broaden the scope to conversion-installations. The bill has been approved in politics by the *Tweede Kamer*, it only needs to pass *Eerste Kamer*. If the amendment gets approved, a battery will be considered as a separate entity in a cable pooling project.

Another potential law change enables system operators to award grid capacity to parties that contribute to social goals. Currently, the system operators are forced to use the "first come first serve" principle where the first project to request grid capacity, receives it, by effect of the Electricity Law following the European non-discrimination principle (ACM, 2023a). ACM proposes a deviation to this to ensure social goals to be reached (ACM, 2023a). With the lack of grid connecting capability in the Netherlands, a deviation of this principle is proposed to allow system operators to prioritize as long as the method is based on "objective and transparent criteria". If a system operator can argue why giving priority to a certain project is needed, ACM will not interfere. This shows that system operators and ACM are receptive to congestion limiting or mitigating projects, such as cable pooling. Cable pooling projects could therefore potentially be awarded (extra) grid capacity more easily. There is a lot of support for the amendment and ACM calls on system operators to get started with objectively prioritizing while the decision is being finalized (ACM, 2023b). The final decision will be published in March 2024.

Furthermore, the government is considering the subsidizing the addition of a battery to a solar farm to relieve the grid (Energy Storage NL, 2023; Solar Magazine, 2023b), by shifting energy from the solar farm. The batteries would be entitled to subsidies structured in a similar way as the SDE++ of which the exact implementation is yet to be published. The expected methodology would be to only allow the system, consisting of storage system and solar farm, to export outside of peak hours, so from 17:00 until 09:00 the next morning (Solar Magazine, 2023a). The batteries would receive subsidy for each kWh of shifted energy, but can also trade on other markets to secure more revenue streams (Solar Magazine, 2023a). For new solar farms this would mean a different business case with more initial CAPEX and possibly different operation, since the grid connection is shared between battery and solar

farm.

2.6. Batteries

Batteries are often mentioned as an important flexible resource in the energy transition, with a potential to also decrease congestion (Jongsma, Van Cappellen, et al., 2021; van Cappellen et al., 2023). As mentioned in subsection 2.5.4, conversion installations, such as storage are potentially added to the legal context for cable pooling. The concept cable pooling agreement including storage has been drafted, ahead of the final decision (Ventolines, 2021). Furthermore, it is likely that subsidized storage will be combined with a new solar farm in the future. Next to all of the above, many of the proposed mechanisms and future developments aim to create a playing field for batteries in the Netherlands. Therefore, the potential revenue streams of a battery are discussed in this section.

2.6.1. Current Revenue Streams

This section focuses on the revenue streams for batteries in the Netherlands and the impact of possible future developments on the grid connecting possibilities for batteries. The CE Delft reports analyse the different markets of interest for the battery business case and are used as an industry benchmark for the turning point on profitability of batteries and their function with regard to congestion (Jongsma, Van Cappellen, et al., 2021; van Cappellen et al., 2023).

When there is any residual imbalance after the Intraday Market, the aFRR and Imbalance Market aim to prevent a frequency deviation. Both have the same purpose, but the aFRR is based on contracted capacity, forcing the parties to reduce the imbalance by ramping up or down with the contracted capacity when activated by the system operator. BRPs can also bid on this imbalance voluntarily. The clearing price determines which contracted parties or voluntary parties are activated to solve the imbalance and for which price.

Any residual imbalance results in a frequency deviation (Jongsma, Van Cappellen, et al., 2021). These deviations give an incentive to ancillary service offering parties to either supply more electricity if the frequency drops or consume more energy if the frequency rises. The frequency deviation is solved using two mechanisms. First Frequency Containment Reserve (”FCR”) and later the manual Frequency Restoration Reserve (”mFRR”) (Jongsma, Van Cappellen, et al., 2021; TenneT, 2023). The characteristics of the FCR is fast response time and availability at all times, in case of a deviation. The size of capacity of the FCR is however limited, so it can only be active for a short period of time. If the FCR does not solve the imbalance, the mFRR is activated, which only happens a few times a year. If a resource contributes to the balancing mechanisms, it must have the capacity subscribed reserved at all times.

Batteries are well-suited for the FCR or aFRR contracts due to the battery’s fast response time (Jongsma, Van Cappellen, et al., 2021). An FCR contract is currently the most profitable business case for a battery in the Netherlands, most batteries are deployed there. The FCR only requires 200 MW contracted, in the latest report the FCR was already saturated (van Cappellen et al., 2023).

CE Delft analysed other potential revenue streams for grid connected batteries and batteries connected to an existing or a new solar farm, focusing on DAM, aFRR or Imbalance Market and stacked-business cases (Jongsma, Van Cappellen, et al., 2021; van Cappellen et al., 2023). Stacked-business cases are business cases taking into account multiple markets to make bids on or reserve capacity for. These scenarios did not consider a battery combined with a wind farm, since the output of a wind farm is less subjected to day and night patterns.

Batteries are currently still expensive to install and operate. By drawing energy from the grid to charge the battery, the battery behaves as a large consumer and has to pay both for the power used and for the usage of the grid. The high costs of installing and operating the battery whilst keeping the project profitable, requires high revenues. CE Delft arrived at the following main conclusions (Jongsma, Van Cappellen, et al., 2021; van Cappellen et al., 2023):

1. **DAM**:

Trading on the DAM alone will not become profitable before 2030 for neither of the three connecting possibilities according to both analyses. For the scenarios where the battery was connected to a solar farm, trading at the DAM could be considered peak shifting. Peak shifting by storing excess energy of the solar farm and trading it at a later time is effectively the same as trading at the DAM, except the reduction in grid tariff costs since no energy has to be drawn from the grid.

According to CE Delft, peak shifting does not result in a positive business case before 2030, even with the reduction in grid tariffs. If the battery wishes to trade on other markets next to peak shifting, the additional grid tariffs outweigh the additional revenues, leading to no net change. The proposed subsidy scheme could significantly improve this business case given that the unprofitable top will be covered.

2. **aFRR or Imbalance Market**:
   For grid-connected batteries, blocking capacity for an aFRR contract or bidding on the Imbalance Market show the best results in the business case and were expected to become profitable for grid-connected batteries by 2021. However, in the later analysis, CE Delft projected this revenue stream to become profitable in the run-up to 2030.

3. **mFRR**:
   Due to the limited activation of the mFRR and the capacity that needs to be reserved at all times, the mFRR is not used as a source of revenue for batteries in the Netherlands.

4. **Stacked-business cases**:
   For grid connected batteries, the stacked-business case of DAM, FCR, aFRR or Imbalance Market yields the highest revenues and is profitable at the time of the first report.

Currently, either stacking of business cases or trading on the FCR market leads to a profitable business case. Since FCR is already saturated, only the stacked option leads to a profitable business case.

In this research, the aim is to analyse how the presence of on-site storage affects the cost-benefit framework. The CE Delft analyses did not consider a renewable resource cable pooling with another renewable resource with a battery. This could potentially lead to different results on the profitability of the business case, so the results of CE Delft are only used as guidelines.

To identify the impact of on-site storage on the cost-benefit framework, the different revenue streams from either contracted ancillary services or aFRR or trading on the DAM or Imbalance Market can be considered. For both balancing mechanisms, FCR and mFRR, the reserved capacity needs to be available on-demand at all times. The same holds for an aFRR contract. CE Delft found that the revenues due to revenue streams with this contracted capacity decrease when the connection is shared with a solar farm, since there is less capacity continuously available to use for FCR or aFRR (Jongsma, Van Cappellen, et al., 2021). With cable pooling, these revenues are likely to decrease even more, since less grid capacity is available to be reserved. Also considering that the FCR market is saturated, the ancillary services and aFRR will not be considered in this study.

The potential revenue streams are therefore DAM or imbalance. Due to the projections of the increasing volatility the DAM and the upcoming subsidy for a battery shifting the output of a solar farm, the value for peak shifting will increase. Therefore, the DAM and peak shifting revenue stream will be considered in this research.

2.6.2. Impact Future Developments

The possible future developments could have significant impact on the grid connecting possibilities for batteries and potentially in the revenue streams too. All four congestion management mechanisms, discussed in subsection 2.5.1, could in theory be of interest for batteries connecting to the grid in the Netherlands, since batteries can steer supply and demand.

The structure of the congestion management mechanisms is now built on a financial and technical limit, as described in ACM, 2022a; Jongsma, van Cappellen, et al., 2021). The financial limit is based on the costs of grid reinforcements. The costs of congestion management should not be higher than the costs of an equally sized grid reinforcement. The limit is currently set to 1.02 EUR/MWh. The technical limit is based on how much extra capacity can be connected to the grid if flexibility is purchased by the grid operator using these mechanisms. The limit is currently set at 50%, so an additional 50% could be connected to the grid.

CE Delft analysed the influence of currently built batteries and systems in the pipeline on congestion and concludes that the current financial limit does not provide enough compensation for batteries to assist in solving congestion (van Cappellen et al., 2023). With the current policies, grid-connected batteries will tend to connect in areas without congestion to apply for a grid-connection there, instead of participating in the congestion mechanisms in congested areas.

Furthermore, CE Delft foresees that the peaks of congestion will have a longer time span than the hours a battery can provide energy at their full capacity. Most batteries contain one, two or at most four hours of flexibility at full capacity, while the congestion peaks can take up to twelve hours. Batteries could still assist in congestion, but currently built batteries or batteries in the pipeline can only do so at reduced capacity. Both factors lead to batteries currently not solving the congestion, and rather contributing to it without fitting policies.

In earlier research on the profitability of batteries, the congestion management market is used as a potential revenue stream as well, emphasizing that the mechanisms are built on compensating the missed revenues and should not be considered a ”direct revenue model” (van Cappellen et al., 2023).

CE Delft concludes that the congestion market in combination with other income sources could result in a profitable business case for batteries. For example, CE Delft projects that combines the Imbalance Market with congestion market is profitable for grid-connected batteries (Jongsma, Van Cappellen, et al., 2021). For a battery connected to a new solar farm, CE Delft concludes that the same combination is the most profitable, but not yet profitable before 2030 (Jongsma, Van Cappellen, et al., 2021). Combining the aFRR or Imbalance Market, FCR and DAM with the congestion market is not projected to become profitable before 2030 (Jongsma, Van Cappellen, et al., 2021).

Next to the trading on GOPACS, congestion management considers different connecting possibilities to the grid in congested areas considering export or import limitations during peak hours. The *capaciteits-beperkende contracten* and alternative transport rights could result in new grid connecting possibilities in congested areas for batteries.

2.7. Cable Pooling Project Examples

This section shows published operational cable pooling projects in the Netherlands.

Pilot: Franeker

A pilot in Franeker showed that sharing an undersized grid connection with two generating sources shows great promise. The wind turbine has a power output of 900 kW and is joined with a solar farm with peak capacity of 512 kW. The generating sources share a grid connection of just 1 MW, which has proven to be sufficient since curtailment was limited (Firan, 2023).

De Grift

Solar farm De Grift has cooperated with an existing wind farm of four turbines with a total capacity of 10 MW. The solar farm has a peak capacity of 5.04 MWp and was added after the start of operation of the wind farm (Firan, 2023; Zonnepark de Grift, n.d.). The total grid connection size is 10 MW, according to the size of the wind turbines. To connect the solar farm to the wind farm, excess room originally left free for a possible fifth turbine, can be used. Furthermore, the metering- and control devices have been changed to be able to track the performance of the two farms separately.

Grid-ON
An existing solar farm and wind turbine cable pooling project has been extended with a battery (Duurzaam ondernemen, 2022), as an exception of the existing cable pooling definition to act as a pilot project. The battery assists in balancing services and trades on the imbalance market. Advanced energy- and power management systems decide which resource is allowed to make use of which part of the cable.

During peak hours, the solar farm and turbine curtail their export and store the excess energy in the battery and receive a compensation of the system operator for the curtailing of the export. This has a positive impact on the battery too. Combined, the farm delivers about 10 million kWh of generation. The battery is 1 MW and can contain up to 2 MWh. This example shows that combining a battery with solar and wind could lead to a more efficient use of the grid and helps the grid too by providing grid services.

2.8. Overview

This section contains an overview of different cable pooling combinations and corresponding revenue streams considered in this research. The different combinations consist of adding a generating resource or a generating resource with a battery BTM.

- **Adding a generating resource: Hybrid Farm**
  To an existing renewable resource, a wind or solar resource can be added to form a hybrid farm. The solar farm can have different orientations. This is confirm the existing law and definition of cable pooling. In congested areas, the added generating farm can only be added to an existing grid connection and has to comply with the existing ATO.

- **Added generating and conversion resource: Hybrid Farm including Battery**
  To an existing renewable resource, a wind or solar resource combined with a battery can be added to form a hybrid farm including battery. The solar farm can again have different orientations. This is confirm the existing law and definition of cable pooling, if the battery is added BTM at the SAP.

  The battery will only be allowed to use excess energy of the added farm to peak shift the output. In congested areas, the added generating farm and battery can only be added to an existing grid connection and have to comply with the existing ATO.

The added generating resource and, if present, battery will trade on the EPEX market. The added generating resource secures the revenues either using a PPA or a SDE++. Another revenue stream is fully market-exposed (”ME”), with no PPA and SDE++ present.

3

Problem Definition and Scope

With the context explained in chapter 2, this chapter discusses the past research in hybrid farms to arrive at the problem definition used in this research. The aim of this chapter is to first analyse the past research. This is used to define the problem formulation with corresponding scope and describe how to determine and optimize the cable pooling potential at a specific site, based on the presented Dutch and literature context.

3.1. Literature Overview

This section discusses the past research conducted to analyse the literature context and to identify how determining and optimizing the cable pooling potential can form a possible contribution.

In literature, there is an interest in researching the co-location of complementary renewable energy sources to form a hybrid farm. One perspective focuses on the potential to reduce the intermittency of the power output. Another perspective focuses on optimally sizing components in hybrid farms using an optimization approach. First, different combinations of energy resources in literature are discussed. Secondly, the potential of co-locating complementary resources is explored, followed by an overview of the methods and approaches used in prior research to optimize hybrid systems.

3.1.1. Combinations of Renewable Resources in Hybrid Farms

In past research, different combinations of renewable energy sources can be identified. This section discusses the variable combinations seen in past literature.

The first combination is wind and solar energy, as used by for example Zhou et al. (2010), both on- and offshore. The weather patterns of wind speed and solar irradiation are (weakly) negatively correlated, making combined wind and solar energy a good fit for a hybrid farm (Stanley and King, 2022).

The second combination is wind and wave energy, as used by for example Stoutenburg et al. (2010). Some research focuses on replacing a fossil resource, such as a diesel generator, by renewable sources as much as the system allows, as used by for example Al-Sharafi et al. (2017).

Batteries can be added in stand-alone situations to ensure the security of supply and in grid-connected situations to further reduce the intermittency in the output, as used by for example Anoune et al. (2020). Another advantage of adding storage is the expected increase in the value of dispatchable energy, in a future with increased penetration of instearable renewable resource (Sioshansi and Denholm, 2013), matching the trends seen in the spot market as mentioned in chapter 2. Another storage method often combined with renewable generation is pumped hydro storage (Farfan and Breyer, 2018; Ma, Yang, Lu, and Peng, 2014).

3.1.2. Identifying the Potential of Hybrid Farms

Quantifying the potential of combining different resources in a hybrid farm is one of the topics analysed in past literature. This section discusses some of the benefits of combining different generation types.

The potential can be quantified using a technical and/or economic feasibility analysis, as used by for example Trikalitis et al. (2021), or by considering the influence of the co-location on the power output, as used by for example Stoutenburg et al. (2010).

The benefits of combining wind and solar have been researched by Venkataraman et al. (2018). The main benefits mentioned are ”a decrease in development costs, better use of available land, the complementary behaviour of the generation profile, both diurnal and seasonal, potential savings in transmission evacuation costs, and the sharing of operations and maintenance (”O&M”) costs” (Venkataraman et al., 2018).

The improved usage of available land, decrease in development costs and reduction of O&M costs, of 14 and 12% respectively, are also reported by Astariz et al. (2015). As mentioned in chapter 2, the potential savings in transmission evacuation costs, complementary behaviour of generation profiles and possible cost reductions (Venkataraman et al., 2018) are also a driving reason for cable pooling in the Netherlands.

The complementary behaviour of two resources is analysed by Stoutenburg et al. (2010). Different configurations of wind and wave energy and the impact on the power system in California in terms of reliability are simulated. It is concluded that the combination of two resources with a low or negative correlation coefficient, wind and wave energy in this case, results in a reduction in the power output volatility reducing the impact on the power system. The same can be concluded for wind and solar. ”Using two or more generation systems can reduce the variability of power production that is common with wind and solar and provide higher quality power to the grid” (Stanley and King).

This is also concluded by Astariz and Iglesias (2016) and Astariz et al. (2015). In a Brazilian offshore wind and solar case, the higher the wind speeds the better the correlation between wind and solar resulting in high complementary behaviour of the resources (de Souza Nascimento et al., 2022). The complementary behaviour can also be visible in a fewer count of no production of the farm (Astariz and Iglesias, 2016) or an increased capacity factor. Increasing the mix of wave energy in an existing wind farm, increases the capacity factor of the combined output up to a certain maximum (Astariz and Iglesias, 2016).

The behaviour of weather patterns of different sources can be an insightful indicator of the complementary behaviour of the co-location of two renewable resources and is used in multiple papers identifying the potential of combining multiple resources in a hybrid farm (Astariz and Iglesias, 2016, 2017; Chen et al., 2010; Diaf et al., 2008; Ma, Yang, Lu, and Peng, 2014; Stanley and King, 2022; Trikalitis et al., 2021; Yang et al., 2007).

3.1.3. Optimization of Hybrid Farm Components

The second perspective on hybrid systems in research is optimally sizing the different components. This section deals with the different optimization approaches used in past research.

Optimization is a tool often used to comply with constraints while obtaining an optimal objective function by varying decision variables. To compare the research in the field of optimally sizing a hybrid farm, the different parts of the optimization will be compared. First of all, the general setup of an optimization problem is introduced. Furthermore, the different parts of the optimization problem are discussed, ranging from objective functions and type of optimizations, to decision variables or solving methods.

The main focus of prior research is stand-alone situations, where the load demand must be met by supply at the lowest cost possible, as used by for example Ma, Yang, and Lu (2014). The sizing of components is crucial to minimize the costs while maintaining the security of supply or to maximize the profits. Configurations impact the potential of the hybrid farm in terms of economic and technical

feasibility.

An overview of the past research considered for the context can be found in Table 3.1, showing the tag used in other tables to indicate the article and the writer and publish year. The hybrid case can either be grid connected (”GC”) or stand-alone (”SA”). The GC focused articles will be discussed in more detail in subsection 3.1.4. The table also indicates the technologies used in the hybrid farm and the location of the case study.

Table 3.1: Overview of past research in optimization of hybrid systems indicating the tag used in the other tables, the writers and year, if the project is Stand-Alone (”SA”) or Grid-Connected (”GC”), the main components of the hybrid system and the location of the case study.

#	Authors, Year	Type	Sources	Location
2006-1	Yang et al., 2007	SA	PV/Wind/Batteries	China
2007-1	Diaf et al., 2007	SA	PV/Wind/Batteries	Corsica
2008-1	Diaf et al., 2008	SA	PV/Wind/Batteries	Corsica
2008-2	Yang et al., 2009	SA	PV/Wind/Batteries	China
2008-3	Yang et al., 2008	SA	PV/Wind/Batteries	China
2009-1	Kaldellis et al., 2009	SA	PV/Batteries	Greece
2009-2	Ekren and Ekren, 2009	SA	PV/Wind/Batteries	Turkey
2010-1	Mousa et al., 2010	SA	PV/Wind	Oman
2010-2	Ould Bilal et al., 2010	SA	PV/Wind/Batteries	Senegal
2010-3	Kaldellis et al., 2010	SA	PV/Storage	Greece
2011-1	Dufo-López et al., 2011	SA	PV/Wind/Diesel/Batteries	Spain
2011-2	Kaabeche et al., 2011a	SA	PV/Wind/Batteries	Algeria
2011-3	Rajkumar et al., 2011	SA	PV/Wind/Batteries	Malaysia
2011-4	Kaabeche et al., 2011b	SA	PV/Wind/Batteries	Algeria
2012-1	Abedi et al., 2012	SA	PV/Wind/Diesel/Batteries/Hydrogen	Iran
2012-2	Ngan and Tan, 2012	SA	PV/Wind/Diesel/Batteries	Malaysia
2013-1	Perera et al., 2013	SA	PV/Wind/Combustion/Batteries	Sri Lanka
2013-2	Engin, 2013	SA	PV/Wind/Batteries	Turkey
2013-3	Hiendro et al., 2013	SA	PV/Wind/Batteries	Indonesia
2014-1	Ma, Yang, Lu, and Peng, 2014	SA	PV/Wind/Hydro	China
2015-1	González et al., 2015	GC	PV/Wind	Spain
2016-1	Tito et al., 2016	SA	PV/Wind/Batteries	New Zealand
2017-1	Abdul Aziz et al., 2017	SA	PV/Battery	Malaysia
2017-2	Al-Sharafi et al., 2017	SA	PV/Wind/Diesel/Batteries	Saudi-Arabia
2018-1	Bakos and Tsagas, 2018	SA	PV/Wind/Natural Gas	Greece
2020-1	Barakat et al., 2020	GC	PV/Wind/Batteries	Egypt
2020-2	Anoune et al., 2020	SA	PV/Wind/Batteries/Electrical heater	Marocco
2020-3	Najafi Ashtiani et al., 2020	GC	PV/Batteries	Iran
2021-1	Golroodbari et al., 2021	GC	PV/Wind	Netherlands
2022-1	Mertens, 2022	SA	PV/Wind	Netherlands
2022-2	Stanley and King, 2022	GC	PV/Wind/Batteries	USA
2022-3	Diab et al., 2022	GC	PV/Wind/Batteries	Netherlands

The aim of a sizing optimization is to find the optimal design of the hybrid farm based on performance indicators, or criteria. The indicators range from minimising the annualised cost or loss load probability, to maximising the NPV. The performance indicator determines the objective and the corresponding approach.

Objective Function

The objective function is to either minimize or maximize a certain goal, or objective which can be linked to economical or technical indicators. An overview of the different objective indicators used can be found in Table 3.2.

Table 3.2: Overview of past research in optimization of hybrid systems indicating the type of objective/indicator used, if the optimization is multi-objective (”MO”) or not, how the optimization is solved and which decision variables are varied. ** Multi-step*

			Solving		
#	**Indicator**	**MO**	**Method**	**Software**	**Decision Variables**
2006-1	LCE	N	-	-	kW PV, wind, kWh batteries
2007-1	LCE	N	-	-	kW PV, wind, kWh batteries
2008-1	LCE	N	-	-	kW PV, wind, storage days
2008-2	ACS	N	GA	-	NPV, NWT, kWh bat, PV tilt, WT hh
2008-3	ACS	N	GA	-	NPV, NWT, Nbat, PV tilt, WT hh
2009-1	EPBP	N	-	-	NPV, mod type, kWh batteries, kW inv/CC
2009-2	CAPEX	N	-	Arena12.0	Area PV, RSA WT, kWh batteries
2010-1	Power, TCS	*Y*	-	GAMS	NPV, NWT, WT hh, WT Rotor D
2010-2	ACS	N	GA	-	NPV, NWT, NBat, Nreg, Ninv
2010-3	NPC	N	-	-	kW PV, kWh storage
2011-1	LCOE, GHG	Y	SPEA	-	NPV, NWT, Nbat, type PV/bat/gen/inv/WT
2011-2	LUEC	N	-	-	kW PV, wind, kWh batteries
2011-3	LCOE	N	ANFIS	-	kW PV, wind, kW batteries
2011-4	TNPC	N	Iterative	-	NPV, NWT, storage days
2012-1	NPC, LPSP, GHG	Y	DEA	-	NPV, NWT, Nbat, Ngen, NFC, Nel
2012-2	NPC	N	-	HOMER	kW PV (in steps of 20 kW), Nbat, NWT
2013-1	LEC, ICC, GHG	Y	SESEA	-	NPV, PV type, kW WT, NWT, Nbat
2013-2	LCS	N	-	-	NPV, NWT, Nbat, CC type
2013-3	LCOE	N	-	HOMER	PV type, WT type, kWh batteries
2014-1	-	N	Iterative	-	kW PV, NWT, volume Hydro, Ncon
2015-1	NPV	N	GA	-	NPV, NWT
2016-1	TCS	N	GA	-	NPV, NWT, Nbat, PV tilt, WT hh
2017-1	LPSP	N	FA	-	kW PV, kWh bat, type PV/bat/CC/inv
2017-2	TPI	Y*	-	-	kW PV, Nbat
2018-1	LCS	N	-	-	EPV, Ewind, Esolar thermal
2020-1	LPSP, COE, REF	Y	MOPSO	-	NPV, NWT, Nbat
2020-2	LCOE	N	GA	-	kW PV, wind, kWh batteries
2020-3	LCOE	N	TLBO	-	kW PV, kWh batteries, kW inverter
2021-1	LCOE	N	Iterative	-	kW PV
2022-1	Unmet load	N	Analytical	-	fraction EPV/EWT
2022-2	LCOE, profits	N	GA	-	Grid variables WT, kW PV, kWh bat
2022-3	-	N	-	-	kW PV, kW WT, kW batteries

Minimizing costs is a commonly used objective function, expressed as annualized cost of system (”ACS”), used by for example Ould Bilal et al. (2010), total cost of system (”TCS”) (Tito et al., 2016), investment costs, used by for example Perera et al. (2013), levelized unit of electricity cost (”LUEC”) (Kaabeche et al., 2011a), life cycle costs or savings, used by for example Javed et al. (2019), net present costs (”NPC”), used by for example Ngan and Tan (2012) or levelized costs of electricity (”LCOE”), used by for example Golroodbari et al. (2021).

Minimizing the loss of power supply probability (”LPSP”), used by for example Barakat et al. (2020), minimizing the unmet load (Mertens, 2022) or optimizing the NPV (González et al., 2015) or profits (Stanley and King, 2022) can also be used as an objective function.

Another possible objective of an optimization, is minimizing the carbon emissions, or greenhouse gasses (”GHG”), used by for example Abedi et al. (2012) or maximizing the renewable energy factor (”REF”) (Barakat et al., 2020). A reduction of emissions often forms a trade-off with a reduction of costs (Al-Sharafi et al., 2017). The same can be said for the increased level of renewable penetration and low costs, used by for example Rajkumar et al. (2011). Depending on the focus, low emissions or low costs, the optimal system design may differ.

The optimization problems may have one or multiple objectives. In a multi-objective approach, two potentially conflicting objectives are both optimized, used by for example Barakat et al. (2020). Multi-objective problems steer the system to find a configuration that obeys both objectives.

In a two-step objective (Al-Sharafi et al., 2017), the two objectives are solved subsequently. An example of a multi-objective case is to maximize the output power while minimizing the total costs (Mousa et al., 2010) or minimizing the LCOE while also minimizing the emissions (Dufo-López et al., 2011). Zhou et al. (2010) consider two criteria in the sizing optimization strategies: the power reliability of a stand-alone system and the system cost.

Decision Variables

Decision variables are varied using different solving methods to find the optimal outcome of the objective function. For a hybrid system containing PV, wind and/or battery storage, different decision variables have been used in past research. The decision variables for each analysed paper can be seen in Table 3.2 and are discussed in this section.

For wind turbines ("WT"), the decision variables can be the number of turbines (NWT), used by for example Yang et al. (2009), or the required capacity (kW), used by for example Kaabeche et al. (2011a). Another approach is to find the optimum rotor swept area (RSA) in m^2 (Ekren and Ekren, 2009), rotor diameter (Mousa et al., 2010) or hub height (hh) as used in by for example Tito et al. (2016).

For solar panels, the required capacity (kW), used by for example Al-Sharafi et al. (2017), or the number of modules (NPV), used by for example Perera et al. (2013), can be used as decision variables. Another approach is to find the required area of PV panels in m^2 (Ekren and Ekren, 2009) or the number of modules and the maximum power point of those modules (Kaldellis et al., 2009). The number of modules and batteries in parallel and the number of wind turbines are used as decision variables by Dufo-López et al. (2011).

The type of wind turbine, PV panel or battery can also be used as a decision variable, used by for example Dufo-López et al. (2011). The slope angle of the modules (Tito et al., 2016; Yang et al., 2009; Yang et al., 2008) and the installation height of the turbines, used by for example Tito et al. (2016), can be used as system design parameters too, subject to minima and maxima.

The decision variable related to the storage is the energy of the battery bank (kWh), used by for example Kaldellis et al. (2009), the number of batteries required (Nbat), used by for example Abedi et al. (2012) to find the number of batteries in series given the voltage level required, or the amount of storage days required to meet a certain energy demand (Diaf et al., 2008; Kaabeche et al., 2011b).

Support system decision variables can be considered too, such as the nominal power of the inverter or charge controller ("CC") employed in the system (Kaldellis et al., 2009), the number of regulators and inverters (Ould Bilal et al., 2010), the number of converters (Ma, Yang, Lu, and Peng, 2014), the battery charger type (Abdul Aziz et al., 2017; Engin, 2013), the number (Abedi et al., 2012) or capacity (Perera et al., 2013) of generators or the number of fuel cells or electrolysers (Abedi et al., 2012). The sizing variables for different technologies can also be expressed using produced energy over a time period instead of the installed capacity (Javed et al., 2019).

Constraints

Constraints are a set of equality of inequality expressions which must be met by the optimal solution of the optimization problem. Constraints impose boundaries on the solution space. The different constraints used in past papers are shown in Table 3.3.

Table 3.3: Overview of past research in optimization of hybrid systems indicating the most important constraint used create the decision space and the variations performed to find the most sensitive inputs.

#	Constraints	Sensitive input
2006-1	LPSP <LPSPmax	Hub height, Orientation of panels
2007-1	LPSP <LPSPmax	Type of module/turbine/battery
2008-1	LPSP <LPSPmax	Battery, Impact of wind/(total energy) ratio
2008-2	LPSP <LPSPmax	-
2008-3	LPSP <LPSPmax	Battery
2009-1	100% autonomy, EPBP<LT	Type of module/battery, Tilt
2009-2	LLP <LLPmax	Auxiliary energy costs
2010-1	Demand must be met by supply	Load profile
2010-2	LPSP <LPSPmax	Load profile
2010-3	Demand must be met by supply	Autonomy values, Storage type
2011-1	Demand must be met by supply	Inflation, Module cost, Module Emissions
2011-2	DPSP <DPSPmax	DPSPmax
2011-3	LPSP <LPSPmax	-
2011-4	DPSP <DPSPmax	Storage days, DPSPmax, Discount rate, CAPEX, LT
2012-1	-	-
2012-2	Demand must be met by supply	Fuel cost
2013-1	Unmet load fraction	Unmet fraction, Fuel cost, WT/PV panel cost
2013-2	Load must be met by supply	-
2013-3	LLP <LLPmax	-
2014-1	LPSP <LPSPmax	LPSPmax
2015-1	Load must be met by supply	CAPEX, Spot price, Inflation, Interest, Efficiency
2016-1	LPSP = 0	Socio-demographics: Load patterns
2017-1	Load must be met by supply	Controller type
2017-2	Load must be met by supply	-
2018-1	Load must be met by supply	-
2020-1	Load must be met by supply	Grid management strategies
2020-2	LPSP <LPSPmax	LPSPmax
2020-3	Load must be met by supply	Load profile, Climatic data, Prices
2021-1	Export <Grid connection	Revenue scenarios
2022-1	Load must be met by supply	% of demand met by hybrid farm
2022-2	P >Pmin	Pmin, Outage duration, PPA type
2022-3	Load must be met by supply	Grid management strategies

The configuration of the hybrid farm must comply with a reliability constraint in stand-alone situations. The reliability is often calculated by use of the Loss of Power Supply Probability (”LPSP”), Loss of Load Probability (”LLP”) or Deficiency of Power Supply Probability (”DPSP”) indicating the security of supply. All represent the probability that a load will experience a loss of power supply.

A maximum value of the LPSP, LLP or DPSP are used as an inequality constraint by for example Yang et al. (2007), Hiendro et al. (2013) and Kaabeche et al. (2011a) respectively or as an equality constraint where the value must be zero (Tito et al., 2016). The reliability can also be expressed as an unmet load fraction (Perera et al., 2013) or by introducing a required level of autonomy of the system (Kaldellis et al., 2009). Different configurations meeting the required reliability levels can be compared in terms of for example costs or emissions, to choose the optimal configuration, as done by for example Diaf et al. (2007).

Next to calculating different indicators of the reliability of the farm, matching supply to demand at all times for a given supply and demand model can also be used as an equality or inequality constraint, as used by for example González et al. (2015). For grid connected hybrid farms an export limitation can be considered (Golroodbari et al., 2021), due to which the power output of the farm can not exceed a certain value, used as an inequality constraint.

A requirement for the minimum output of the hybrid farm can also be formulated (Stanley and King, 2022). To consider the environmental impact of a hybrid system, the energy pay-back period ("EPBP") can also be used as a constraint by forcing the system configuration to be such that the EPBP is smaller than the lifetime of the project (Kaldellis et al., 2009).

Solving Methods

After setting up the objective function, decision variables and constraints, the problem can be solved resulting in the value of the objective function and the decision variables. Different solving methods and tools are discussed in this section. An overview of the solving methods and tools can be found in Table 3.2. The solving methods will be discussed differentiating between direct solvers to a (numeric) problem and heuristic solvers, translating a problem to an advanced algorithm to efficiently find the optimal solution. Different integrated tools will be discussed at the end of the section.

First, the graphical solving method is discussed, followed by the iterative or manual approach. Solving methods can be analytical, as used by for example Mertens (2022), by use of a graphical construction method (Zhou et al., 2010) or manual, by varying the size of one component of the farm manually until an optimum of the objective function is reached. For example, since batteries represent the highest costs in research by Yang et al. (2008), different battery sizes are considered to choose the lowest cost configuration. Ekren and Ekren (2009) vary the cost of auxiliary energy to compare the optimum configuration and corresponding costs. Barakat et al. (2020) change the grid management strategy to choose the most optimal one.

The graphical construction method limits the number of decision variables to two parameters (Zhou et al., 2010) and the manual approach is dependent on the step size chosen and the number of iterations and is time-intensive. The iterative approach is also computationally intensive and may lead to sub-optimal solutions (Zhou et al., 2010).

Heuristic solving methods using advanced algorithms such as the genetic algorithm ("GA") prove useful in the optimisation of non-linear systems and finding the global optimum. GA imitates the evolution of genetics in nature (Yang et al., 2008). GA is used in many past research, as can be seen in Table 3.2. Strength Pareto Evolutionary Algorithm ("SPEA") is used by Dufo-López et al. which finds the configurations resulting in minimized costs and emissions, in combination with a GA algorithm. Other examples of advanced algorithms as heuristic solving methods are:

- A solving approach called Adaptive Neuro Fuzzy Inference System ("ANFIS") simulating the neural networks, learns from input and output data to adjust decision variables iteratively (Rajkumar et al., 2011).
- The Firefly Algorithm ("FA") based sizing algorithm can be used for sizing decision variables by simulates the flashing behavior of fireflies, where the brightest fireflies attract other fireflies (Abdul Aziz et al., 2017).
- A similar approach is called the Teaching Learning Based optimization ("TLBO"), where a teacher teaches its pupils and the pupils also learn from each other (Najafi Ashtiani et al., 2020).

For multi-objective optimization problems ("MO"), specific heuristic methods can be used. A multi-objective fuzzy method in combination with a Differential Evolution Algorithm ("DEA") (Abedi et al., 2012) can be used to deal with multi-objective, non-linear optimizations. The Steady ϵ-State Evolutionary Algorithm (Perera et al., 2013) or the Multi-Objective Particle Swarm Optimization ("MOPSO") (Barakat et al., 2020) can be used to deal with multi-objective optimizations as well. The multi-objective optimizations can also be solved by solving the objectives separately and creating a total performance index ("TPI"), assigning weights to certain objective functions or performance indicators (Al-Sharafi et al., 2017).

Integrated optimization software and tools are often used in past research. Zhou et al. (2010) discusses a software to optimise and/or simulate hybrid farms and the different optimisation approaches and techniques at that point in time. Another example is the Hybrid Optimisation Model for Electric Renewables ("HOMER") is an open-tool software by NREL (source) aiming to find the optimal size of a stand-alone system based on an objective function using meteorological and load inputs given a set

of constraints, as used by for example Ngan and Tan (2012) . The obtained design can be improved using HYBRID2 with smaller time frames available (Zhou et al., 2010). Optimisation software using the iterative approach are also used in past research, for example in Ma, Yang, Lu, and Peng (2014).

The GA solving method is also available as an integrated optimisation software such as HOGA (Zhou et al., 2010). ARENA 12.0 software can be used to incorporate the weather statistics and predict distributions of weather data and demand (Ekren and Ekren, 2009). GAMS can also be used as an optimization software (Mousa et al., 2010).

Sensitivities

To test the robustness of the optimization results, the inputs can be varied. This way, the most sensitive inputs, where a small derivation leads to an impacting change in the results, can be identified. This section discusses different sensitivity analyses performed in past research. An overview of the different sensitivities performed can be seen in Table 3.3.

In Yang et al. (2007), the hub height of the turbines and the orientation of the module are varied and are considered sensitive using that the output power of a turbine depends on the wind speed cubed, which is determined by the hub height. The impact of changing the module, turbine, controller and battery type is also considered (Abdul Aziz et al., 2017; Diaf et al., 2007; Kaldellis et al., 2009).

Varying the load patterns, the required amount of storage days or a different maximum DPSP are also used to determine the impact on the output of the optimization (Anoune et al., 2020; Kaabeche et al., 2011a; Kaabeche et al., 2011b; Ma, Yang, Lu, and Peng, 2014; Mertens, 2022; Mousa et al., 2010; Najafi Ashtiani et al., 2020; Ould Bilal et al., 2010; Perera et al., 2013; Tito et al., 2016).

Another approach is varying external factors, such as the discount rate, capital cost, lifetime or inflation (Dufo-López et al., 2011; González et al., 2015; Kaabeche et al., 2011b; Najafi Ashtiani et al., 2020), fuel prices (Ngan and Tan, 2012; Perera et al., 2013), or revenue scenarios (Golroodbari et al., 2021; Stanley and King, 2022).

3.1.4. Optimization of Grid-Connected Hybrid Farms - In Depth Analysis

The past research yields a good overview of the different methodologies used to optimally size a hybrid farm. However, Table 3.1 clearly shows the abundant research in SA projects and limited focus on GC projects. Since this research focuses on GC projects, a deep dive into the GC research is performed by analyzing a few relevant papers in detail to further identify the gap to which identifying the potential of a cable pooling location could contribute.

González et al. (2015) conclude that the link between hourly production and market prices is studied in few articles. Therefore, the time-scale of the grid connected hybrid farm is hourly, using hourly weather data. The market prices are not considered per hour, but are divided into three subgroups: peak, off-peak and flat hour tariffs, with corresponding time periods in different seasons. The values are constant within the time periods. The aim is to ”not see the electricity production as steady profits but looking at it as a dynamic cost term, strongly linked to actual market conditions”.

The hybrid farm is designed to minimize the Net Present Value (”NPV”) which takes into account the time-value of money. The yearly cash-flows are discounted by use of a discount rate indicating the value of the money in the year in question and summed to find the NPV. In this research, the costs are considered positive and the income negative.

The optimal NPV is found by varying the area covered by Photo-voltaics (”PV”), directly related to the number of modules, and the number of turbines. The optimization is based on the constraint of matching total annual supply and total annual demand, constructing a net power production (”NPP”) using this annual energy balance. If the systems’ NPP is negative and the system produces too little energy, the residual energy must be purchased from the electricity market. If the NPP is positive, the residual electricity production is sold, contributing to a lower NPV.

The optimization is solved using the GA in Matlab. The decision variables may not be negative and have no active upper limit. Two grid-connected scenarios are considered: a non-Hybrid Renewable Energy System ("HRES") scenario, supplying all demand by purchasing from the electricity market, and a HRES scenario, supplying part of the demand by the hybrid farm and buying the additional part from the electricity market.

The NPV of the HRES scenario is lower than the non-HRES scenario, implying a cost reduction by substituting the traditional farm configuration by a renewable system on the long-term, but requires a large initial investment. The sensitivities of the results are tested by increasing the Capital Expenditure ("CAPEX"), electricity price, inflation rate, efficiencies and interest rate by 10%. The CAPEX of the wind turbines show the largest impact on the results, also considering the large share of wind of 95% in the total system. The electricity price barely influences the results, since the aim is to reduce the consumption from the grid in the first place. The increase in the interest rate results in a decrease in the NPV and is attributed to a higher discounting of the cash flows. The increase in efficiency for wind and consequently PV leads to different farm configurations. A higher PV module efficiency results in less required area to achieve the same installed capacity and a higher turbine efficiency results in less installed WT.

In this research, the costs and benefits of the electricity market are simplified by the use of a peak, off-peak and flat price and do not represent the real market incentives linked to the weather data and thus electricity output of the different resources. Furthermore, this approach sizes both the wind and PV capacity, instead of adding one resource to an existing resource, as could also be the case in a cable pooling scenario. The case is system-wide and solely focuses on meeting demand by supply for the lowest costs. It therefore does not consider a grid or export constraint or the business case of the farm itself. No relevant upper boundaries are considered, such as the maximum space for PV panels.

Barakat et al. (2020) considers a grid connected hybrid farm in Egypt and optimizes its size by varying wind turbines, PV modules and batteries. The objective is to minimize the LCOE and the LPSP and to maximize the renewable energy fraction ("REF"). The emissions for each configuration are considered to choose between the different configurations. The energy balance is used as a constraint requiring the farm to supply the load at all times. In times of energy deficiencies, electricity can be bought from the grid for a constant price. In times of excess supply, the excess electricity can be sold to the grid for a constant feed-in rate.

Different grid purchase and sell management strategies are incorporated to see the effect on the results. The first scenario allows the system to buy and sell from the grid, while the second and third scenario only allow the system to buy from (2^{nd}) and sell to (3^{rd}) the grid. The solving method used is the multi-objective particle swarm optimization algorithm ("MOPSO"), an evolutionary optimization technique using a population of particles to look for optimal solutions at the same time resulting in a set of different optimal solutions. Increasing the renewable energy fraction induces higher costs and higher LPSP values. Not allowing the system to buy from the grid increases the system costs as well, but does result in the lowest emissions.

This article again sizes the total farm at once and does not use any grid export constraints. The constant feed-in rate again do not represent time-dependent incentives of the electricity market on the sizing of different components. The focus is on comparing the three different management scenarios for the load demand in terms of costs, LPSP, REF and consequent emissions.

A similar research is performed by Najafi Ashtiani et al. (2020). This article also focuses on reducing the costs of a system which can extract energy from the grid for a constant price in case the renewable farm does not supply the demand. The optimization is solved using the Teacher Learning-Based Optimization ("TLBO"), a population-based optimization algorithm imitating the behaviour of pupils learning from their teacher and other pupils. The costs will determine if the system remains grid connected or aims to not draw energy from the grid. Due to the low prices for electricity from the grid in Iran, the non-renewable farm design lead to the lowest costs. This project focuses solely on the cost-side and not on the revenue side, even though the hourly market price and weather data might influence the

optimal configuration of the hybrid farm.

Golroodbari et al. (2021) considers a grid connection of an offshore wind farm in the Dutch part of the North Sea and the possible addition of a floating solar farm by effect of cable pooling. The paper tries to find the optimal added solar capacity, given a limiting cable capacity. The combination of the offshore wind and floating solar is validated by considering the correlation of the two resources, by finding a linear fit to the scatter plot. From the correlation analysis, a negatively, yet weak, correlation can be found and the conclusion is therefore that adding solar could increase the usage of the cable and thus the cable capacity factor. Another result is a less variable power output which is also considered favorable.

The research is divided in a technical and economical analysis where the technical part focuses on minimizing the cost of electricity subject to the size of the cable and finds the energy output of the total farm. The economical analysis focuses on the value of this energy output and uses it to calculate NPV as the financial indicator. Important input variables to the optimisation are CAPEX, degradation, capacity of the cable, the energy price and the amount of hours the farm is producing energy.

Historic weather data is used to find the so-called potential energy production of total farm consisting of the wind and solar farm, where the size of the solar farm is varied. The total power output may not be larger than the cable capacity. The annual energy of one panel is defined using a performance ratio, the efficiency, the irradiance on the panel and the area of the panel. The performance ratio deals with the losses due to temperature and the impact of PV panel efficiency and other losses in the system, such as the inverters. The PV output can be curtailed by use of a curtailment factor C_{PV} which is always between 0 and 1. The total output of the system $E_{tot}(h)$ is calculated as shown in equation Equation 3.1 (Golroodbari et al., 2021) by adding the output of the existing wind farm $E_{WF}(h)$ and the output of the solar system $E_{PV}(h)$ which can be curtailed using C_{PV}.

$$E_{tot}(h) = E_{WF}(h) + C_{PV} \cdot E_{PVF}(h) \leq 700 \quad \text{for} \quad h \in [1, 8760] \tag{3.1}$$

The installed solar capacity is increased linearly and used to find the corresponding energy output of the solar farm $E_{PV}(h)$, total farm output $E_{tot}(h)$ and the cable capacity factor. The economical value of these energy outputs is found based on simplified revenue scenarios. The scenarios deal with subsidies, where the first scenario considers no subsidies and the second and third scenario consider SDE+, the subsidy policy before SDE++, and a doubled SDE+ respectively. The power price is divided in to off peak and peak hours and the produced energy is categorised accordingly. The approach is later generalised to find the optimal installed wind and floating solar capacity, given that the two farms share a grid connection.

To conclude, this paper aims to find the optimal floating solar size, based on existing production and a grid connection, and to identify its technical and economical potential. However, the method to find this optimal size is not mentioned explicitly. The optimal size seems to have been found manually by adding solar capacity in steps of 100 MW_p and considering the output for the increased solar capacity. This method could be more efficient when using an optimisation software to find the optimal output given the constraints which combines the technical and economical optimisation instead of treating them separately. The revenue simplification of using averaged peak- and off-peak hours does not take into account the value of the free capacity on the cable for each hour, which might impact the installed capacity. Furthermore, the focus is solely on offshore wind and floating solar and no variations in orientations of the solar panels is considered. There is no constraint mentioned but the export cable, while other factors could impact the optimisation too, such as the size of the space to build the new farm.

Stanley and King (2022) designs a hybrid farm consisting of wind, PV and storage. The hybrid design must be such that the output of the hybrid farm can withstand certain disruptions like power outages. The PV modules are placed between the turbines and therefore a shading model is developed. The focus is on the physical design of the model, using an x-y grid with row and column spacing, grid shear and rotation and the grid center location in (x,y) coordinates (Stanley and King, 2022). The shading model aids the design process.

The optimization problem is solved using GA. The hybrid farm is optimized for the lowest LCOE and for maximizing profits, while supplying the minimum power requirement. The objective function chosen significantly impacts the optimal configuration. The robustness was tested by removing the varying the power requirement, varying the outage duration, varying the PPA scenario, constant, daytime peak or nighttime peak PPA. The research does not implement the value of electricity produced at an hourly level, which may again cause the farm componenet sizing to be different. It also designs the full farm at once, only regarding the inter-resource spacing, but no other constraints for the design, or constraints for the export of electricity.

3.2. Possible Contributions to Research

When considering the past research discussed above, most research sizes the total hybrid farm, instead of optimally sizing a resource to be added to an existing resource. Furthermore, the main focus so far has been on SA applications where reliability of the system is the most important indicator. So, limited research has been performed with an export limitation of the hybrid farm.

Additionally, the type of hybrid farm was always predetermined, the share of each component could only be varied. Only Golroodbari et al. (2021) add a resource to an existing one and use an export constraint on the grid cable, but the added resource was predetermined. An addition could be to allow the optimization to consider different resource additions, like wind and solar, in multiple orientations, to fully exploit the current Dutch context for cable pooling with these resources.

Furthermore, the impact of the electricity prices on the configuration of the farm have not been explored yet. This also lacks in the article by Golroodbari et al. The free space on the cable for each hour can have a different value, based on the market prices at that time. Since the renewable additions are subject to the weather patterns, the sizing of different technologies depends on the value of the free space of the grid connection. The market prices will have an influence on the outcome of the optimization. Using current Dutch revenue streams, such as SDE++ and Dutch PPA values, is an addition as well.

Lastly, on the long-term the increased penetration of renewable resources might lead to decreased value of renewable resources in the future. Long-term market outlooks should be used to consider these developments and use them in the optimization.

Therefore, the aim of this research, identifying and optimizing the potential of a cable pooling location, contributes to research if:

- Hourly free cable capacity is considered with corresponding hourly weather values and spot market prices;
- Multiple resources are considered in the optimization;
- Long-term market outlooks are used to take into account the long-term value of the different resources;
- Dutch revenue models are incorporated, such as the SDE++ subsidy and Dutch PPA values

3.3. Decision problem

This section discusses the general decision problem. As mentioned in chapter 2, the addition of a generating resource to an existing resource with a grid connection is considered cable pooling, which could lead to an improved usage of the grid connection.

With a cable pooling location, in this research a renewable generation project with a secured grid connection is meant, called the existing renewable resource. The project can be already built or still in development, but the assumption is that there is a grid connection capacity secured based on solely the existing renewable resource. Since the existing renewable resource does not use the grid capacity to the full 100% at all times, there is free capacity at the cable. This free capacity forms the input of the decision problem.

The assumption is made that the existing and new renewable resource do not necessarily belong to the same owner. To create a tool that can be put to practice in many cases, the approach is used that the residual capacity on the cable after export of the existing resource is the only exporting capacity available to the potential new farm. Another assumption is that the new renewable resource will be built on a separate piece of land. The available land area to develop the new resource on is used as input too.

The existing renewable resource can be two types of renewable generation: solar or wind. The new renewable resource is either a wind farm or a solar farm. The combination of two generating resources leads a hybrid farm. A battery can be added to the hybrid farm, leading to a hybrid farm & battery. Since a battery changes the operations of the system, the battery decision problem will be discussed separately.

Conventionally, solar panels are orientated to the south to maximize power output leading to peak production at noon (Sheffield Solar, 2023). The focus for cable pooling has been mostly on combining solar energy orientated to the south and wind energy. The large growth of solar production in the Netherlands due to large-scale solar development and rooftop solar has led to large production peaks and low prices at noon (Jongsma, van Cappellen, et al., 2021). Due to the low and sometimes even negative prices during the solar peak, interest in solar panels orientated to the east and west is growing (Sheffield Solar, 2023). Solar panels orientated to the east and west generate electricity spread out throughout the day, with peaks coinciding more with the demand pattern (Sheffield Solar, 2023). The possible new solar farms will therefore be considered with two orientations: south and east-west.

Identifying and optimizing this cable pooling potential can be done using long-term economics and an economic indicator to show whether or not a cable pooling location of interest meets a basic requirement, taking into account both technical and financial parameters. The hybrid farm decision problem aims at finding the value of installed capacity leading to an optimized economic indicator for all possible additions, based on the residual cable capacity, land size and economic parameters.

To solve the decision problem on whether or not to further investigate the cable pooling location, the economic indicator Net Present Value ("NPV") is used. The NPV is a method to take into account the time value of money by using the discount rate. The discount rate r shows how much more money is worth to an investor now, instead of in the future, considering the option to make investments elsewhere and expecting some annual return based on this discount rate.

The NPV of a project can be found by discounting all yearly positive incoming and negative outgoing cash flows to the present value and summing them for the full lifetime of the project. If the NPV is positive, the project is profitable enough based on the desired discount rate and generates a higher return than the investment elsewhere. If the NPV is negative, it is not interesting to invest in, since more return can be earned with other investments. The NPV is calculated using Equation 3.2

$$NPV = \sum_{t=0}^{T} \frac{C_t}{(1+r)^t} \tag{3.2}$$

Where C_t are the net cash flows in year t and r is the discount rate. The net cash flows of year t can be found using the revenues of selling energy and the costs of installing and operating the installed capacity.

Each type of new renewable resource has its own typical generation profile, each with their own correlation to the existing renewable resource and thus the residual cable capacity and revenues that can be earned. Next to that, each new resource has different capital expenditures (CAPEX) and operational expenditures (OPEX) per installed capacity and revenues by selling electricity. Therefore, each option for the new resource will yield a different optimal NPV and installed capacity.

4

Methodology

This chapter deals with the modelling approach for the decision problem and shows the calculation methodology for different components used in the problem definition and other system components with corresponding losses or constraints.

The first step is to create an approach solely focusing on the hybrid farm, considering only wind and solar as possible options. The next step is to add a battery to the hybrid farm. Section section 4.1 and section 4.2 discuss the general optimization methodology, including objective, constraints and decision variables, and introduce the different parameters that need to be defined.

In section 4.3, section 4.4 and section 4.5 different parameter calculation approaches are discussed. Performance indicators and their calculation methods will be discussed in section 4.6, followed by the most important assumptions and simplifications in section 4.7.

4.1. Hybrid Farm Optimization Problem Formulation

This section uses the description of the decision problem to formulate the optimization. First, the sets will be introduced which will be used to iterate over. Next, the parameters are defined which form the input for the optimization. Some parameters will be discussed in separate sections, section 4.3, section 4.4 and section 4.5. The parameters are followed by the decision variables which will be sized to find the optimal solution to the objective function, which is discussed after the variables. The objective function is subject to constraints, which are mentioned afterwards.

Indices

Indices are used to describe parameters or decision variables of the optimization problem that take different values for these indices. In this optimization problem, three indices can be defined.

The optimization is chosen to take data steps of one hour into account. The first index i deals with the set containing all hours in one year.

$$i \in I = \{1, \ldots, 8760\}$$

The second index j deals with the different additions that can be made to an existing farm. Based on the regulatory and legal framework, solar and wind are chosen as generation types. As discussed before, due to the increasing interest in east-west oriented solar farms, the possible solar additions are either oriented to the south ("S") or to the east west ("EW"), leading to three possible additions j in total.

$$j \in \{\text{Wind, Solar EW, Solar S}\}$$

To account for the long-term trends, the business case will be considered over the full lifetime of the project. This leads to the third index: years t which run up to the lifetime of the project, which can be different per resource j, expressed as T_j.

$$t \in T = \{1, \ldots, T_j\}$$

Parameters

The parameters are the input for the optimization, either constant or depending on an index.

To account for the land area available for the new resource, the first input parameter is the amount of land available in m^2. It is the same for all three options will be used to determine the maximum size of the new renewable resource:

$$\text{land}$$

To find the maximum size of the new renewable resource, a power density is used. It is the installed power density, so based on peak or rated power, in W/m^2 for all three options j:

$$\text{P}_{\text{dens},j}$$

The land and $\text{P}_{\text{dens},j}$ together determine the upper boundary of the installed capacity for that specific site. The calculation method of the power density for each technology is discussed in section 4.3.

The output of wind and solar farms depend on the hourly weather data. Furthermore, the systems have fixed losses, such as electrical losses, and time dependent losses, which also depend on the hourly weather pattern. An example of hourly weather dependent losses is the temperature dependent efficiency of modules. The overall system Weather and Losses Factor ("WLF") can be calculated for each renewable resource j at time i which accounts for all reductions from the installed capacity for that hour i and is used to find the maximum produced energy at that hour i for technology j:

$$\text{WLF}_{i,j} \quad \forall i \in I$$

The calculation method of the WLF will be discussed separately in section 4.4.

The assumption is made that only the residual space on the cable, after export of the existing farm, can be used to export electricity on to the grid and thus earn money. Therefore, the energy output of the existing farm for each hour i determines the cable capacity, which is then used as an upper boundary for the exported energy of the new farm:

$$\text{Cap}_{\text{cable},i} \quad \forall i \in I$$

The size of the grid connection $\text{Cap}_{\text{cable,max}}$ and the hourly power output of the existing resource $\text{P}_{\text{out,existing},i}$ thus determine the residual capacity on the cable $\text{Cap}_{\text{cable},i}$ for each hour i, as shown in equation Equation 4.1.

$$\text{Cap}_{\text{cable},i} = \text{Cap}_{\text{cable,max}} - \text{E}_{\text{out,existing},i} \quad \forall i \in I \tag{4.1}$$

The grid connection size is often expressed in MVA, which is translated to MW using the power factor. For simplicity, a power factor of 1 is used in this report. The output power of the existing farm can either be based on actual production data or can be constructed using farm specifications.

To determine the revenues made by the new renewable resource, the price to which the energy output can be sold for all hours in a year i in euro (€) per MWh is used. This price corresponds to the EPEX spot market price for that hour i:

$$\text{price}_i \quad \forall i \in I$$

Three revenue scenarios are used. One scenario uses the yearly addition of the SDE++ to make up for the unprofitable part. The second scenario uses a fixed price for each hour, determined by the PPA. The third scenario is market exposed ("ME"), solely dependent on the spot market prices. Each create a separate objective function.

To account for the inflation, a yearly inflation factor will be used. The inflation in year t is accounted for using the yearly inflation rate k. The inflation is considered from a base year in which the final investment decision ("FID") is taken t_{FID}. The farm is operational from the commercial operation date ("COD") in year t_{COD}. The difference between those years is called $\delta t = t_{COD} - t_{FID}$. After COD, the counting of t until lifetime T_j runs.

$$\text{inf}_t = (1+k)^{\delta t}(1+k)^t \quad \forall t \in T_j \tag{4.2}$$

To account for long-term economics, the discount rate is considered. The discount rate r determines the yearly discounting factor disc_t. The discounting factor determines the present value of a future cash flow.

$$\text{disc}_t = \frac{1}{(1+r)^t} \quad \forall t \in T_j \tag{4.3}$$

The output of the new and existing farm are expected to degrade each year t. For the existing farm, degradation results in less output and thus potentially more space on the cable available for the new farm. For the new farm, degradation results in less output and thus less revenues.

The yearly degradation impacts the energy that can be produced and exported per hour. To account for degradation while limiting the computational efforts, a yearly degradation factor for the existing farm deg_{E_t} and the new farm $deg_{j,t}$ is introduced. These factors are used to approximate the impact of the degradation on the income for one full year instead of considering the impact per hour.

$$\text{deg}_{j,t} \quad \forall t \in T_j \quad \text{deg}_{\text{E}_t} \quad \forall t \in T_j$$

First, the method to approximate the degradation of the new farm using the degradation factor $\text{deg}_{j,t}$ is introduced. Using t as the year of operation and T_j the lifetime of the modules or turbines, the reduction in the revenues in year t due to degradation can be approximated by the degradation factor d_t depending on the degradation in year t for each technology j δ_j.

$$\text{deg}_{j,t} = (1-\delta_j)^t \quad \forall t \in T_j \tag{4.4}$$

Secondly, the method to approximate the degradation of the existing farm using the degradation factor deg_{E_t} is introduced. Using t as the year of operation of the new farm, age as the age of the existing farm, and T_E the lifetime of the existing farm, the degradation factor deg_{E_t}, depending on the degradation in year t δ_{E}, can be found.

$$\text{deg}_{\text{E}_t} = (1-\delta_{\text{E}})^{\text{age}+t} \quad t \leq (T_{\text{E}} - \text{age}) \tag{4.5}$$

This factor can be used to approximate the reduction in the output of the existing farm. This reduction is assumed to create additional space on the cable for export of energy produced by the new farm. The degradation factor of the existing farm deg_{E_t} is used to approximate the impact of this additional space on yearly revenues, by dividing the yearly revenues by this factor. This assumes that the existing farm indeed allows the new farm to use the additional free space on the cable.

Each technology has a technical availability av_j. At times of for example scheduled or unscheduled maintenance, the resource is not available. It is used in this approach as a percentage to correct the yearly revenues.

$$\text{av}_\text{j} \tag{4.6}$$

To account for the long-term development of the EPEX spot market, a long-term outlook (”LTMO”) is used. The LTMO is used to determine the long-term projections of the average price on the EPEX spot market, LT, and the expected value of the electricity produced of different technologies j, $\text{LT}_{\text{f},j,t}$. The latter accounts for different production patterns of solar and wind energy and the expected value this pattern has, given the expected increased penetration of these renewable resources.

$$\text{LT}_t \quad \forall t \in T_j \quad \text{LT}_{\text{f},j,t} \quad \forall t \in T_j$$

The costs of building the new renewable resource are represented by Capital Expenditures (“CAPEX”), the total investment costs per installed MW of new renewable resource j. The total operations and maintenance costs (”OPEX”) per installed MW of new renewable resource j for each year t:

$$\text{CAPEX}_j \quad \text{OPEX}_{j,t} \quad \forall t \in T_j \tag{4.7}$$

The costs for a shared grid connection will differ per project and system operator. Since the new resource only uses the residual space on the grid connection and to create a generalized approach, all costs related to the grid connection are per default zero. Case-specific grid connection fees can be added manually.

Decision variables

The decision variables are varied to obtain the optimal objective function and represent decisions made during planning or operation. In this problem formulation, three decision variables are used.

The first decision variable is the installed capacity, related to the costs of building and maintaining the system. The installed capacity will be found for each renewable resource j.

$$\mathsf{P}_{\mathsf{installed},j} \tag{4.8}$$

The other two decision variables are the sold and curtailed energy throughout that year, which depend on the installed capacity and the hourly production patterns of the existing and new resource. The amount of energy sold per hour i for each renewable resource j depends on the residual space on the cable and the produced energy and determines the revenues.

$$\mathsf{E}_{\mathsf{sold},i,j} \quad \forall i \in I \tag{4.9}$$

Since the cable forms a constraint, the output of the new renewable resource needs to be curtailed in some hours i for each renewable resource j.

$$\mathsf{E}_{\mathsf{curtailed},i,j} \quad \forall i \in I \tag{4.10}$$

Objective

The objective function attempts to maximize the NPV, considering the discounted revenues and costs over the lifetime of the project. As briefly introduced in section 3.3, the inputs are the net cash flows for each year t, $C_{j,t}$, and the required discount rate r.

The NPV is maximized for each of the new renewable resources j and the results can be compared manually to make a decision on the best addition to the existing farm. This might also depend on other factors, such as local policy or stakeholders, resulting in one technology to be favored over the other. Therefore, the approach is used to show the optimal NPV for all three options j, leaving the decision on the best addition to the specific situation.

$$max\left(\mathsf{NPV}(j) = \sum_{t=0}^{T} \frac{C_{j,t}}{(1+r)^t}\right) \tag{4.11}$$

Year $t = 0$ is considered as the year before the start of the operation of the added resource. The initial investment costs CAPEX represent the net cash flow in year 0 $C_{j,0} = -\mathsf{CAPEX}_j \cdot \mathsf{P}_{\mathsf{installed},j}$. The net cash flows for year $t \in T_j$, $C_{j,t}$, consist of revenues and costs during operation. Three different revenue models have been introduced, each resulting in different formulations of the yearly net cash flows $C_{j,t}$.

All three revenue models are corrected for the long-term developments using the inflation inf_t, long-term market factor LT_t and technology specific long-term value factor $\mathsf{LT}_{j,t}$. Furthermore, the degradation $\mathsf{deg}_{j,t}$ of the new farm and the degradation of the existing farm $\mathsf{deg}_{\mathsf{E},j,t}$ are used to correct for the energy that can be exported.

For all three models, the hourly revenues are summed for all the hours in the year j, after which the costs of operating the system $\mathsf{OPEX}_{j,t} \cdot \mathsf{P}_{\mathsf{installed},j}$ are subtracted from this yearly revenue to arrive at the net cash flow for that year. The operational costs differ per technology and are depicted here as to be subject to inflation as well. Not all OPEX are in fact subject to inflation, which will be clarified in chapter 5. The different formulations are discussed per revenue scenario.

1. **SDE++**
   The working principle of the SDE++ has been discussed in subsection 2.4.1. The determination of the price of the subsidy is summarized Equation 4.12.

$$\mathsf{subsidy}_{j,t} = \begin{cases} 0 & \text{if } MV_{j,t} > BB_j \\ BB_j - CB_{j,t} = BB_j - MV_{j,t} & \text{if } MV_{j,t} < BB_j \\ BB_j - CB_{j,t} = BB_j - BEB_j & \text{if } MV_{j,t} < BEB_j \end{cases} \quad \forall t \in T_j \tag{4.12}$$

In Equation 4.13, $\text{subsidy}_{j,t}$ represents the height of the total subsidy awarded in year t, using the technology specific FLH_j and the installed capacity $\text{P}_{\text{installed},j}$.

$$\text{subsidy}_{j,t} = \text{SDE}_{j,t} \cdot FLH \cdot \text{P}_{\text{installed}} \tag{4.13}$$

The subsidy is a yearly addition to the revenues earned on the spot market. The yearly cash flows the SDE++ scenario is shown in Equation 4.14.

$$\begin{aligned} C_{\text{SDE},j,t} = &\text{disc}_t \cdot \text{inf}_t \cdot \Big(\text{subsidy}_{j,t} + \text{av}_\text{j} \cdot \text{LT}_t \cdot \text{LT}_{\text{f},j,t} \cdot \frac{1}{\text{deg}_{\text{E},t}} \cdot \text{deg}_{j,t} \cdot \sum_{i=1}^{8760} (\text{E}_{\text{sold},i,j} \cdot \text{price}_i) \\ &- \text{OPEX}_{j,t} \cdot \text{P}_{\text{installed},j}\Big) \quad \forall t \in T_j \end{aligned} \tag{4.14}$$

The subsidy usually has a duration shorter than the lifetime of the project. After the subsidy ends, the revenues earned solely depend on the spot market prices and can be considered ME.

2. **PPA**
   The PPA considers a fixed PPA price received by the generating resource PPA_j. The generation receives this PPA price for each generated unit of energy during the duration of the PPA. During the period that the PPA is active, the yearly revenues do not need to be corrected for the long-term market factor LT_t and the technology specific value factor $\text{LT}_{\text{f},j,t}$ given the constant price used. The PPA cash flows are shown in Equation 4.15.

$$\begin{aligned} C_{\text{PPA},j,t} = &\text{disc}_t \cdot \text{inf}_t \cdot \Bigg(\text{av}_\text{j} \cdot \frac{1}{\text{deg}_{\text{E},t}} \cdot \text{deg}_{j,t} \cdot \sum_{i=1}^{8760} (\text{E}_{\text{sold},i,j} \cdot \text{PPA}_j) \\ &- \text{OPEX}_{j,t} \cdot \text{P}_{\text{installed},j}\Bigg) \quad \forall t \in T_j \end{aligned} \tag{4.15}$$

   The long-term price agreement usually has a duration shorter than the lifetime of the project. After the PPA ends, the revenues earned solely depend on the spot market prices and can be considered ME.

3. **ME**
   This revenue scenario solely depends on the spot market price. As mentioned before, both SDE++ and PPA become ME after the duration of the subsidy or agreement respectively. The ME cash flows are shown in Equation 4.15.

$$\begin{aligned} C_{\text{ME},j,t} = &\text{disc}_t \cdot \text{inf}_t \cdot \text{av}_\text{j} \cdot \Bigg(\text{LT}_t \cdot \text{LT}_{\text{f},j,t} \cdot \frac{1}{\text{deg}_{E,t}} \cdot \text{deg}_{j,t} \cdot \sum_{i=1}^{8760} (\text{E}_{\text{sold},i,j} \cdot \text{price}_i) \\ &- \text{OPEX}_{j,t} \cdot \text{P}_{\text{installed},j}\Bigg) \quad \forall t \in T_j \end{aligned} \tag{4.16}$$

The cash-flows thus depend on decision variables $\text{E}_{\text{sold},i,j}$ for the revenues and $\text{P}_{\text{installed},j}$ for the initial and operating costs. The sold energy $\text{E}_{\text{sold},i,j}$ is matched with the installed power $\text{P}_{\text{installed},j}$ by use of the weather and losses factor $\text{WLF}_{i,j}$ and curtailed energy $\text{E}_{\text{curtailed},i,j}$.

Constraints

The objective function tries to maximize the NPV by varying $\text{P}_{\text{installed},j}$ and interlinked $\text{E}_{\text{sold},i,j}$ and $\text{E}_{\text{curtailed},i,j}$, which are bounded to constraints. Since there is an export limitation, the energy sold $\text{E}_{\text{sold},i,j}$ must always be lower than the cable capacity $\text{Cap}_{\text{cable},i}$ for each hour i. The residual cable capacity depends on the energy produced by the existing farm.

$$\text{E}_{\text{sold},i,j} \leq \text{Cap}_{\text{cable},i} \quad \forall i \in I \tag{4.17}$$

The Weather and Losses Factor $\text{WLF}_{i,j}$ accounts for all reductions in energy due to hourly weather data and losses in the system and links the installed capacity to the produced energy. The power values are assumed to be directly proportional to energy with a time step used of Δt = 1h. The sold and curtailed energy added up must therefore be equal to the installed capacity multiplied by the WLF for

each technology j for all hours in the year i.

The optimization will try to maximize the sold energy as much as possible, to maximize the revenues and thus NPV. So if there is residual space on the cable to export the produced energy, it will be assigned to $E_{sold,i,j}$. If there is no or too little space available on the cable to export the produced energy, it will be assigned partly or fully to $E_{curtailed,i,j}$.

$$WLF_{i,j} \cdot P_{installed,j} == E_{sold,i,j} + E_{curtailed,i,j} \quad \forall i \in I \tag{4.18}$$

To stay within the land boundaries, the installed capacity must be smaller than some upper boundary defined by the land size multiplied by the installed power density.

$$P_{installed,j} \leq land \cdot P_{dens,j} \tag{4.19}$$

All decision variables must be larger than zero and are real values.

$$P_{installed,j}, E_{sold,i,j}, E_{curtailed,i,j} \geq 0 \qquad \forall i, j \in \mathbb{R} \tag{4.20}$$

Hybrid Farm Optimization Overview

The output of the objective function is the NPV for each new renewable resource j, regarding the discount rate r. The objective function and constraints are all linear, so the optimization problem is a linear problem ("LP") and can be solved using linear solvers. The problem has been translated into a code in Python, using the optimization software Pyomo and open source solver Gurobi. A simplified overview of the system can be found in Figure 4.1 and Figure 4.2.

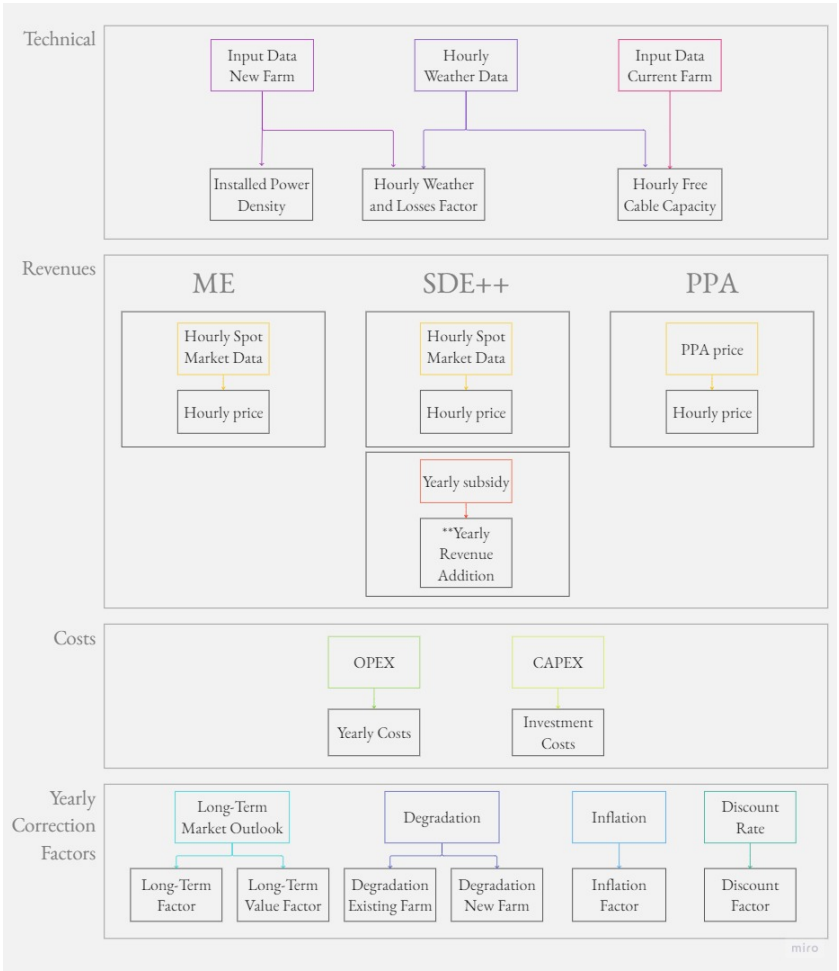

Figure 4.1: Cable Pooling Hybrid Farm Optimization Inputs Overview showing the technical inputs, revenue and costs and yearly correction factors. ** Only in case of the SDE++ revenue scenario, the yearly revenue requires a yearly addition.

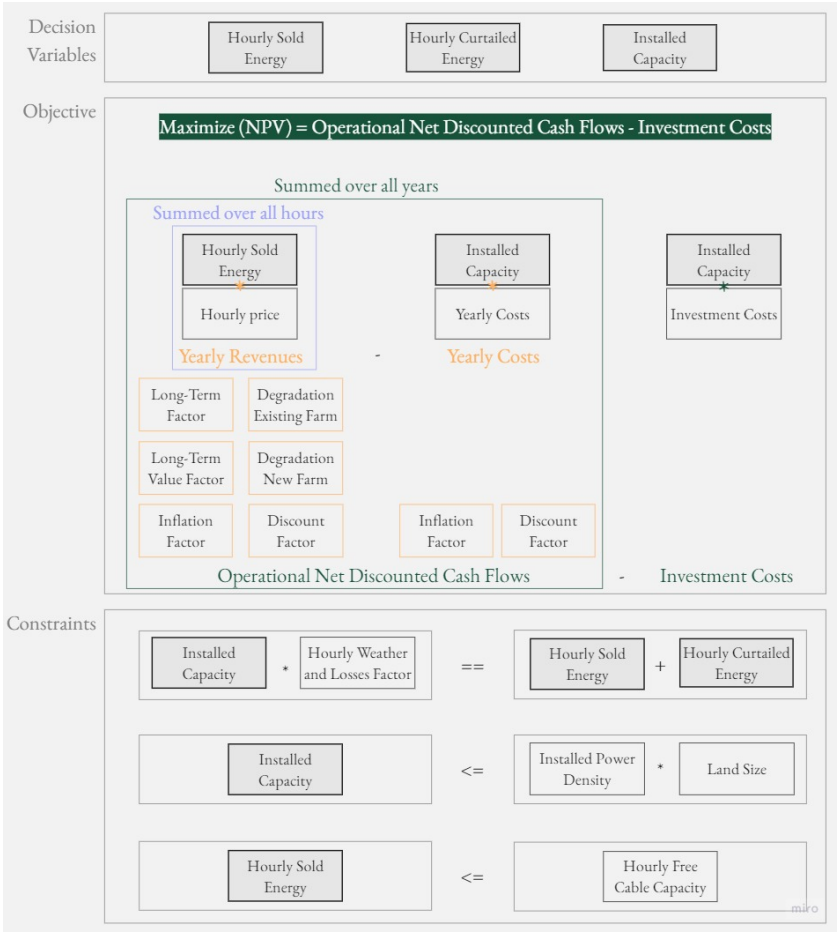

Figure 4.2: Cable Pooling Hybrid Farm Optimization Overview showing the decision variables, the general objective and constraints. It shows how the inputs are used.

4.2. Hybrid Farm with Battery Optimization Problem Formulation

This section will describe the expansion of the hybrid farm with a battery. First, the main characteristics of the chosen battery configuration are discussed, followed by the modelling approach and assumptions.

As mentioned in chapter 2, the battery revenue stream considered in this research will be shifting the energy exported to the grid. This is effectively the same as trading on the spot market, which is the ME revenue model for the hybrid farm.

A large cost contribution in a battery system in the Netherlands are the grid costs, since the installations are considered large-scale consumers and are charged accordingly. To limit the costs of a battery, the battery is considered behind-the-meter (BTM) and is only allowed to charge from the energy generated by the added generating unit. Therefore, the costs of charging are assumed to be zero.

The possible expansion of the cable pooling definition in the electricity law, allowing more than two resources, including conversion-installations, to share one grid connection, expands the connecting possibilities for a battery in a cable pooling scenario, rather than just a hybrid farm with a battery added BTM to the new resource. These other possibilities are not considered in this research yet.

A subsidy will be introduced for a battery added to a solar farm and is awarded per kWh of shifted energy. For a battery added to a wind farm, so far, no subsidies are planned to be introduced. Therefore, the impact of the presence of on-site storage on the cost-benefit framework will only be examined for a battery added to solar farms. Since the timeline and height of the possible subsidies are still unclear

and the modelling of other revenue streams adds difficulty, a worst-case scenario is considered only focusing on the ME generation revenue model, with the addition of the battery.

New parameters, decision variables and constraints are introduced to add the battery to the hybrid farm. This leads to a new objective function as well. This section discusses the additional parameters, decision variables and constraints.

Parameters

A battery is characterized by its power and energy, which can be translated by the C-rate. The C-rate denotes the ratio between the power and energy of a battery.

$$\text{C-Rate} = \frac{\text{P}_{\text{bat}}}{\text{E}_{\text{bat}}} \tag{4.21}$$

It effectively represents the speed at which the battery can charge and the depth to which the battery can be charged, and can therefore be explained as the inverse of the time required to fill up the battery completely. Most currently developed batteries in the Netherlands contain one, two or at most four hours of depth (van Cappellen et al., 2023). The C-rate and P_{bat} are input parameters, automatically leading to E_{bat}.

Charging and discharging the battery is subject to an efficiency eff, which is assumed to be the same for charging and discharging, based on the square root of the round-trip efficiency ("RTE").

$$\text{eff} \tag{4.22}$$

Installing the battery results in the CAPEX of the battery, CAPEX_b and the yearly operation and maintenance, OPEX_b, throughout the lifetime of the battery T_{bat}. Both costs are often expressed as costs per unit energy.

$$\text{CAPEX}_b \quad \text{OPEX}_b \quad \forall t \in T_{\text{bat}} \tag{4.23}$$

Furthermore, the battery degrades with each cycle, which can also be presented as a yearly degradation factor $\delta_{\text{bat},t}$. The impact of the degradation of the battery on the revenues earned by the battery is again approximated by a yearly degradation factor $\text{deg}_{\text{bat},t}$ and can be calculated using the approach in Equation 4.4.

$$\text{deg}_{\text{bat},t} \quad \forall t \in T_{\text{bat}} \tag{4.24}$$

Decision Variables

The decision variables are expanded with three variables. The first variable deals with the state of charge. Batteries degrade fast and often have charge and discharge limitations to prevent accelerated degradation. The state of charge ("SoC") of a battery can be used to express these limits. A minimum and maximum SoC are enforced, expressed by SoC_{min} and SoC_{max} respectively.

$$\text{SoC}_{\text{min}} \leq \text{SoC}_i \leq \text{SoC}_{\text{max}} \quad \forall i \in I \tag{4.25}$$

The other two variables show the hourly charge and discharge behaviour of the battery. The energy charged by the battery is represented by $\text{E}_{\text{ch},i}$ and the energy discharged by the battery by $\text{E}_{\text{dch},i}$. The battery can charge with at most the power rating of the battery P_{bat}.

$$0 \leq \text{E}_{\text{ch},i}, \text{E}_{\text{dch},i} \leq \text{P}_{\text{bat}} \quad \forall i \in I \tag{4.26}$$

Objective Function

The objective function is similar to the ME objective function for the hybrid farm. The battery sells energy on an hourly bases $\text{E}_{\text{dch},i}$. Effectively, there is extra energy that can be sold each hour. The new net cash flow expression is shown in Equation 4.27.

$$\begin{aligned} C_{\text{ME},t} =& \text{disc}_t \cdot \text{inf}_t \cdot \Bigg(\text{LT}_t \cdot \frac{1}{\text{deg}_{E,t}} \cdot \left(\text{deg}_t \cdot \text{av}_j \cdot \left(\sum_{i=1}^{8760} \text{E}_{\text{sold},i} \cdot \text{EPEX}_i \right) + \text{deg}_{\text{bat},t} \cdot \left(\sum_{i=1}^{8760} \text{E}_{\text{dch},i} \cdot \text{price}_i \right) \right) \\ & - \left(\text{OPEX}_t \cdot \text{P}_{\text{installed}} + \text{OPEX}_{\text{bat},t} \cdot \text{E}_{\text{bat}} \right) \Bigg) \quad \forall t \in T_j \end{aligned} \tag{4.27}$$

In the objective function used in the optimization, the yearly long-term value factor $LT_{f,t}$ for solar energy is not used. The revenues earned by the solar farm and battery for the optimal solution are stored separately. The solar revenues are later corrected for the long-term value factor $LT_{f,t}$ for solar energy, leading to a corrected NPV value. Otherwise, the selling energy via the battery is preferred over selling directly from the solar farm, which would result in increased degradation of the battery.

Constraints

The discharged energy $E_{dch,i}$ and energy directly sold from the solar farm $E_{sold,i}$ can not exceed the free cable capacity at that hour i, leading to the new export constraint.

$$E_{sold,i} + E_{dch,i} \leq Cap_{cable,i} \quad \forall i \in I \tag{4.28}$$

Furthermore, a new constraint is introduced to account for the SoC bounds.

$$SoC_i = SoC_{i-1} + eff \cdot E_{ch,i} - \frac{1}{eff} \cdot E_{dch,i} \quad \forall i \in I \tag{4.29}$$

The energy generated by the system can now either be sold directly, charged or curtailed, leading to a new energy balance constraint.

$$P_{installed} \cdot WLF_i = E_{sold,i} + E_{ch,i} + E_{curtailed,i} \quad \forall i \in I \tag{4.30}$$

Hybrid Farm with Battery Optimization Overview

The objective function and constraints are again all linear, so the optimization problem is a linear problem ("LP") too and can also be solved using linear solvers. The problem has been translated into a code in Python, using the optimization software Pyomo and open source solver Gurobi.

It must be noted that the battery trading in this optimization is based on market data which is fully available for the optimization. The model thus has perfect foresight, which causes the trading behaviour and thus the value of the objective function to be different different than situations where this data is not fully available. The trading mechanisms of batteries are often assisted by a forecasting algorithm, predicting the behaviour of the market prices and steering the battery on when to discharge and charge.

A simplified overview of the system can be found in Figure 4.3 and Figure 4.4.

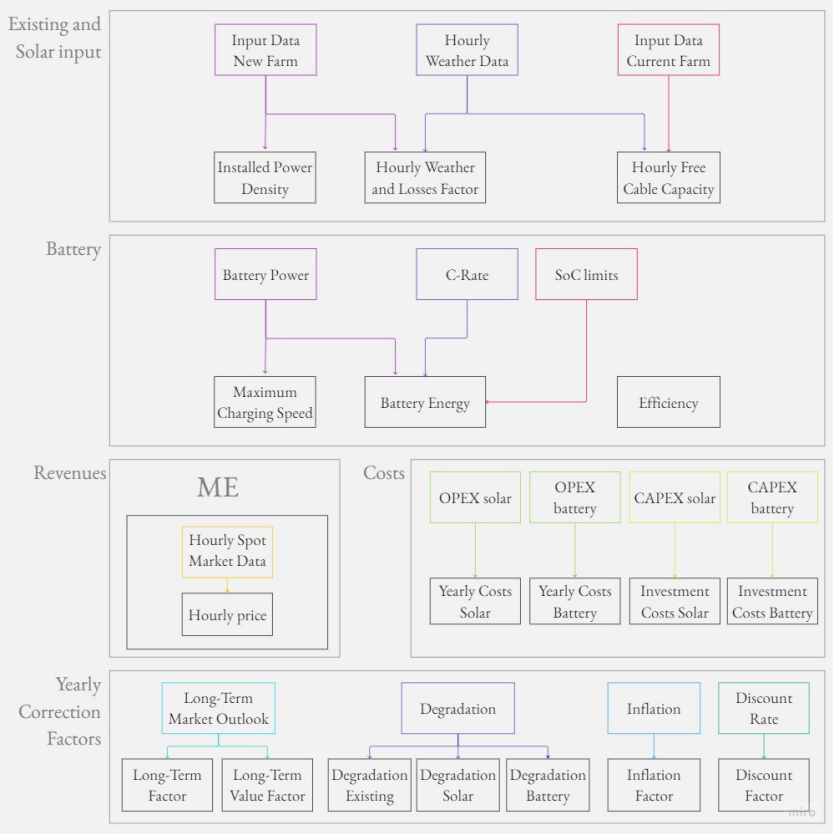

Figure 4.3: Cable Pooling Hybrid Farm including Battery Optimization Inputs Overview showing the technical inputs, revenue and costs and yearly correction factors.

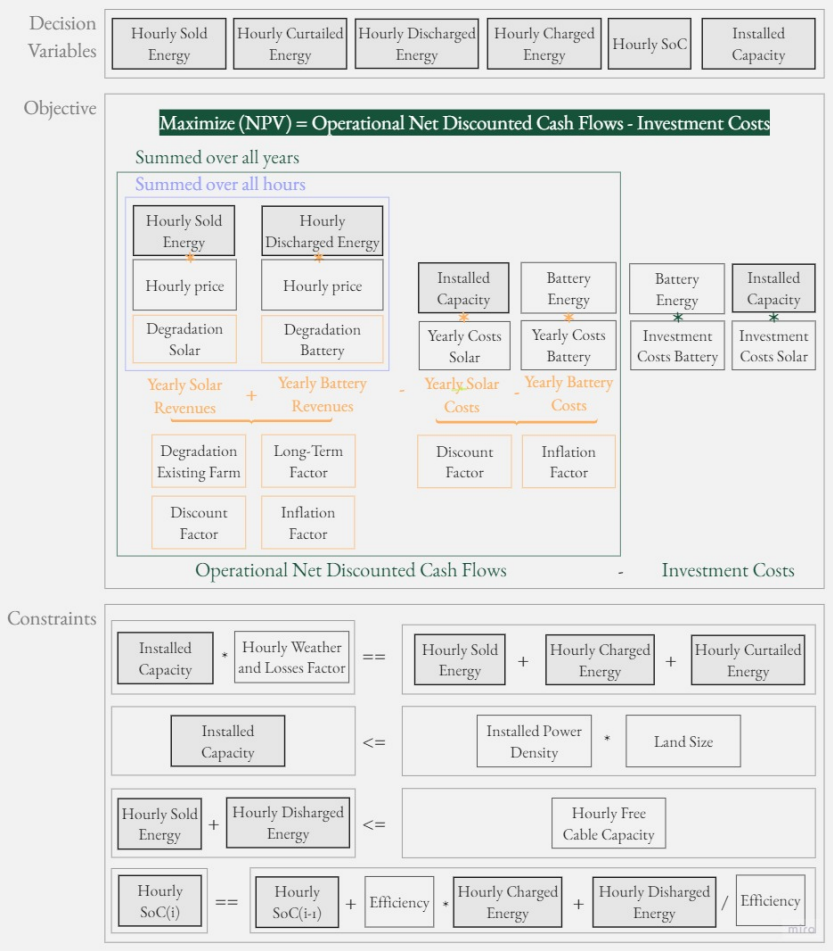

Figure 4.4: Cable Pooling Hybrid Farm including Battery Optimization Overview showing the decision variables, the general objective and constraints. It shows how the inputs are used.

4.3. Installed Power Density

The installed power densities are used to consider the boundaries of the available land. First, the solar installed power density calculations and assumptions are discussed, followed by the wind installed power density approach.

Solar

For the solar panels, the installed power density can be calculated a geometric approach. The installed power density can be approximated using the configuration of a table, to which multiple modules are attached in series. The configuration of the table depends on the voltage requirements of the inverter used. The maximum power P_{MPP} of a table per a certain area, corresponding to a certain width and length, indicates the power density.

Tables can stack multiple modules in either portrait or landscape mode. In this report, a portrait mode table is considered. Figure 4.5 and Figure 4.6 show and example of the top and side view of a south orientated geometry respectively. In this figure, M modules are placed next to each other in vertical direction, determined by the table height, and N modules next to each other in horizontal direction, determined by the voltage requirements of the inverter.

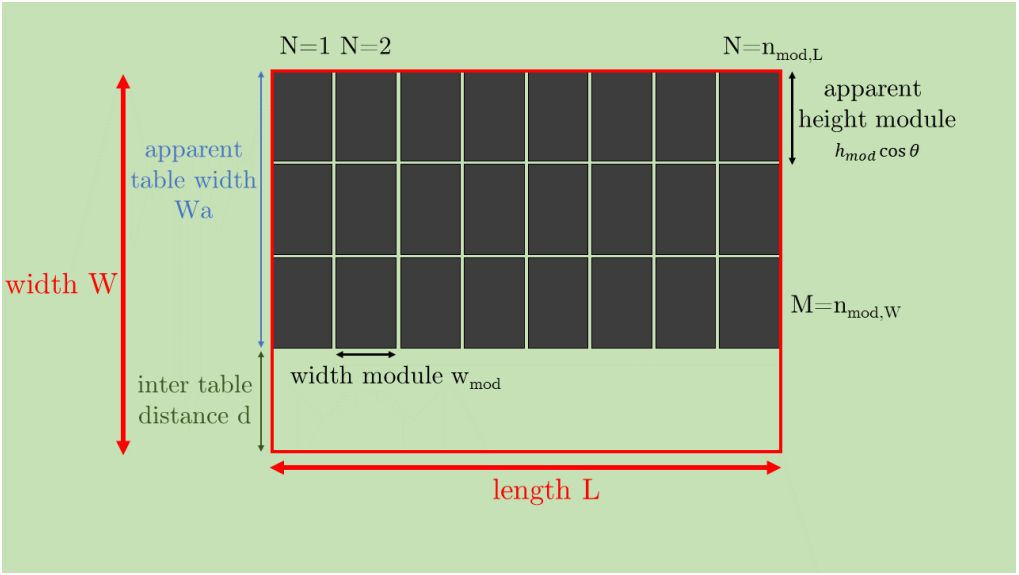

Figure 4.5: Simplified top view of south oriented table and corresponding geometries

The width and length determining the power density are determined by the size of the modules and the geometrical spacing approach which will be discussed in more detail using Figure 4.6.

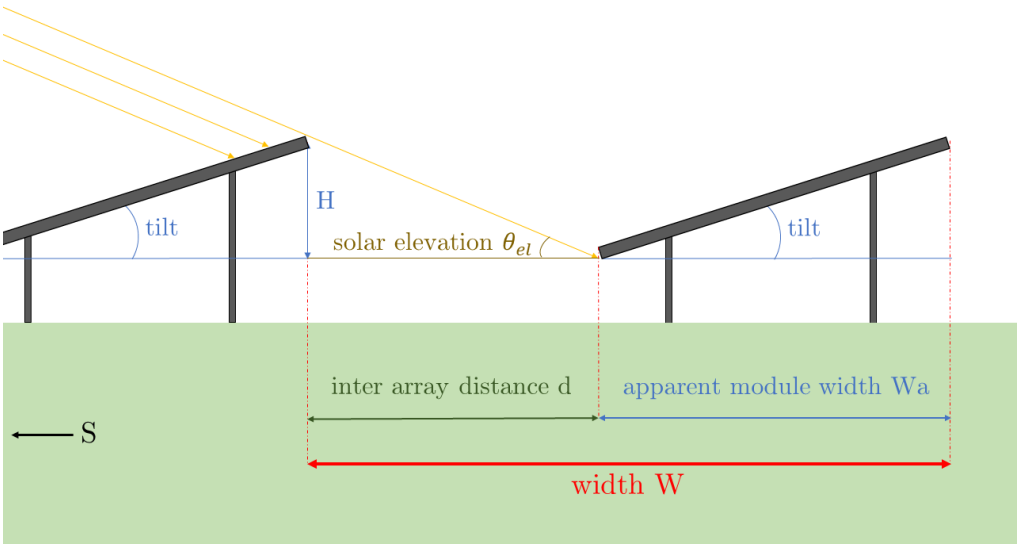

Figure 4.6: Simplified side view of south oriented tables and corresponding geometries and solar irradiance

The width W used for the power density is determined by the apparent table width W_a, depending on the tilt, the height of the modules h_{mod} and the number of modules in that direction $n_{mod,W}$, and the required inter table distance d, based on reducing the inter table shading. The apparent table height W_a is shown in blue and corresponds to the width of the table corrected for the tilt, as calculated in Equation 4.31

$$W_a = (n_{mod,W} \cdot h_{mod}) \cdot cos(tilt) \tag{4.31}$$

Where h_{mod} is the height of the module and $n_{mod,W}$ is the amount of modules this direction.

The inter array distance for solar south orientated is shown in green, d. The inter array distance is determined by shading geometries (Green Tech Renewables, 2020; The Solar Labs, 2021). The inter array distance can be calculated using different low solar elevation irradiance scenarios at certain dates

and times. If no shading is caused in these scenarios, the impact of shading at other times of the year is assumed to be limited.

The approach used in this report considers times at which the farm is supposed to generate the most electricity of the day, so at noon solar-time for solar oriented to the south, and considering a day where, at this time, potentially a large shade could be generated from one row of panels to the next.

This instance for south oriented tables is at noon solar-time on the day with the lowest solar elevation in the Northern hemisphere and the shortest day of the year, 21st of December. The solar position at this instance can be identified with the solar azimuth azimuth$_S$ and the solar elevation angle $\theta_{el,S}$. The azimuth of the solar farm needs to be corrected for the solar azimuth at this instance. For a south orientated panel, with an azimuth of 180 °, the azimuth correction $\theta_{az,S} = 180 -$ azimuth$_S$ °.

To find the inter array distance d, the height H and the solar elevation θ_{el} are used, as can be seen in Figure 4.6. The height H can be found using the tilt, the height of the modules and the number of modules in that direction $n_{mod,W}$, represented by M.

$$H = (n_{mod,W} \cdot h_{mod}) \cdot sin(tilt) \tag{4.32}$$

Height H, the azimuth correction $\theta_{az,S}$ and solar elevation $\theta_{el,S}$) are then used to find inter array distance d.

$$d = H \cdot \frac{cos(\theta_{az,S})}{tan(\theta_{el,S})} = (n_{mod,W} \cdot h_{mod}) \cdot sin(tilt) \cdot \frac{cos(\theta_{Az,S})}{tan(\theta_{el})} \tag{4.33}$$

The apparent module with W_a and inter array distance d are summed together determine the width considered for this installed power density W.

$$W = d + W_a \tag{4.34}$$

The length L is determined by the width of the modules w_{mod} and the number of modules in that direction $n_{mod,L}$, represented by N.

$$L = n_{mod,L} \cdot w_{mod} \tag{4.35}$$

Where w_{mod} is the width of the module

East-west orientated modules consist of two adjacent tables, so the width is determined by the apparent table width of two tables and the required inter table distance until the next set of tables. For east-west orientated panels, the same approach holds for finding the apparent table height W_a.

The instances used for east-west oriented tables is at 09:00 and 15:00 solar-time for east and west oriented tables respectively on the day with the lowest solar elevation in the Northern hemisphere and the shortest day of the year, 21st of December. The solar position at this instance can be identified with the solar azimuth azimuth$_E$ for 09:00 and azimuth$_W$ for 15:00 and the solar elevation angle $\theta_{el,EW}$, which is the same at 09:00 and 15:00 given the symmetry of the solar pattern.

The azimuth of the solar farm needs to be corrected for the solar azimuth at this instance. For a east orientated panel, with an azimuth of 90°, the azimuth correction can be found by $\theta_{az,E} = 90 -$ azimuth$_E$ °. For a west oriented panel, with an azimuth of 270°, the azimuth correction can be found by $\theta_{az,W} = 270 -$ azimuth$_W$ °. Given the symmetry of the solar trajectory, the correction is the same for 09:00 as for 15:00 and one instance can be considered to calculate the installed power density, characterized by $\theta_{az,EW}$ and $\theta_{el,EW}$.

The top and side view of the geometries used can be found in Figure 4.7 and Figure 4.7 respectively.

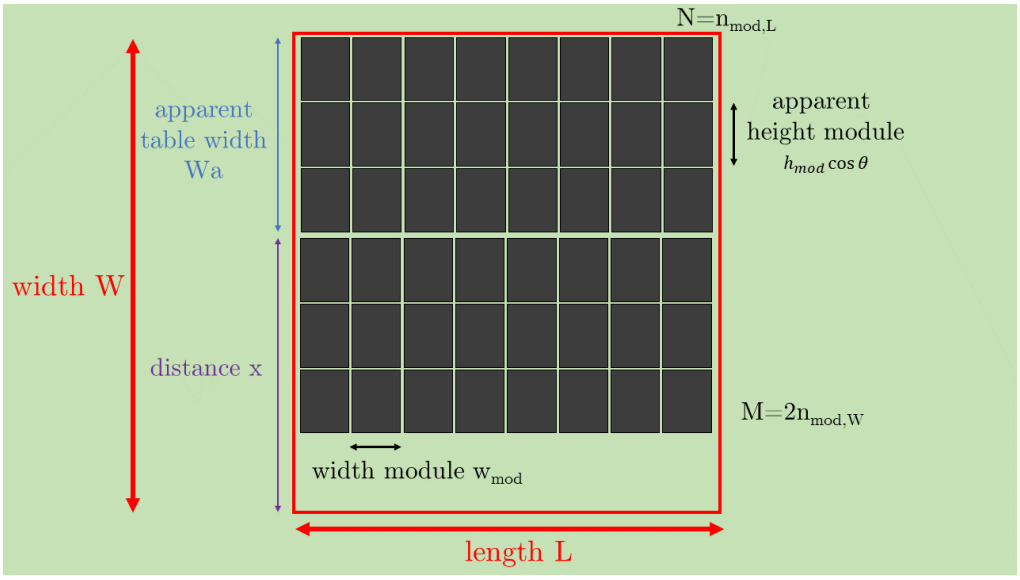

Figure 4.7: Simplified top view of east-west oriented table and corresponding geometries

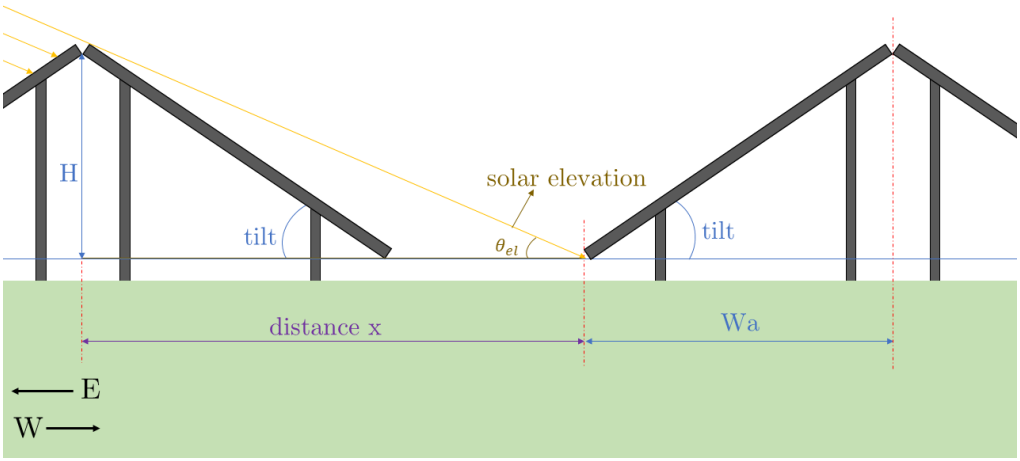

Figure 4.8: Simplified side view of east-west oriented tables and corresponding geometries

The total width W can be found by adding the distance x and the apparent table width W_a, as indicated in Figure 4.7.

$$W = x + W_a \tag{4.36}$$

The apparent width W_a again depends on the tilt, the number of modules in that direction $n_{mod,W}$ and the height of the modules h_{mod}. The same equation can be used as for the south oriented case, as seen in Equation 4.31. The distance x depends on height H.

The height H can be found using the tilt and table height, as shown in Equation 4.32. The height H, the solar elevation $\theta_{el,EW}$ and the azimuth correction $\theta_{az,EW}$ are used to find the following expression for distance x.

$$x = H\frac{cos(\theta_{az,EW})}{tan(\theta_{el,EW})} = (n_{mod,W} \cdot h_{mod}) \cdot sin(tilt) \cdot \frac{cos(\theta_{az,EW})}{tan(\theta_{el,EW})} \tag{4.37}$$

Summing this distance x and the apparent module with W_a leads to the total width W. The length L is found by using Equation 4.35.

A factor to account for a margin between the panels is used, called the ground coverage ratio ("GCR"). A margin could be needed for other equipment than solar panels or civil works. A margin could also be used for initiatives to maintain biodiversity and ecosystems (van Aken et al., 2021). The GCR will be implemented for both South and East-West oriented farms. The power density for south orientated scenario can be found using Equation 4.38.

$$\begin{aligned} \mathsf{P}_{\text{dens,Solar S}} &= GCR \frac{n_{\text{mod},L} \cdot n_{\text{mod},W} \cdot \mathsf{P}_{\text{MPP}}}{L \cdot W} \\ &= GCR \frac{n_{\text{mod},L} \cdot n_{\text{mod},W} \cdot \mathsf{P}_{\text{MPP}}}{n_{\text{mod},L} \cdot w_{\text{mod}} \cdot (d + W_a)} \end{aligned} \tag{4.38}$$

The power density for east-west orientated scenario can be found using Equation 4.39.

$$\begin{aligned} \mathsf{P}_{\text{dens,Solar EW}} &= GCR \frac{n_{\text{mod},L} \cdot n_{\text{mod},W} \cdot 2 \cdot \mathsf{P}_{\text{MPP}}}{L \cdot W} \\ &= GCR \frac{n_{\text{mod},L} \cdot n_{\text{mod},W} \cdot 2 \cdot \mathsf{P}_{\text{MPP}}}{n_{\text{mod},L} \cdot w_{\text{mod}} \cdot (x + W_a)} \end{aligned} \tag{4.39}$$

Wind

Wind turbines disturb the wind after it passes the rotor, called the wake, leading to reduced power outputs if the turbines are placed too close together, which are called wake losses. In order to minimize the wake losses an approach can be used where the wind turbines are placed several rotor diameters D_{rotor} apart, based on an ellipse shape as used within Vattenfall.

The turbine nacelles are usually placed to face the direction the wind comes from predominantly. The wake effects are largest in the area behind the turbine if the wind would blow from the dominant direction. Therefore, the distance between turbines parallel to the dominant direction is larger than the distance between the turbines perpendicular to the dominant wind speed.

For the direction of the wind speed, a distance of 2 and a halve times the rotor diameter on each side of the turbine is assumed until the next turbine can be built, so five times the rotor diameter $5D_{rotor}$ in total per turbine. For the direction perpendicular to the predominant wind direction, a distance of 1 and a halve times the rotor diameter on each side of the turbine is assumed until the next turbine can be built, so three times the rotor diameter $3D_{rotor}$ in total per turbine.

This approach does not take into account any distance regulations from residential areas due possible noise and health issues. It assumes that any electrical or civil works, such as transformers or roads, can be added in between the turbines. To account for these aspects, a margin is created by using a rectangular shape. The visualisation can be found in Figure 4.9.

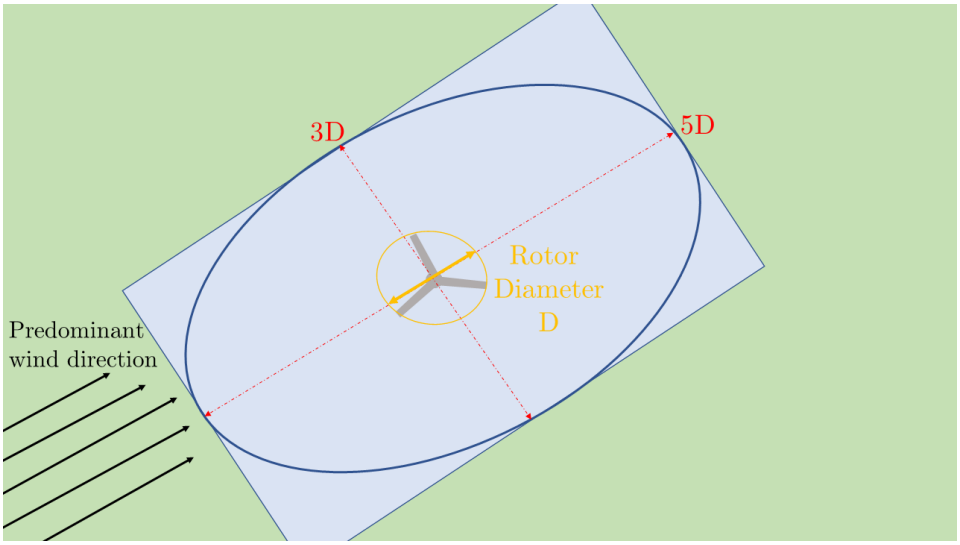

Figure 4.9: Simplified top view of turbines and corresponding geometries

The power density can be found using the area calculation of a rectangle and the turbine diameter D_{rotor}.

$$\begin{aligned} \mathsf{P}_{\text{dens,wind}} &= \mathsf{P}_{\text{rated}}/(3 \cdot D_{rotor} \cdot 5 \cdot D_{rotor}) \\ &= \mathsf{P}_{\text{rated}}/15 \cdot D_{rotor}^2 \end{aligned} \tag{4.40}$$

4.4. Weather and Losses Factor ("WLF")

This section discusses the calculation method of the Weather and Losses Factor (”WLF”) for both wind and solar. The WLF is chosen to consist of reductions in the power output compared to the installed capacity based on weather influences and resource dependent losses. It is an hourly parameter to connect the installed capacity to the actual sold or curtailed power. The solar approach will be discussed first, following by wind.

Solar

The power output of a solar module is determined by different aspects (Holmgren et al., 2018; Smets et al., 2016): (1). The voltage and current characteristics, which depend on the irradiance at the site and electrical layout and determine the power output; (2). The size of the panels, which determines how much irradiance can be captured by the panel; (3). Ambient temperature and wind speed, which determine the temperature of the model, which influences the efficiency; (4). The orientation and tilt of the panels, which influence the effective irradiance on the panel.

As discussed before, in this approach, solar farms consist of solar modules which are connected in series to form a table, also called a string. The amount of modules connected in series determines the output voltage of the farm. Strings can be connected in parallel and determine the output current of the farm.

Multiple strings can be connected in parallel to an inverter which converts the DC energy to AC energy. The inverter has DC and AC characteristics. As briefly introduced before, the inverter is limited by the maximum DC input current and voltage. Depending on the required DC/AC ratio, the DC output of the farm may reach higher values than the DC input capacity of the inverter, resulting in inverter clipping (Inverter.com, 2020).

As mentioned before, the DC input voltage of the inverter determines the number of modules in series in a string. The amount of strings connected to an inverter in parallel can be varied and determines the DC/AC ratio of the farm. The total number of modules on the DC side $\mathsf{N}_{\text{mod, inv}}$ are thus determined by the number of modules per string and the number of strings per inverter. The DC/AC ratio is defined in

Equation 4.41.

$$\text{DC/AC} = \frac{\text{P}_{\text{MPP}} * \text{N}_{\text{mod,inv}}}{\text{P}_{\text{AC}}} \tag{4.41}$$

Modules are installed on the ground using mounting racks and are connected to each other via cabling.

For the WLF calculations of a certain string, the most important input characteristics are project location, panel orientation and tilt, module and inverter type and electrical layout. Using these input characteristics and weather data, the output of one inverter can be extracted from the Python library *PVLib* (Holmgren et al., 2018).

The latitude and longitude determine the hourly weather data including amongst other the radiation specifics, wind speed and ambient temperature. The radiation specifics contain hourly radiation data in W/m^2 and contains the global irradiation on a horizontal plane (GHI), diffuse irradiation on a horizontal plane (DHI) and direct irradiation at normal incidence (DNI). The GHI can be decomposed into DNI and DHI using the solar zenith angle z_s as seen in Equation 4.42 (Smets et al., 2016).

$$\text{GHI} = \text{DHI} + cos(z_s) \cdot \text{DNI} \tag{4.42}$$

By defining a certain tilt and azimuth, the effective irradiance on a module can be found. The module orientation is assumed to be either to either towards the south with an azimuth of 180 degrees in PVlib, or towards the east and west with equal capacities, with corresponding azimuth of 90 and 270 degrees respectively. The module tilt can change with different orientations.

PVlib has in-built module and inverter parameters used to determine DC and AC output of the module and inverter respectively. Each module has specific temperature parameters which can be used in the PVlib temperature models to calculate the efficiency loss of a module by finding the module temperature.

The weather data and effective irradiance determine the hourly output of the modules on the DC side of the inverter. The DC output of the modules, the configuration of the number of modules in series to form a string and number of strings in parallel connected to one inverter and the inverter efficiency, determine the AC output of the inverter.

The AC output of an inverter can be found for each hour of meteorological year in the following steps:

1. The hourly effective irradiance, or plane of array ("POA") is found in PVLib using weather and solar trajectory data based on longitude and latitude, tilt and orientation;
2. The POA and module parameters result in the hourly DC output $\text{P}_{i,\text{DC,output}}$ of a module in PVLib, considering module specific losses;
3. The DC output of the modules and the configuration per inverter, considering the DC/AC ratio, lead to the hourly AC output per inverter $\text{P}_{i,\text{AC,output}}$ in PVLib, considering DC/AC conversion, potential clipping of the inverter and other inverter specific losses;
4. A fixed loss and gain factor η_{solar} is multiplied by the AC output per inverter. The losses and gains considered in η_{solar} are system specific losses, such as electronic losses and soiling losses.

Dividing the hourly AC output of the inverter $\text{P}_{i,\text{AC,output}}$ by the amount of panels on one table connected to the inverter $\text{N}_{\text{mod,inv}}$ multiplied by the peak power output of a module P_{MPP}, results in the hourly WLF.

The hourly WLF for a solar farm with east-west orientation is shown in Equation 4.43. The AC output values of the inverters connected to the east oriented strings and the west oriented strings are summed and multiplied by the fixed loss and gain factor and divided by the number of modules connected to the two inverters.

$$\text{WLF}_{i,\text{Solar E-W}} = \frac{\eta_{\text{solar}} \cdot (\text{P}_{i,\text{AC,output, E}} + \text{P}_{i,\text{AC,output, W}})}{2 \cdot \text{N}_{\text{mod,inv}} \cdot \text{P}_{\text{MPP}}} \quad \forall i \in I \tag{4.43}$$

The hourly WLF for a solar farm with east-west orientation is shown in Equation 4.44. The AC output values of the inverter connected to the south oriented strings are multiplied by the fixed loss and gain

factor and divided by the number of modules connected to the inverter.

$$\mathsf{WLF}_{i,\mathsf{Solar\ S}} = \frac{\eta_{\mathsf{solar}} \cdot \mathsf{P}_{i,\mathsf{AC,output,\ S}}}{\mathsf{N}_{\mathsf{mod,inv}} \cdot \mathsf{P}_{\mathsf{MPP}}} \quad \forall i \in I \tag{4.44}$$

Wind

Wind farms consist of wind turbines which consist of a tower and blades. Turbines are installed in the ground using foundations and are connected to each other via cabling.

To determine the output of a wind farm, the wind velocity at hub height is required. The weather data shows the wind velocity at measured height, called the potential wind speed. If the measured height is below the blending height, the wind speed values can be extrapolated to hub height using the logarithmic boundary layer law (Zaaijer and Viré, 2021). To extrapolate the wind speeds from the blending height to the hub height of the turbine considered, the power law can be used (Zaaijer and Viré, 2021).

This method is based on the influence of the surface on the wind profile. The surface influences the wind speed up to the blending height. The logarithmic boundary layer law considers the surface roughness z_0, indicating the friction of the surface. From the blending height h_{blend}, the influence of the local terrain is no longer felt by the wind velocity and the wind velocity profile no longer depends on surface roughness z_0.

So, if the measurement height $\mathsf{U}(h_{ref})$ is below the blending height $\mathsf{U}(h_{blend})$, the logarithmic boundary layer law can be used to extrapolate the wind speed at measurement height to the wind speed at the blending height (Diab et al., 2022; Zaaijer and Viré, 2021).

$$\mathsf{U}(h_{blend}) = \mathsf{U}(h_{ref}) \cdot \frac{ln(h_{blend}/z_0)}{ln(h_{ref}/z_0)} \tag{4.45}$$

Where h_{ref} is the reference measurement height and h_{blend} is the blending height.

To get from wind speed at blending height $\mathsf{U}(h_{blend})$ to the wind speed at hub height $\mathsf{U}(hh)$, the power law can be used. The power law depends on the factor α which depends on the surroundings (Diab et al., 2022; Diaf et al., 2007; Diaf et al., 2008; Hiendro et al., 2013; Kaabeche et al., 2011a; Yang et al., 2007; Yang et al., 2009; Yang et al., 2008; Zaaijer and Viré, 2021).

$$\mathsf{U}(hh) = \mathsf{U}(h_{blend}) \cdot \left(\frac{hh}{h_{blend}}\right)^{\alpha} \tag{4.46}$$

If the measurement height $\mathsf{U}(h_{ref})$ is higher than the blending height $U(h_{blend})$, the power law can be used directly, depending on the factor α again.

$$\mathsf{U}(hh) = \mathsf{U}(h_{ref}) \cdot \left(\frac{hh}{h_{ref}}\right)^{\alpha} \tag{4.47}$$

Where h_{ref} is the blending height and hh is the hub height.

The hourly power output of a turbine depends on the hourly wind speed at hub height $\mathsf{U}_i(hh)$ and can be found by using the power curve of the turbine. The power production curve runs from cut-in wind velocity $\mathsf{U}_{\mathsf{cut\text{-}in}}$ until cut-out wind velocity $\mathsf{U}_{\mathsf{cut\text{-}out}}$. For all wind speeds lower than the cut-in or higher than the cut-out wind velocity, the power output is zero. A turbine produces at its maximum rated power from the rated wind velocity $\mathsf{U}_{\mathsf{rated}}$ up to the cut-out wind velocity. From the cut-in until the rated wind velocity, the output power depends on the wind velocity cubed. In summary, the power curve can be constructed as following (Anoune et al., 2020; Diab et al., 2022; Zaaijer and Viré, 2021):

$$\begin{aligned}
\mathsf{U}_i(hh) < \mathsf{U}_{\text{cut-in}} \quad & \mathsf{P}_i = 0 && \forall i \in I \\
\mathsf{U}_{\text{cut-in}} < \mathsf{U}_i(hh) < \mathsf{U}_{\text{rated}} \quad & \mathsf{P}_i = \tfrac{1}{2} c_p \pi \rho \tfrac{D^2_{\text{rotor}}}{4} \mathsf{U}_i(hh)^3 && \forall i \in I \\
\mathsf{U}_{\text{rated}} < \mathsf{U}_i(hh) < \mathsf{U}_{\text{cut-out}} \quad & \mathsf{P}_i = \mathsf{P}_{\text{rated}} && \forall i \in I \\
\mathsf{U}_i(hh) > \mathsf{U}_{\text{cut-out}} \quad & \mathsf{P}_i = 0 && \forall i \in I
\end{aligned}$$

Where c_p is the power factor, ρ is the air density and D_{rotor} is the rotor diameter.

The hourly output P_i can be found by obtaining the power for each hour using the wind velocity at hub height at that hour $U_i(hh)$. To find the WLF, the hourly power output should be corrected for the losses in the system η_{wind}. The losses contain electrical losses, wake losses, and other internal losses and do not consider icing and site specific losses, impacted by for example shade, noise, bird or bat restrictions.

The largest impact on the output are the wake losses caused a disturbance of the wind pattern by turbines. If the turbines are spaced too closely to one another, the losses impact the output significantly (Zaaijer and Viré, 2021). As introduced in section 4.3, the wake losses depend on the geometry of the wind farm resulting in the approach used to minimise the wake losses.

The hourly WLF parameter can be found by dividing the corrected output $\mathsf{P}_i \cdot \eta_{\text{wind}}$ by the rated output of the turbine $\mathsf{P}_{\text{rated}}$ in question.

$$\mathsf{WLF}_{\text{wind},i} = \frac{\mathsf{P}_i \cdot \eta_{\text{wind}}}{\mathsf{P}_{\text{rated}}} \quad \forall i \in I \tag{4.48}$$

4.5. Cable Capacity and Electrical Components

This section discusses the approach to find the residual space on the cable in more detail. Some general remarks regarding the electrical components used in a cable pooling system are also discussed.

4.5.1. Cable Capacity

Cables to connect a resource to the grid are sized by the system operator based on degradation models, which differ per system operator. Cables degrade faster if the cable internal temperature rises above a certain threshold. The temperature rises with higher current running through the cables. To keep the operating temperature below this threshold, the cables are sized based on the expected generation patterns, determining the current carrying capability.

With intermittent generation, there will be times of no generation where the cable can cool down, which is accounted for by system operators when sizing the cable. Cables connecting a solar farm, which has no production at night, to the grid are sized differently compared to wind farms, which produce more continuously throughout the day.

Adding an extra generating resource to the same cable to the grid connecting point, may result in less time to cool the cable down and thus higher temperatures in the cable and faster degradation. This could imply that the grid operator would change the ATO to limit the degradation on the cable due to the changed production profile.

Since the degradation models and assumptions used differ per system operator, the current carrying capability will not be considered in this research and the assumption is made that all grid capacity as specified in the ATO may be used.

4.5.2. Electrical Components

When sharing one grid connection with two generating resources, the electrical component configuration has to be altered compared to the situation with one generating resource. When one generating resource exports power to the grid, the control and metering configuration is based on only one re-

source exporting electricity. When another resource is added, this configuration needs to be expanded.

The existing metering structure measures the total output at the grid connection point. When another resource is added, metering components for the new resource need to be added, together with an additional metering structure to measure the output of the existing resource separately. In practice, the metering is performed by metering transformers, which measure current and voltage.

The existing control system controls the output of the total farm, so apart from a control system for the new resource, an additional control system will need to be installed for the existing resource separately. In practice, the control is performed by fuses and switches, based on SCADA systems collecting data from the system.

The additional losses and costs due to the extra metering and control equipment are considered negligible for this research. The assumption is made that the required equipment is present and the output at the grid connection point does not cross any ATO or temperature limits.

4.6. Performance Indicators

The system is sized to maximise the NPV for all three technologies j. The optimised system can be expressed in other economical or technical performance indicators in order to compare the different technologies.

Different indicators and the calculations methods are summed below.

1. **Total Costs**
   An interesting indicator are the total costs. The total costs are found by summing all the yearly operational costs $\text{OPEX}_{j,t}$ and adding the initial investment costs CAPEX_j.
2. **Capacity Factor** c_f
   The capacity factor shows the real output compared to the theoretical output. The capacity factor of the output of the hybrid farm can be calculated using Equation 4.49 (Golroodbari et al., 2021).

$$c_f = \frac{\sum_{i=1}^{8760} (\mathsf{E}_{\text{out,existing},i} + \mathsf{E}_{\text{sold},i})}{(\mathsf{P}_{\text{installed,existing}} + \mathsf{P}_{\text{installed}}) \cdot 8760} \tag{4.49}$$

3. **Cable Capacity Factor** cc_f
   The cable capacity factor shows the export on the cable compared to the theoretical maximum export. The cable capacity factor of the output of the hybrid farm can be calculated using Equation 4.50 (Golroodbari et al., 2021).

$$cc_f = \frac{\sum_{i=1}^{8760} (\mathsf{E}_{\text{out,existing},i} + \mathsf{E}_{\text{sold},i})}{\mathsf{Cable}_{\text{cap,max}} \cdot 8760} \tag{4.50}$$

   For the hybrid farm including a battery, a similar method can be used as shown in Equation 4.51.

$$cc_{f,\text{bat}} = \frac{\sum_{i=1}^{8760} (\mathsf{E}_{\text{out,existing},i} + \mathsf{E}_{\text{sold},i} + \mathsf{E}_{\text{dch},i})}{\mathsf{Cable}_{\text{cap,max}} \cdot 8760} \tag{4.51}$$

4. **Curtailment**
   If the cable size is limiting or the prices on the spot market are negative, the farm will curtail energy. The curtailed energy of technology j for a year is found by summing the hourly curtailed energy $\mathsf{E}_{\text{curtailed},i,j}$ over all hours in the year, as shown in Equation 4.52.

$$\text{Curtailment} = \frac{\sum_{i=1}^{8760} \mathsf{E}_{\text{curtailed},i}}{\mathsf{P}_{\text{installed}} \cdot 8760} \tag{4.52}$$

4.7. Assumptions and Simplifications

The problem formulation and methodology are derived using assumptions and simplifications. This section discusses the most important simplifications and assumptions.

- The hourly weather data input for the farm is assumed to be constant during the time step (Diaf et al., 2007). The power values are assumed to be directly proportional to energy with a time step used of Δt = 1h.

  The power factor, linking apparent in MVA to real power in MW, is assumed to be one. The power values are therefore assumed to be directly proportional to export capacity on the cable.

- Hourly exported energy generates hourly revenues, which are summed to find the yearly revenues. The yearly revenues are corrected for the approximated impact of the degradation of the existing and new resource. This is a simplification, since the degradation of the existing and new resource each influence the export on the cable for each hour of the year. The simplification is made to indicate the impact on the revenues earned, while minimizing computational efforts.

- It is assumed that the degradation of the existing farm results in an increase in the business case of the new resource, which is not necessarily the case.

- Degradation of other components in the system are not considered.

- Only the residual space on the cable can be used for the new renewable resource. If the existing resource does not produce power at the cable capacity, there is room for the new renewable resource to export. This approach is chosen to consider a worst case with no negotiating power to use a certain share of the grid capacity. In case the developer would have negotiating power and could secure a certain percentage of the grid connection capacity for a certain price, this might lead to upsides in the business case.

- If the cable forms an active constraint, the generated energy can not be sold and will be curtailed.

- The maximum residual cable capacity is considered to be the same as the size of the grid connection before the possible addition of the new resource, even though temperature models used by the system operator might change the grid capacity at the PAP in the ATO if another resource is added.

- All costs related to the grid connection are assumed to be zero.

- The goal was to create a scalable optimization, where the installed capacity could be increased or decreased to find the optimal objective function. The power density and WLF are defined to link the sold energy, earning revenues, to the installed power, determining the investment and operational costs.

- The power density is a measure of the installed power per square meter and is used to check whether or not the installed capacity exceeds the land bounds. This assumes that the land has a certain shape and the installed capacity can be built in that same shape, without any losses due to the shape of the land.

- Furthermore, the layout of the farm does not create extra losses in terms of shading losses for a solar farm and wake losses for a wind farm. Certain distancing from residential or agricultural areas may also be required, but is situation dependent and therefore disregarded in the general model. A buffer is created by use of the GCR for solar and the rectangular shape for wind, which can be used for layout requirements, such as roads and fences, and components not considered in the power density.

- Shading of solar panels by wind turbines is not considered since the distance between the two farms is assumed to be sufficiently large.

- Additionally, the grid is assumed as an infinite power source and infinite demand to which electricity can be transported up to the cable capacity amount at any moment in time.

- In this approach, it is assumed that grid code requirements can be met by using the right equipment, such as measurement equipment and controllers. No constraints from the grid are therefore considered. Given the minimal power losses and extra costs of extra equipment, the exact requirements are disregarded in this research.

- The current methodology assumes perfect day-ahead forecast for trading energy.

5

Case study

This chapter discusses the case study used in this research to obtain results from the model. The chapter first discusses the case study location and later discusses the input used.

5.1. Case Study Description

The location used for the case study is a solar farm in Overijssel, the Netherlands. The region selected is an earmarked area for solar energy assigned by the provincial authorities by use of the Regional Energy Strategies (”RES”). One party has started developing in this area and acquired the last available grid connection at the nearest station, with a size of 13 MVA. The size of the piece of land of party one was limiting the size of the solar farm the party could develop, resulting in an oversized grid connection.

Vattenfall secured a piece of land adjacent to the plot of the first party, aspiring to develop their own project. Given that the party one had secured the last space on the grid connection closest to the location, Vattenfall was forced to deviate to another grid connection point, inducing high costs. After negotiations, the first party and Vattenfall have agreed to share the grid connection based on a 50/50 ratio. The total farm will have a size of 28.5 MWp and is divided into two separate farms of approximately the same size on two pieces of land. The two farms have applied for SDE++ separately.

This case will serve as a benchmark against which the results of optimization models can be evaluated. The existing farm will be a 15 MWp east-west oriented solar farm, owned by the first party, and the potential new farm is located on a piece of land adjacent to this farm. The size of the piece of land secured by Vattenfall is 12 ha. Considering the grid connection of 13 MVA, the model will optimally size the new wind or solar farm, in either of the orientations.

5.2. Case Study Inputs

This section discusses the inputs used in this case study. First, weather and spot market input is discussed in subsection 5.2.1, followed by economical inputs, including SDE++ or PPA prices, the long-term market outlook and costs in subsection 5.2.2. Furthermore, the inputs used to determine the yield and losses are discussed in subsection 5.2.3.

5.2.1. Weather and EPEX Data Input

The weather data influences the market prices increasingly due to the high penetration of renewable energy. The market prices are steered by supply and demand curves and with increasingly volatile supply, the price can reach high spikes, both positive and negative. A full year of weather data and EPEX data of the corresponding year should be used to take this dependency into account.

To find the most representative full year of data to use, the past data is analysed. The average EPEX spot market data has seen a steady increase since 2020 and the spread between the minimum and the maximum value has grown, as can be seen in Figure 5.1. The spot market data has been obtained

from the internal data collection of Vattenfall.

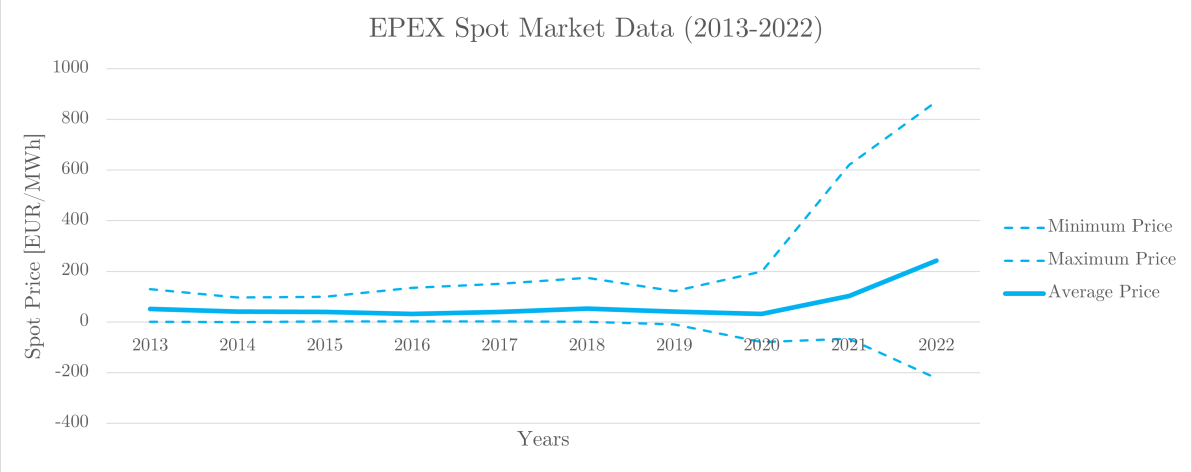

Figure 5.1: Average, minimum and maximum EPEX spot prices from 2013 until 2023

Before 2020, the prices usually fluctuated somewhere between 0 and 150 EUR/MWh, as can be seen in Figure 5.2. This increase in spread can partially be attributed to the influence of the renewable energy sources in the electricity mix on the mismatch between supply and demand and political issues. At times of high supply, i.e. high radiation or high wind speeds, the demand is not necessarily high, inducing low prices prices. Negative prices also occur more often in the past years, as a result of inflexibilities or subsidies. The same derivation can be made for high demand and low supply, inducing high price spikes.

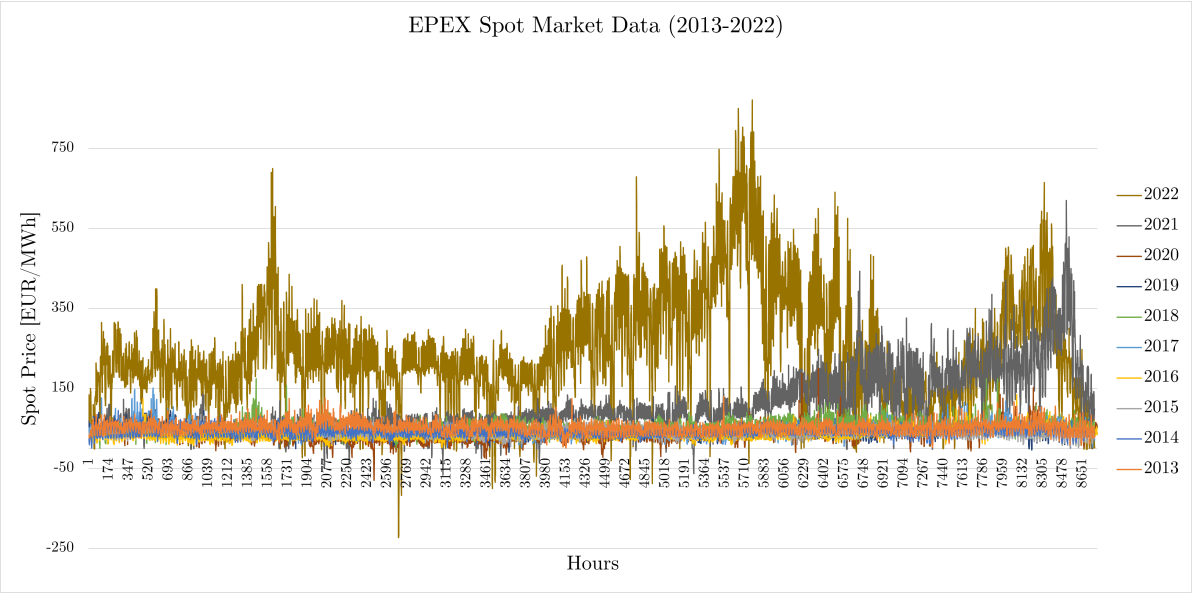

Figure 5.2: Hourly EPEX spot prices from 2013 until 2023

The share of renewable energy sources in the total electricity production in the Netherlands has increased over the past years, as can be seen in Figure 5.3. From 2019, the share sees a steep increase, accompanied by a decline of the share of fossil fuels.

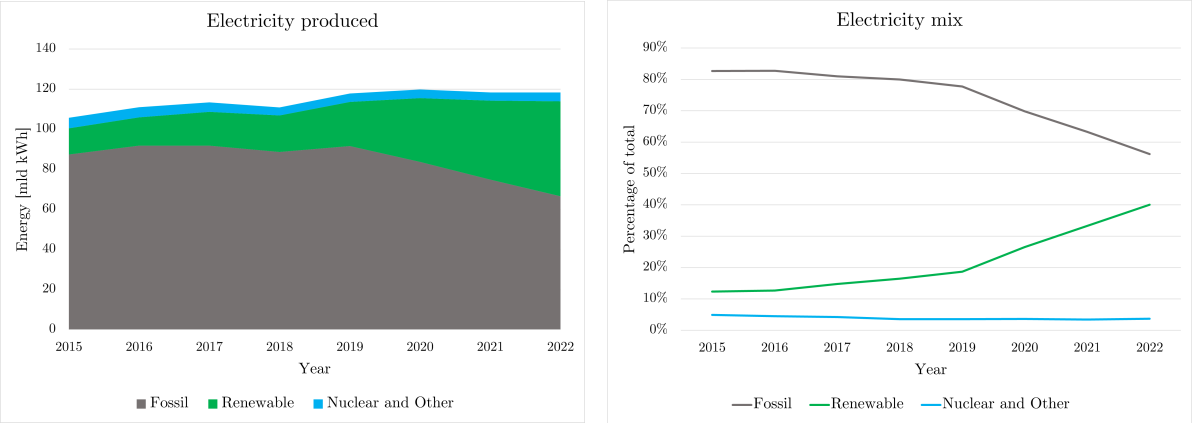

Figure 5.3: Electricity production by fossil, renewable and nuclear and other sources from 2015 until 2022 and their share of the total electricity (Centraal Bureau voor Statistiek, 2022, 2023)

When considering the share of renewables in the electricity mix and their influence on the volatility of the EPEX prices, more recent years of data, 2019 until 2022, can be considered more representative for the future and are shown separately in Figure 5.4. The spikiness and average price show an increase from 2019 until 2022, with exceptionally high spikes in 2022. In 2022, the average EPEX price was 242 €/MWh, the minimum price was -222 €/MWh and the maximum price was 871 €/MWh.

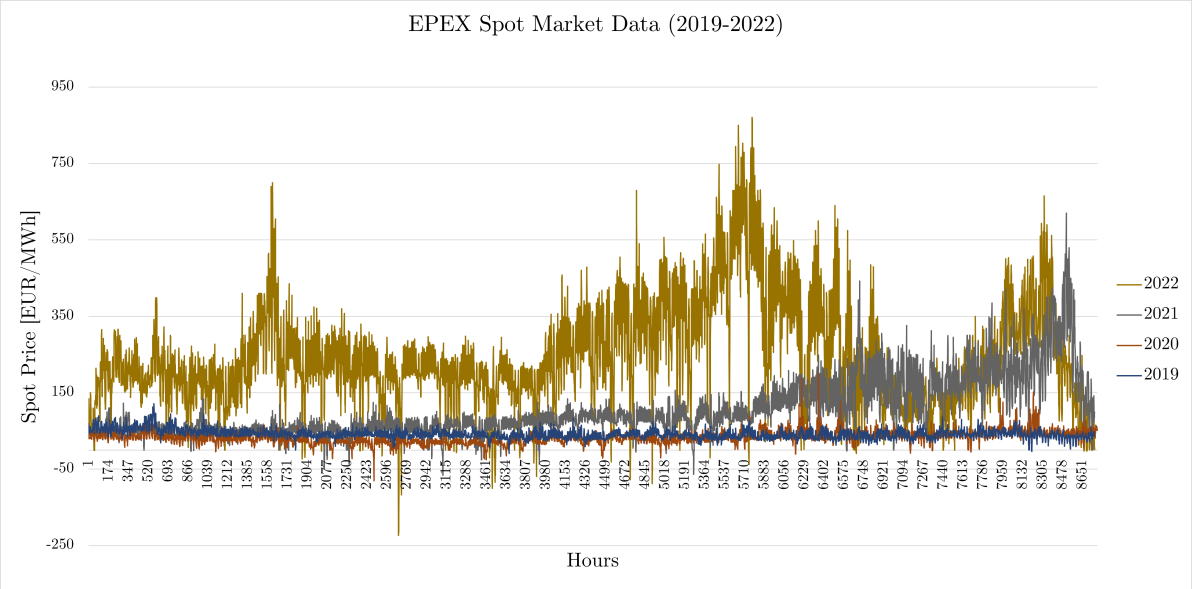

Figure 5.4: Hourly EPEX spot prices from 2019 until 2023

Following this reasoning, the year 2022 can be considered the most representative year for the future, given that the share of renewables will only increase in the future. However, the extremely high prices occurred can largely be attributed to the Ukraine War. To compare, in 2023 the average price so far 98,9 €/MWh with a maximum of 270 €/MWh and a minimum of -500 €/MWh, again showing volatility but a decreased average price. The decrease in the average price can be partially attributed to the count of negative hours and less geopolitical influences impacting the market prices. The count of negative hours in 2023 was already 205 hours until September, compared to a total of 92 hours in 2022. This again shows the increased volatility of the spot market.

The year 2019 is a less volatile and a less extreme high price year, but also saw far less renewable energy in the mix, as seen in Figure 5.3. In 2019 the average EPEX price was 41.9 €/MWh, the minimum price was -9.02 €/MWh and the maximum price was 121 €/MWh. This clearly shows the increased

volatility and height of the EPEX prices in 2022 compared with 2019. The year 2020 can be considered an exception, due to Covid-19. The year 2021 shows a steep increase in electricity prices by the end of 2021, which can be attributed to the decrease in Covid-19 restrictions and a sudden increase in electricity demand (Engie, 2022).

Since 2022 is most representative for the share of renewables and 2019 is the year with the least situation dependent influences on the price, considering both full years of weather data and corresponding EPEX data is preferred. Chapter 2 addresses the possible cable pooling combinations in the current context: wind-wind, solar-wind, or solar-solar. Therefore, weather characteristics for wind and solar are obtained for 2019 and 2022.

Wind speed data at location is obtained using the ERA5 database (Copernicus, 2023) containing wind speed at 10 and 100 meters and the air temperature. Solar irradiation data is obtained from CAMS Radiation Service (Copernicus Atmosphere Monitoring Service, 2023). It contains hourly radiation data in W/m^2 for the global irradiation on a horizontal plane (GHI), diffuse irradiation on a horizontal plane (DHI) and direct irradiation at normal incidence (DNI). The solar irradiation discussed here only covers the global irradiance for solar energy. The orientation of the solar farm is not yet taken into account.

Wind speed and solar irradiance are proven to be complementary (Gajewski and Pieńkowski, 2021; Javed et al., 2019; Zhou et al., 2010). This makes the potential for combining solar and wind together positive. The combinations considering wind-wind or solar-solar do not have this advantage. To analyse the behaviour of the wind speed and solar irradiation at the case study location, the seasonal pattern of wind speed and solar irradiation and the correlation between the two is analysed.

Figure 5.5 and Figure 5.6 show the daily average wind speed at 100 m and GHI for each month in 2019 and 2022 respectively illustrating the seasonal complementary behaviour of the GHI and the wind speed in the case study location in Overijssel. The solar resource shows a seasonal pattern with the peak in the summer months and a big drop in the winter months. The wind pattern shows a more stable behaviour throughout the years, with the peaks mostly occurring in the winter times. However, 2019 also showed some peaks in the summer. This confirms the seasonal complementary behaviour of solar and wind.

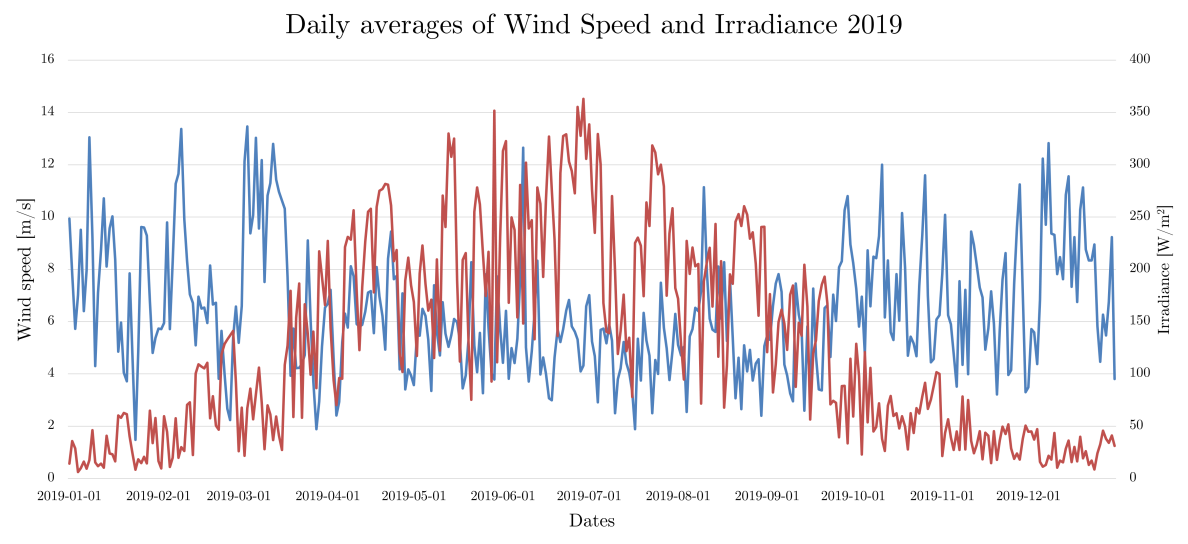

Figure 5.5: Daily average GHI and wind speed for the year 2019.

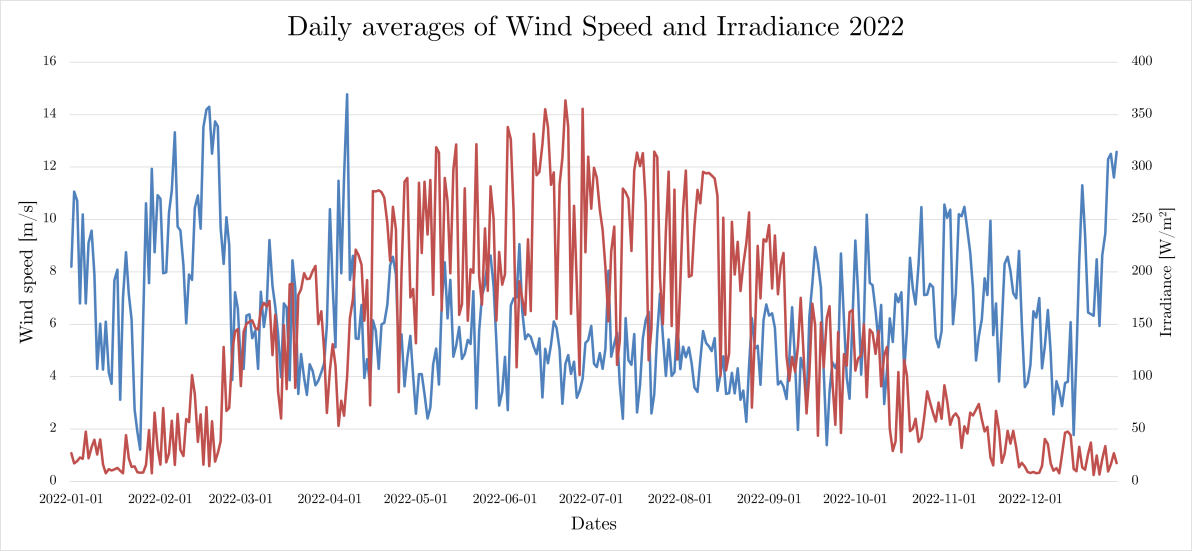

Figure 5.6: Daily average GHI and wind speed for the year 2022.

Figure 5.7 and Figure 5.8 show the correlation between the wind speed and GHI in Overijssel for 2019 and 2022 respectively. High wind speeds do not often occur simultaneously with high irradiation values, affirming the potential of co-locating wind and solar. In 2022, the wind speeds show range up to almost 25 m/s, compared to a maximum of around 17 m/s in 2019, while the maxima for the GHI remained somewhat constant. The extremely high wind speeds of 18 m/s and higher in 2022 almost explicitly occur with low GHI values.

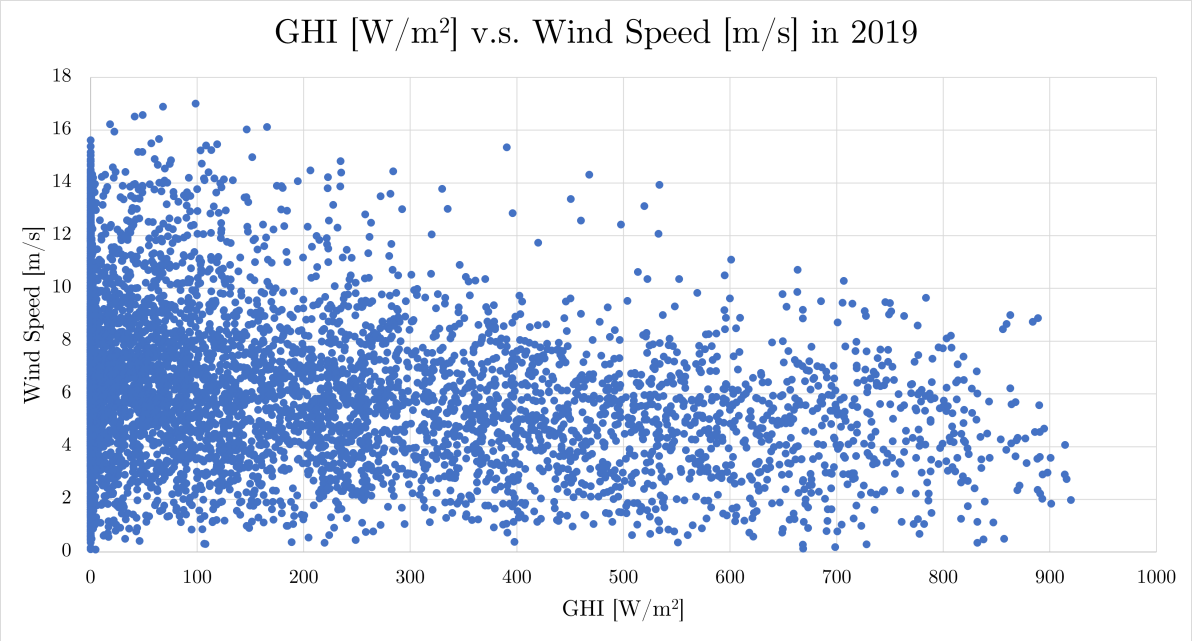

Figure 5.7: The correlation between GHI and the wind speed in the year 2019.

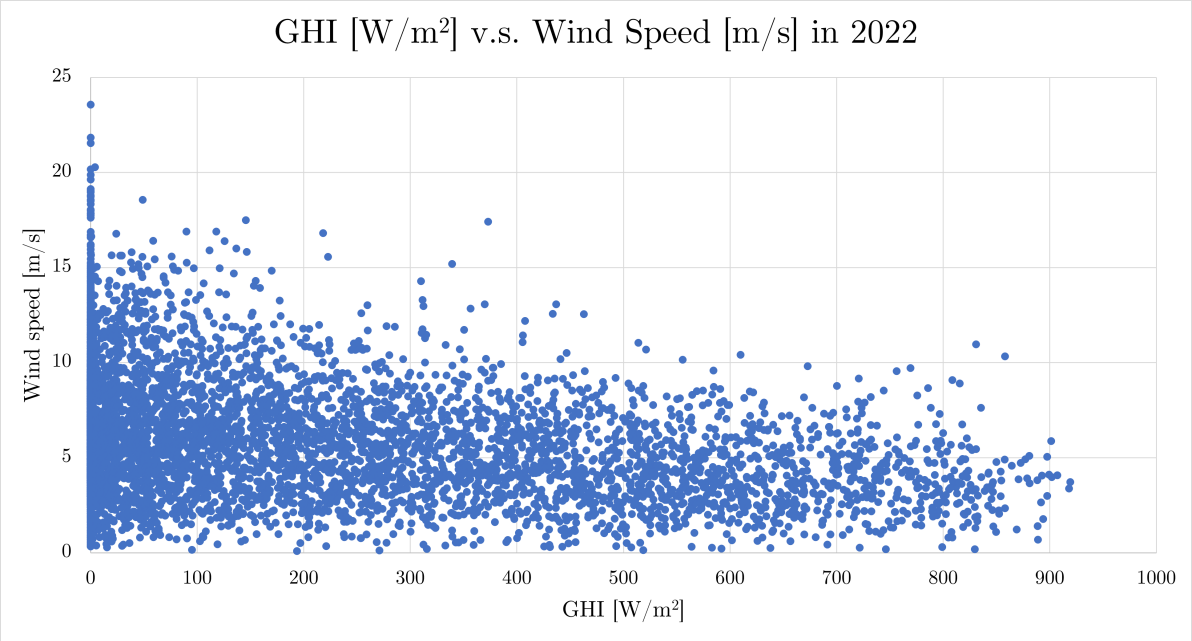

Figure 5.8: The correlation between GHI and the wind speed in the year 2022.

The general statistics are shown in Table 5.1 and Table 5.2. The average GHI was higher in 2022, which also translates lightly into the median. In 2022, the standard deviation was bigger, indicating a larger variability of the data points. The maxima are similar.

Table 5.1: Comparison of GHI Data (2019 vs. 2022)

	2019	2022
Mean [W/m^2]	127.89	137.99
Median [W/m^2]	4.48	4.57
Std [W/m^2]	204.09	214.90
Max [W/m^2]	919.67	919.25

For the wind data, it can be seen the mean was higher in 2019, which can be seen in the median as well. The standard deviation was again higher in 2022, indicating a higher variability in the data points again. The maximum wind speed at the site was significantly higher in 2022 than 2019.

Table 5.2: Comparison of Wind Data (2019 vs. 2022)

	Wind 2019	Wind 2022
Mean [m/s]	3.75	3.63
Median [m/s]	3.46	3.31
Std [m/s]	1.74	1.82
Max [m/s]	11	15.15

Considering the weather data, it is expected that a wind farm at this site would produce more energy based on 2019 data compared to 2022 data, while this is opposite for solar farms.

5.2.2. Economic Input

This section discusses the economical inputs used for the case study. First, the revenue inputs are discussed, containing the revenue streams, long-term market outlook, inflation and discount rate. Secondly, the cost side is discussed, containing CAPEX and OPEX.

The revenue streams, apart from ME, considered are SDE++ and PPA. The inputs required for the SDE++ are the Basisbedrag (BB), the Market Value (MV), a maximum number of full-load hours (FLH) per year and the duration of the subsidy. The MV, used to calculate if there is a subsidy paid, is calculated using the expected average value of the spot market based on the long-term market outlook (LTMO), which will be discussed later. The BB and number of FLH depend on the technology. The duration of the SDE++ subsidy is expected to be 15 years (RVO, 2023d).

The BB SDE++ values of 2023 as determined by RVO are used as inputs for the SDE++ values (RVO, 2023d). For solar farms on land different values are specified for different sizes of solar farms. For wind, the advised BB is dependent on the average wind speed at the location. Using Windviewer (Geocontent RVO, 2023), the average wind speed of a turbine located at the case study site in Overijssel is determined to be 7.31 m/s, within the >7.0 and <7.5 m/s wind speed bin, leading to a BB of 0,0624 EUR/kWh for a maximum allowed number of full load hours based on a P50 production scenario.

The P50 production scenario is the number of FLH which has a 50% chance to be reached or exceeded. Considering the weather data and expected production data and sorting them, the 50^{th} percentile of the production the P50 FLH value for a wind farm at this site, and hub height, is expected to yield 1501 hours based on 2019 and 1414 hours based on 2022 data, in line with the higher expected generation in 2019 based on the weather data.

An overview of all the values can be seen in Table 5.3.

Table 5.3: SDE++ Revenue Stream Input

Type	Basisbedrag (BB) [EUR/kWh]	Full-Load Hours [h]	Duration [y]
Solar <20 MW_p	0.0701	840	15
Solar >20 MW_p	0.0667	840	15
Wind 7.0 m/s < U_{10m} < 7.5 m/s	0.0624	1414-1501	15

For the PPA, the internal PPA values used by Vattenfall are used. For solar, a PPA price of 70 EUR/MWh is assumed. For wind, a PPA price of 78 EUR/MWh is assumed. The duration of the PPA is assumed to be 10 years. Since the duration of both the SDE++ and PPA's is shorter than the lifetime, both are combined with a ME business case for the remaining years, using the EPEX market data. An overview can be found in Table 5.4.

Table 5.4: PPA Revenue Stream Input

Type	PPA price [EUR/kWh]	Duration [y]
Solar	0.070	10
Wind	0.078	10

To account for the market developments on the long term, a long-term market outlook (LTMO) is used. The LTMO consists of multiple market outlooks blended into one curve running from 2023 up to 2070 and was provided by Vattenfall. It can be split up into two projections: (1). the expected value factors for onshore wind and solar energy, as shown in Figure 5.9 and (2). the expected average EPEX spot market price, as shown in Figure 5.10.

The value of solar and wind energy is depicted in Figure 5.9. The percentages can be used as value factors $LT_{f,j,t}$ to correct the yearly revenues to account for the future value of the produced energy of that specific technology j. The value factors for solar and wind are both expected to decrease, due to the increased supply of electricity at times of high wind speeds or high irradiance, leading to lower electricity prices at those instances.

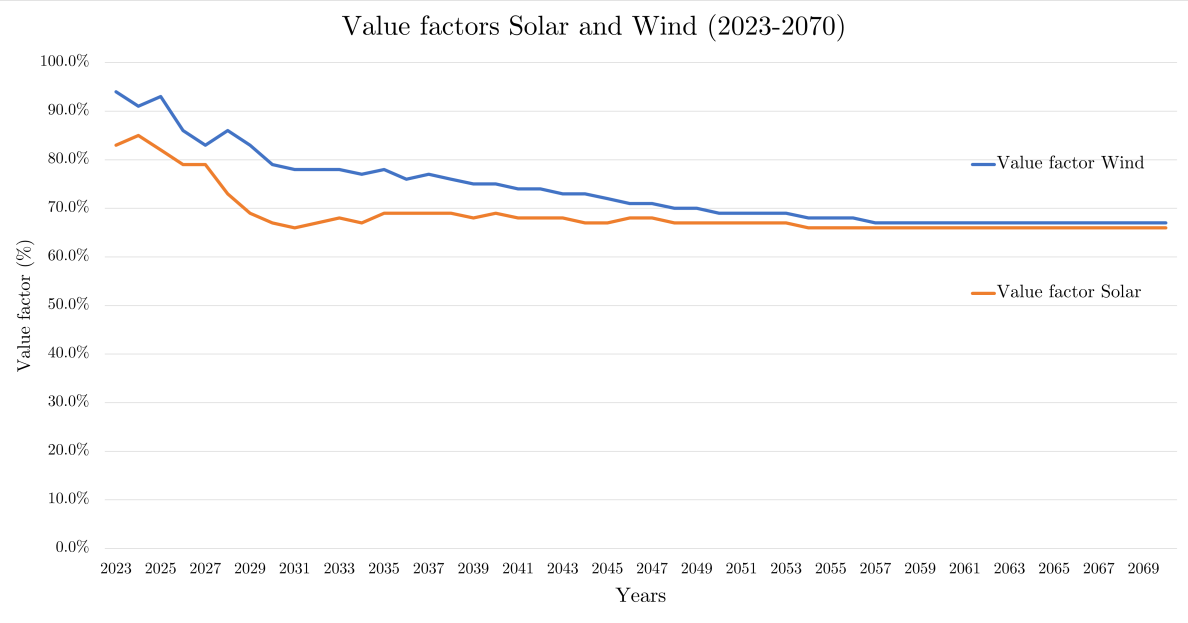

Figure 5.9: Hourly EPEX spot prices from 2019 until 2023

The value factor for wind and solar first show a steep decrease and later stabilize from around 2057 onward to a value factor of around 68%. Solar energy shows a value factor around 10% lower than onshore wind in 2023, due to the high penetration of solar panels in the system and the weather and daily pattern dependency.

The expected average price of the EPEX spot market is depicted in Figure 5.10. It also shows the expected average price for wind and solar energy based on expected average price corrected for the expected value factor of solar and wind energy.

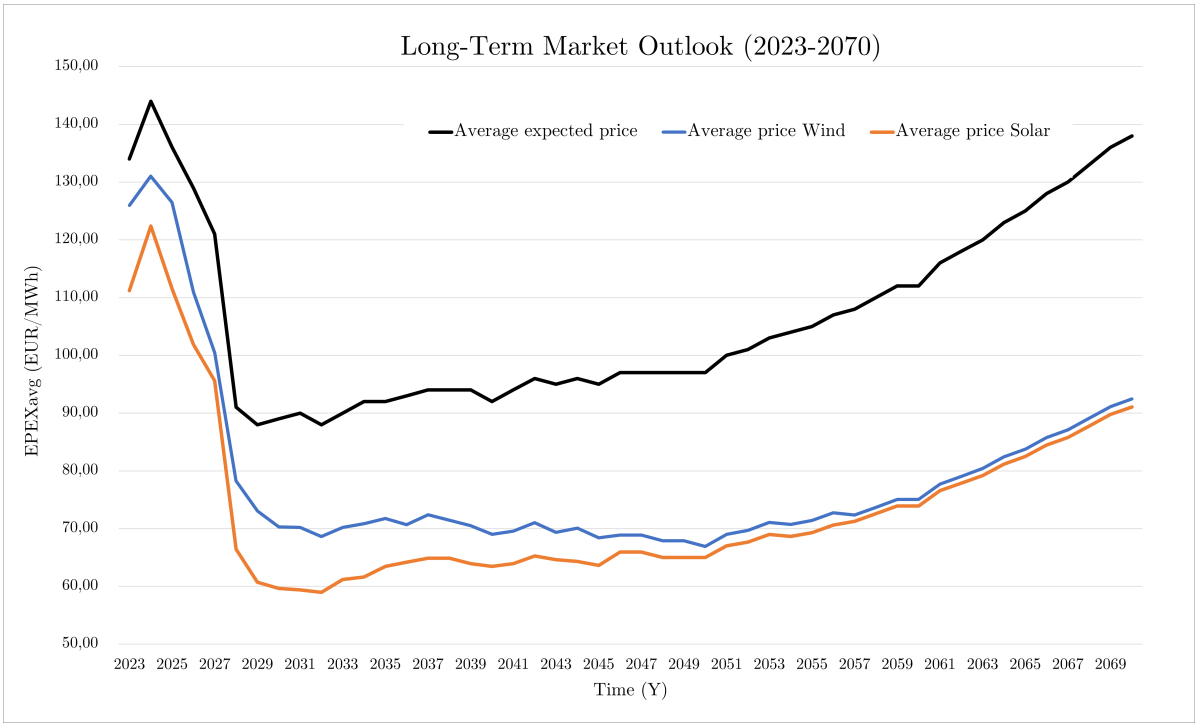

Figure 5.10: Long-term market outlook from 2023 until 2070 showing the projected average EPEX prices and the technology specific average spot market prices.

The average price of the EPEX spot market is expected to increase until 2025, after which a steep decrease until 2030 is expected. After 2030 the average price gradually increases. The steep decrease until 2030 can potentially be attributed to the expected increased presence of storage solutions, stabilizing the supply and demand. The gradual increase after 2030 can be attributed to the expected increased demand due to the electrification of the energy system, driving up the average prices of electricity.

The expected averages can be used to correct the yearly revenues for the expected market developments in the years considered by introducing the long-term market value LT_t. To find the long-term market value LT_t, the average of the EPEX data of the year used t_0, 2019 or 2022, will be compared to the average expected price from the LTMO. The LT_t is determined by Equation 5.1.

$$\mathsf{LT}_t = \frac{EPEX_{avg,t}}{EPEX_{avg,t_0}} \tag{5.1}$$

The average of the EPEX data of 2019 $EPEX_{avg,2019}$ is 41.9 €/MWh and of 2022 $EPEX_{avg,2022}$ is 242 €/MWh.

Multiplying the value factor of onshore wind and solar $\mathsf{LT}_{f,j,t}$ by the expected average prices indicates the value of onshore wind and solar energy produced on the long-term, which converge towards 2070, as can be seen in Figure 5.10. These values are used to determine the yearly market value $MV_{j,t}$ used to derive the height of the subsidy received in the SDE++ regulation.

If the average expected price multiplied by the value factor of the technology in question, so the expected market value for that technology, is below the BB for that technology, the difference is paid for the predetermined number full load hours multiplied by the installed capacity of the farm. For example, using the values for BB for solar smaller than 20 MW_p, 70 EUR/MWh, the project is expected to receive SDE++ subsidy from around 2028 until 2055 approximately, since the expected market value is below 70 EUR/MWh in those years as can be seen in Figure 5.10.

The LTMO is a projection based on the situation of a single farm with no export constraints, but is applied to this cable pooling situation. The estimations therefore might not always represent the long-term developments for this cable pooling project specifically. Furthermore, the average values specified in the blended LTMO might have been calculated differently than the average of the EPEX prices of the base years used.

Next to the LTMO, the time value of money is captured using the discount rate and the inflation. The inflation rate will likely stabilize from 2025 to approximately 2% (Statista, 2023). This rate is used for the full lifetime of the project. The financial investment decision ("FID") is assumed to be made in 2023 and the farm is assumed to be operational from the commercial operation date ("COD") in 2025. All costs are inflated from FID to COD, using this same inflation rate of 2%. The discount rate is based on renewable projects and the desired return on investments. For onshore wind and solar energy, discount rate is often between 3 and 6% (International Energy Agency, 2021). The conservative case of 6% will be used.

The costs consist of both CAPEX and OPEX. The CAPEX are made in year 0, before operation, and are subject to inflation from the final investment decision ("FID") year. The CAPEX_j are assumed to be the same for a cable pooling project as a regular renewable generation project, except for the grid connection down-payment and investment, which are assumed to be zero. The CAPEX are expressed in costs per installed MW capacity to be scalable with the installed capacity. The CAPEX are based on internal Vattenfall values from past projects and are clustered in five main topics, as can be seen in Table 5.5.

Table 5.5: Solar and wind system costs per MW installed capacity (”MWIC”)

Solar CAPEX		Wind CAPEX	
Item	Costs [EUR/MWIC]	Item	Costs [EUR/MWIC]
Modules & Inverters	210,000	Turbines	1,000,000
Balance of Plant	180,000	Balance of Plant	275
Grid connection	0	Grid connection	0
DEVEX and CM	60,000	DEVEX and CM	150
Other	40,000	Other	50
Total	**490,000**	**Total**	**1,000,475**

The Balance of Plant (”BoP”) consists of mounting systems including foundations, low/medium voltage equipment, LV and MV stations, landscaping and civil works, monitoring and security and a financial margin. The grid connection costs consist of both the down-payment of the grid costs and the costs of the grid connection, both assumed to be zero. The DEVEX and CM costs consist of all development (”DEVEX”) and construction management (”CM”) costs, containing contractor and other engineering, procurement and construction costs. Others of spare parts, other non EPC costs, contingency, CAR insurance and other costs are considered in other. The CAPEX for wind are more than twice as expensive as solar CAPEX.

The OPEX consist of non-inflatable and inflatable costs. Again, the OPEX for the grid connection are assumed to be zero. The solar OPEX can be seen in Table 5.6. For the wind farms, the OPEX are only 32.5 EUR/MWIC for preventive O&M.

Table 5.6: Solar system OPEX per MW installed capacity (”MWIC”). *The inverter replacement costs range from 1 euro for the first five years, to 2,700 for the years 6 until 20. The last 10 years, year 21 to 30, the inverter replacement costs are 40 EUR/MWIC.

Inflate?			
Yes		**No**	
Item	Costs [EUR/MWIC]	Item	Costs [EUR/MWIC]
O&M	750	O&M	3500
Inverter replacement*	1-2,700	Module replacement	40
Total	**2,051-4,700**	**Total**	**3,540**

Furthermore, a yearly land lease payment is performed from the year the land lease is signed. This can even be before the FID and is therefore inflated from a different base year. The same inflation rate of 2% has been used. The land lease considered for this case study is has been signed in 2019. The land lease used is not mentioned explicitly to guard the privacy and prevent possible tracing of the land owners.

5.2.3. Yield and Losses Inputs

This section deals with the inputs for the yield calculations, including turbine and module specifics, geometry and losses. First the inputs for solar, both east-west and south are discussed, followed by wind.

Solar

The module type used is the Maxeon Solar Tech Ltd. SPR-P5-550-UPP and the inverter type Sungrow SG 250 HX US, specifications can be found in table 5.8 and 5.7 respectively.

Table 5.7: Inverter specifics (NREL SAM, 2020)

Sungrow Power Supply Co - Ltd : SG250HX-US [800V]			
Variable	Value	Variable	Value
V_{ac} [V]	800	$P_{ac,0}$ [W]	226,997
$P_{dc,0}$ [W]	230,396	$V_{dc,0}$ [W]	1,080
C_0 [1/W]	-4.39E-03	C_1 [1/V]	-8.57E-01
C_2 [1/V]	-0.000791432	C_3 [1/V]	-0.000320828
$V_{dc,max}$ [V]	1,300	$I_{dc,max}$ [A]	213.33

Table 5.8: Module specifics (NREL SAM, 2020)

Maxeon Solar Technologies Ltd. SPR-P5-550-UPP			
Variable [Unit]	Value	Variable [Unit]	Value
Technology	Mono-c-Si	Bifacial	0
P_{STC}	550.832	P_{PTC}	495.2
A_c [m2]	2.6	Length [m]	2.384
Width [m]	1.092	N_s [-]	115
$I_{sc,ref}$ [A]	14.86	$V_{oc,ref}$ [V]	48
$I_{mp,ref}$ [A]	13.84	$V_{mp,ref}$ [V]	39.8
α_{sc} [A/K]	0.0068356	β_{oc} [V/K]	-0.14352
T_{NOCT} [C]	46.4	a_{ref} [V]	211.474
$I_{L,ref}$ [A]	150.307	$I_{o,ref}$ [A]	2.02E-04
R_s [Ohm]	0.139794	$R_{sh,ref}$ [Ohm]	948.365
Adjust [%]	348.554	γ_r [%/K]	-0.493

As discussed in section 4.3 and section 4.4, Vattenfall uses mounting tables to construct the panels. The table type used is a three-portrait table, with three modules stacked in portrait mode. As described before, the maximum amount of modules that can be arranged per mounting table in series is determined by the maximum DC voltage input of the inverter. With a maximum voltage on the DC side of 1300 V, the maximum amount of modules with an open circuit voltage V_{oc} of 48 V that can be arranged in series, rounded down to a multiple of three, is 27. Therefore, the table configuration, always consisting of three panels height, will have a 9 modules width.

The required or desired DC/AC ratio determines the amount of tables, or strings, connected in parallel per inverter. In order to receive SDE++, the allowed inverter size is only 50% of the peak capacity, leading to a required DC/AC ratio of 2.0 (PBL, 2022). With a DC/AC ratio of 2.0, the amount of tables per inverter is 30. The DC/AC ratio used for PPA and ME is 1.6. According to K. Zipp (2018), this DC/AC ratio results in the lowest levelized cost of energy ("LCOE"), regarding both costs and produced energy. With a DC/AC ratio of 1.6, the amount of tables per inverter is 24.

To take into account the impact of the DC/AC ratio on the revenue streams, the costs of the inverter and transformer are scaled with the DC/AC ratio, as apposed to the generalised price per installed MW capacity from Vattenfall data that is mentioned in Table 5.5. The amount of modules connected per inverter can be used to determine the CAPEX and inverter replacement costs per installed MW_p.

Furthermore, the maximum amount of inverters that can be connected to the transformer should be taken into account. The transformer used is the Meins SPS-7000 33 kV, which can connect 7000 kVA and steps up the voltage to 33 kV. The maximum amount of Sungrow inverters that can connect to one transformer is 19, given past experience of Vattenfall and the transformer and inverter specifics.

The unit costs of one transformer can be linked to the number of inverters and therefore the number of modules connected the inverters. This way, the costs of an inverter and transformer per MW_p are smaller with a higher DC/AC ratio, since less inverters and transformers are required per installed MW_p.

The detailed breakdown of the costs can be seen in Table 5.9. The total CAPEX for solar with a DC/AC ratio of 2.0 and 1.6 become 0.49 €/MWIC and 0.50 €/MWIC respectively.

Table 5.9: CAPEX and OPEX for inverter and trafo incorporating DC/AC ratios for different revenue streams.

DC/AC Ratio	2	1.6	Unit
Modules per Inverter	810	648	#Mod / Inv
MW_p per Inverter	0.4455	0.3564	MW_p / Inv
CAPEX Inverter	€ 5,725.00		€ / Inv
	€ 12,850.73	€ 16,063.41	€ / MW_p
Replacement OPEX Inverter y 1-5	€ 0.60		€ / Inv
	€ 1.35	€ 1.68	€ / MW_p
Replacement OPEX Inverter y 6-20	€ 1,868.91		€ / Inv
	€ 4,195.09	€ 5,243.86	€ / MW_p
Replacement OPEX Inverter y 21-25	€ 27.62		€ / Inv
	€ 62.00	€ 77.50	€ / MW_p
Replacement OPEX Inverter y 26-30	€ 27.62		€ / Inv
	€ 62.00	€ 77.50	€ / MW_p
Max Inverters per Trafo	19		#Inv / Trafo
Modules per Trafo	15,381	12,305	#Mod / Trafo
MW_p per Trafo	8.46	6.77	MW_p / Trafo
CAPEX Trafo	€ 185,369.42		€ / Trafo
	€ 21,912.44	€ 27,390.11	€ / MW_p

The break-down of the fixed loss and gain factor η_{solar} can be seen in Table 5.10. The module and inverter specific losses are included in the PVLib calculations.

Table 5.10: Solar system losses based on past Vattenfall projects

Fixed Loss and Gain factor η_{solar}		
Mismatch losses	0.6%	Module mismatch losses
	0.1%	String voltage mismatch losses
Soiling losses	2.0%	Agricultural land
Ohmic losses	0.6%	DC wiring, at STC
	0.5%	AC wiring, at STC
Conversion losses	0.1%	Iron loss
	1.0%	Inductive loss
Auxiliary losses	0.3%	
Averaged shading	2.0%	
Total	**7.2 %**	

The azimuth for a south oriented farm is 180°, based on the PVlib convention. The azimuth for the east-oriented farms is 90°and west-oriented is 270°. The tilt of the tables is constrained due to height restrictions. Given the table lay-out and height restrictions, the tilt of both east-west and south oriented farms is no larger than 10°.

To calculate the power density using the shading approach as discussed in section 4.3, the width and height of the module, as seen in Table 5.8, and the solar position at the instances are required for the inter-array distance calculations. A summary is shown in Table 5.11 for south oriented farms and Table 5.12 for east-west oriented farms.

For south oriented farms, the instance used is 12:00 solar time on the 21^{st} of December. The solar position at this instance is shown in Figure 5.11.

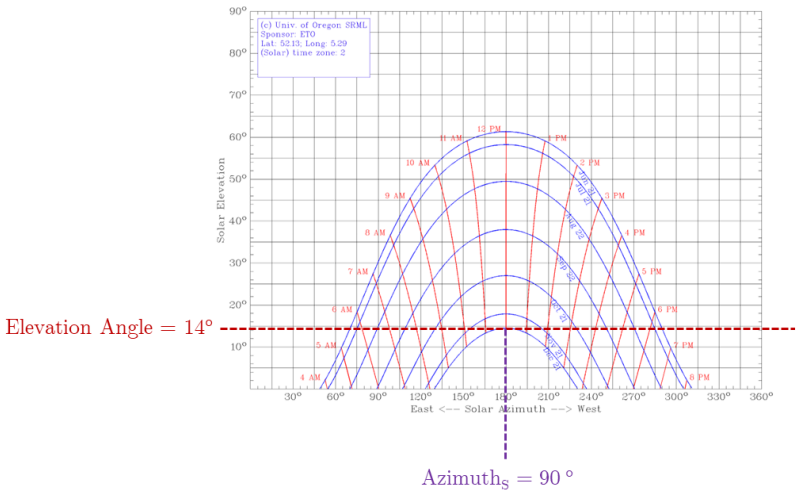

Figure 5.11: Solar position at 12:00 solar time on the 21st of December and the azimuth for a south oriented farm (Solar Dat, 2023)

The solar azimuth at this instance 180°and the solar elevation angle θ_{el} is 14°(Solar Dat, 2023). The azimuth of the solar farm therefore does not need to be corrected for the solar azimuth. An overview of the input values can be found in Table 5.11.

Table 5.11: Solar elevation and azimuth at 12:00 on the 21st of December and the azimuth for a south oriented farm (Solar Dat, 2023)

Solar Position South	
$\theta_{el,S}$	14 °
$azimuth_S$	180 °
$\theta_{az,S}$	$cos(0)$

For east-west oriented farms, the instances used are 09:00 and 15:00 on the 21st of December as shown in Figure 5.12.

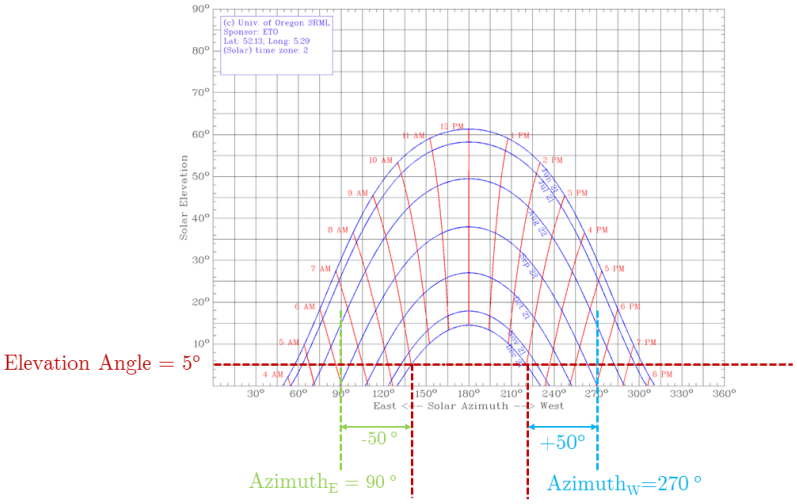

Figure 5.12: Solar position at 06:00 and 18:00 solar time on the 21st of December and the azimuth for a east- and west oriented farm (Solar Dat, 2023)

The solar elevation angle θ_{el} is 5°and the solar azimuth at the first and second instance are 140°and 220°(Solar Dat, 2023). The azimuth of the solar farm needs to be corrected for the solar azimuth. For an east and west orientated panel, with an azimuth of 90°and 270°respectively, the azimuth correction θ_{Az} is $\pm$ 50°. Both instances result in the same correction and calculation, so only one instance needs to be used.

Table 5.12: Solar elevation and azimuth at 09:00 and 15:00 solar time on the 21^{st} of December, abbreviated to "AM" and "PM", and the corrected azimuth for a east- or west oriented farm (Solar Dat, 2023).

Solar Position East-West	
$\theta_{el,EW}$	5 °
$azimuth_{AM}$	140°
$azimuth_{PM}$	220°
$\theta_{az,EW}$	$cos(50)$

Following the values from the case study and the approach of section 4.3, the power density values for the south oriented farm and east-west oriented farm are 94.24 and 140.18 W/m^2 respectively. Please note that the values used in results are 94.82 W/m^2 for the south-oriented farm and 123.31 W/m^2 for the east-west oriented farm based on a previous different calculation method.

The degradation is assumed to be 1.5% in the first year and 0.3% in the following years. The yearly unavailability of solar farms is assumed to be 0.5%, so the technical availability is 99.5%. The values used for degradation and unavailability in this case study correspond to values used by Vattenfall.

Wind

The turbine used in this case study is the Siemens Gamesa 6.6 MW turbine with 170 m rotor diameter. The specifications can be seen in Table 5.13.

Table 5.13: Wind turbine specifics (Siemens Gamesa, 2021)

Wind Turbine Specifics	
P_{rated} [MW]	6.6
hh [m]	145
A_{rotor} [m^2]	22697
R_{rotor} [m]	85

To calculate the WLF, the output power of a turbine for all hours of the year must be determined using the wind speed at hub height. As mentioned in chapter 4, the logarithmic and power law can be used to arrive at the wind speed at the hub height. The inputs for these laws are blending height h_{blend}, power law factor α and surface roughness z_0. The blending height h_{blend} is 60 m, after which the influence of the terrain is no longer visible in the wind pattern (Zaaijer and Viré, 2021).

The measurement heights of the ERA5 data are 10 and 100 meters. The 100 m value is used as reference height, eliminating the use of the logarithmic law. Only the power law is thus required to arrive at the wind speed at hub height U(hh) from the reference height h_{ref}. The power law factor α is 0.143 over land (Zaaijer and Viré, 2021). The surface roughness over land can be considered z_0=0.03 meters.

Table 5.14: Wind power law inputs (Zaaijer and Viré, 2021)

Wind Power Law Inputs	
h_{ref} [m]	10, 100
h_{blend} [m]	60
α [-]	0.143
z_0 [m]	0.03

An overview of the losses considered in the Fixed Loss and Gain factor η_{wind} can be found in Table 5.15. The main part of the losses can be attributed to the wake losses between turbines. This only plays a role if there are a multiple of turbines installed, but the losses are considered here to account for the conservative case. The losses due to the transformer and losses within the cable are 1% and between 0.2-0.4% respectively. The worst-case of 0.4% is used. Next to losses, Vattenfall considers an unavailability of the turbines during 4% of the year and thus an availability of 96%.

Table 5.15: Losses in the wind system.

Fixed Loss and Gain factor η_{wind}	
Wake losses	10%
Trafo losses	1%
Cable losses	0.2-0.4%
total	**11.20-11.40 %**

The power density for wind farms considered is 15.22 W/m^2, following the approximation from section 4.3. The power density is only considered when the upper boundary based on the land size and the power density has a value higher than the rated capacity of one turbine. This ensures at least one turbine can be built. The degradation is assumed to be 1.6% every year (Staffell and Green, 2014).

5.3. Battery

This section describes the case study dependent and general inputs for the battery addition to the hybrid farm. First, the different configurations will be discussed, followed by technology specific inputs.

As mentioned in section 4.2, the battery configuration can be determined by specifying the power of the battery and the C-rate, automatically defining the capacity of the battery. Given the projected use-case of peak shifting, the C-rate is chosen to be either $\frac{1}{2}$ or $\frac{1}{4}$, based on van Cappellen et al.(2023), corresponding to two or four hours of charging required to fully charge the battery.

The approach is to add a predetermined battery type to the optimization and to optimally size the solar farm based on the addition of this battery and all other constraints. The power size considered are 0.5 MW, 1 MW, 2 MW and 3 MW. All power sizes are used with both C-rates. This leads to the following battery configurations.

Table 5.16: Battery configurations

Power	**C-rate**	**Energy**
0.5 MW	1/2	1 MWh
0.5 MW	1/4	2 MWh
1 MW	1/2	2 MWh
1 MW	1/4	4 MWh
2 MW	1/2	4 MWh
2 MW	1/4	8 MWh
3 MW	1/2	6 MWh
3 MW	1/4	12 MWh

The battery type used is lithium-ion. To indicate how on-site storage affects the cost-benefit framework, general lithium-ion battery energy system specifics are used, instead of a specific manufacturer or datasheet. Based on NREL (Cole et al., 2021), a typical round-trip efficiency (”RTE”) for a lithium-ion battery energy storage system is 85%. The efficiency for charging and discharging is therefore eff$= \sqrt{0.85}$=0.92%.

As mentioned in section 4.2, the batteries degrade over the lifetime of the battery. A battery is assumed to be at the end of life (”EoL”) when the degradation reaches two thirds of the original capacity. An aver-

age of 15 years until EoL is used by Cole et al. (2021), leading to a yearly degradation of approximately 2.5%. The battery is allowed to charge and discharge at a maximum rate of the power rating of the battery. Furthermore, the capacity level in the battery may not drop below or be higher than the minimum and maximum SoC, which are assumed to be 10% and 90%, to limit degradation.

The costs of the battery are first disregarded to analyse the added revenues due to the addition battery. Given the new NPV of the system, the costs can be used to find the NPV including the battery costs. Given that the batteries are not expected to become profitable before 2030 by using a single revenue stream, as discussed in chapter 2, a subsidy is likely needed to make up for the unprofitable part of this business case. Adding the costs after the optimization shows the affect of on-site storage on the cost-benefit framework the subsidy or additional revenue streams required to have an added value. The CAPEX and OPEX can be based on the NREL estimations for 2025, resulting in a CAPEX of 250 €/kWh and an OPEX of 35 $/kWh per year (Cole et al., 2021).

6

Results and discussion

This chapter shows the results of the optimization and discusses the outcomes. For the base case, the optimization will be performed for two base years, 2019 and 2022, and for three revenue models, SDE++, PPA and ME. Some base case inputs are discussed in section 6.1. The results of the base case of the hybrid farm are discussed section 6.2. The sensitivity of the base case results will be analysed by varying various inputs and is discussed in section 6.3. The results of the hybrid farm including a battery are discussed in section 6.4.

6.1. Base Case Inputs

In this section, inputs of the optimization that are calculated by the tool are discussed. First, the weather data introduced in subsection 5.2.1 is shown in more detail in subsection 6.1.1. After the weather data, two important time dependent calculated inputs are discussed: (1) The modeled output of the existing farm and the resulting free cable capacity in subsection 6.1.2, followed by (2) the WLF of the new resources subsection 6.1.3. These inputs are later used to explain the results.

6.1.1. Weather data

The weather data has been generally discussed in chapter 5 using the statistics of the weather data to compare 2019 and 2022 data. The wind speed data of 2019 had a slightly higher average than 2022, while the wind speeds showed more variability in 2022. The solar irradiance data showed a higher average and variability in 2022 compared to 2019.

The weather data is shown in more detail in Figure 6.1. The figures show hourly GHI and wind speed at 100 meters for 2019 and 2022 for the first seven days of January, April, July and October. The average wind speeds are higher in January, April and October than in July, corresponding to the seasonal behaviour of wind. The seasonal behaviour is also visible in the irradiation patterns: in July the irradiation levels run up to 800 W/m^2 while in October and April this reduces to 500 W/m^2, with the lowest irradiation in January where the peak touches 250 W/m^2. Furthermore, the irradiation patterns show daily patterns with no generation at night and a peak at noon.

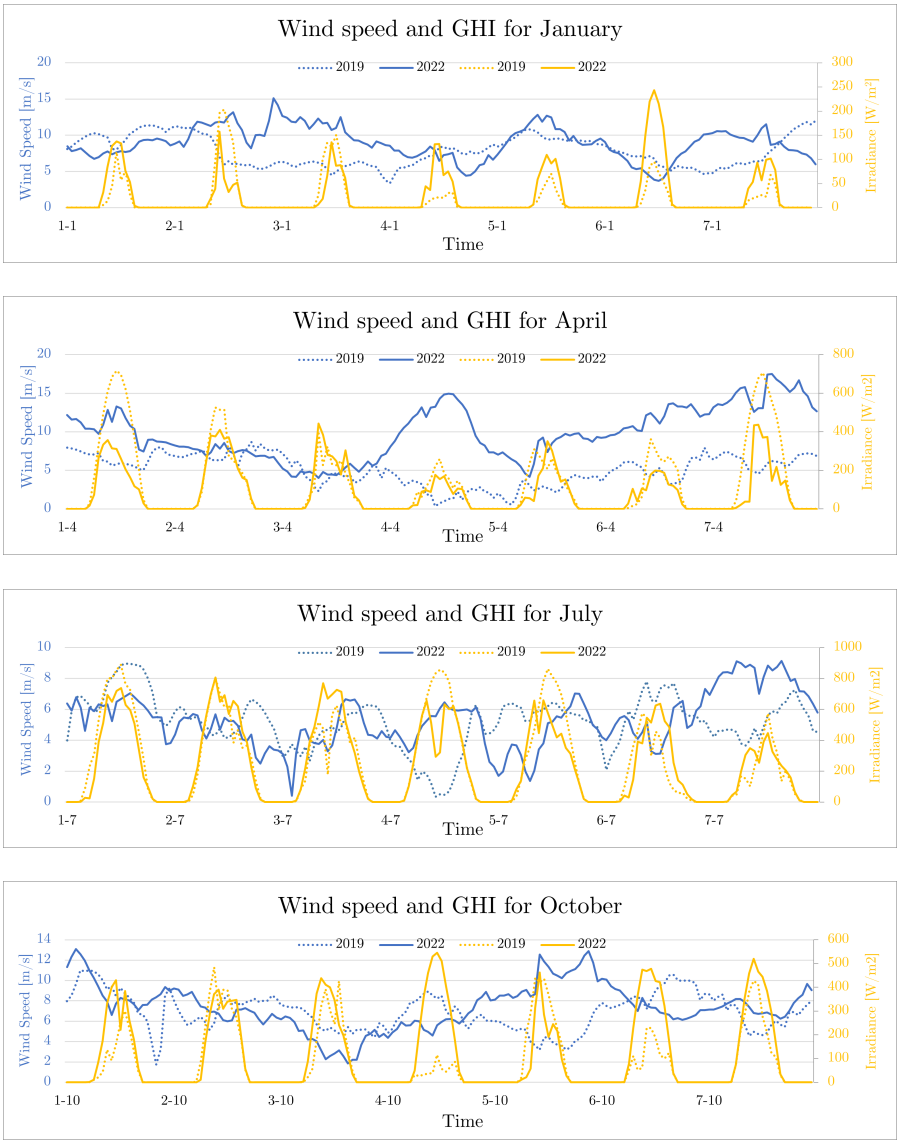

Figure 6.1: Weather data in different months of 2022 and 2019.

The expectation is that for both farms, the weather patterns are proportional to the output of the existing farm, the WLF and ultimately the sold and curtailed energy profiles of the new farms resulting from the optimization.

6.1.2. Output of Existing Farm and Cable Capacity

The residual space on the cable can be found based on the output pattern of the existing farm. As mentioned in chapter 5, the existing farm considered is a solar farm oriented to the east and west. The size is approximately 15 MWp and the grid connection size is 13 MVA. The assumption is that the inverters are sized to match the grid connection size, corresponding to a DC/AC ratio of 1.2.

For 2019 and 2022, the output of the existing farm are shown for a full year in Figure 6.2 and for for the first weeks of January, April, July and October in Figure 6.3. The yearly pattern shows a high production in summer and a low production in winter, corresponding to the seasonal behaviour of solar energy.

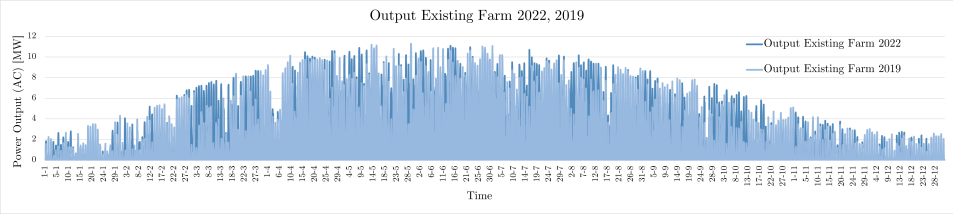

Figure 6.2: Expected hourly output of existing farm based on weather data from 2022 and 2019.

Considering the output on a one week scale the differences on a smaller scale are visible. The different weather and thus solar irradiation patterns of 2019 and 2022 create varying outputs. April 2019 showed higher irradiance values and therefore output of the solar farm than 2022, but October showed the opposite trend.

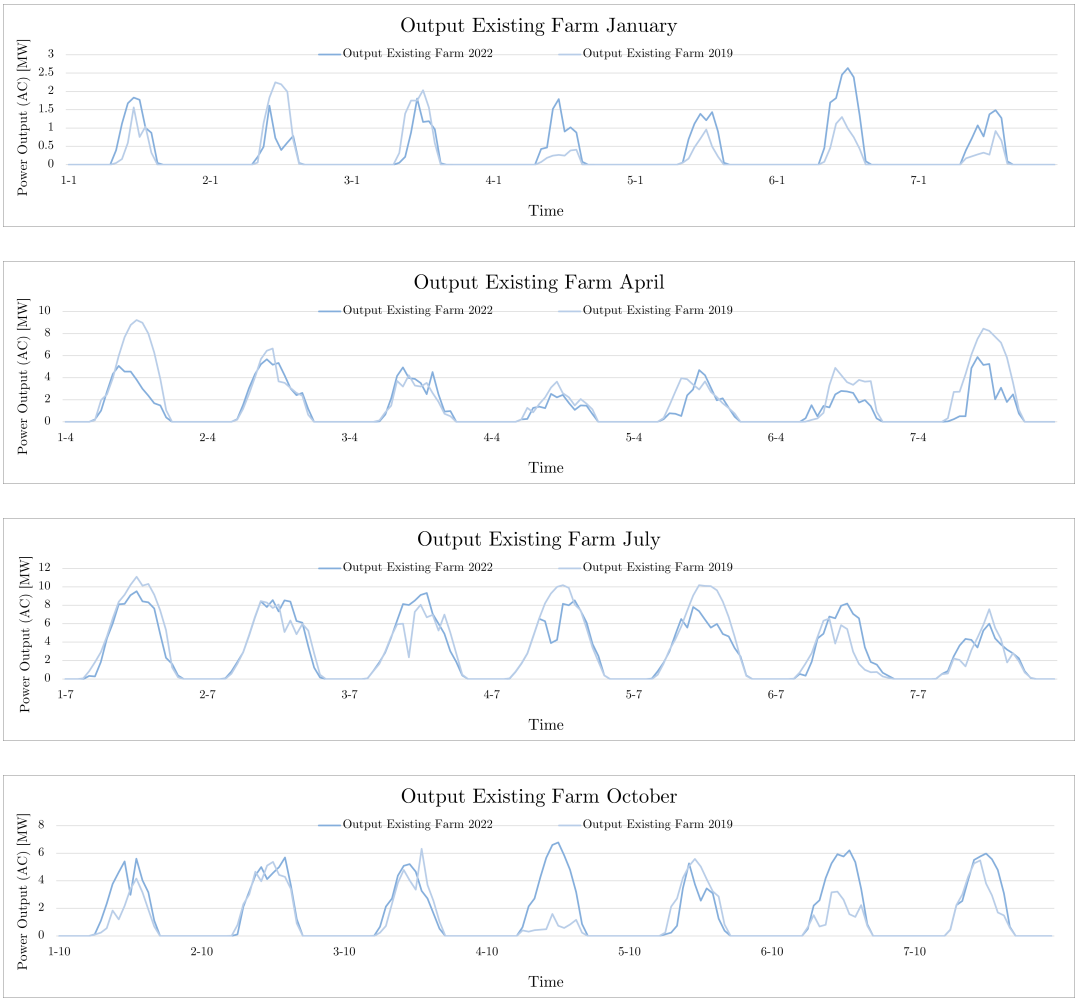

Figure 6.3: Comparison of expected hourly output of the existing farm for different months based on weather data from 2022 and 2019.

To quantify the difference between 2019 and 2022, the mean, median and the sample standard deviation are presented in Table 6.1.

Table 6.1: Comparison of Solar Farm Output Data (2019 vs. 2022)

	2022	2019
Mean [MW]	1.71	1.60
Median [MW]	0.0306	0.0293
Std [MW]	2.63	2.51

The expected mean and median of the solar farm output are higher based on 2022 than 2019 data, indicating that on average, the expected output of the existing farm is higher using 2022 than 2019 data, in line with the weather statistics. The standard deviation of the expected power output using 2022 weather data is higher than 2019, also similar to the weather statistics.

The hourly output of the existing farm is used to determine the residual space on the cable, which forms an export constraint for the new resources. The expected residual cable capacity will on average be higher using the 2019 weather data.

6.1.3. Weather and Losses Factors

The WLF for solar and wind farms are dependent on the weather data. First the WLF for solar farms in different revenue models are shown, followed by the weather and losses factor of wind.

Solar

The WLF is calculated based on the output of one inverter which is based on the configuration of modules connected to that inverter. As discussed in chapter 5, the revenue model influences the DC/AC ratio, which impacts the configuration of modules connected to one inverter and thus the expected AC output of that one inverter. The DC/AC ratio is 1.6 for both PPA and ME revenue models and 2.0 for the SDE++ revenue model.

In Figure 6.4a, Figure 6.5a and Figure 6.6a the expected output of one inverter are shown for both SDE++, and PPA, also representing ME, for the first seven days of January 2022, July 2019 and October 2019. The separate curves for the east and west oriented strings, both connected to separate inverters, are shown.

The hourly output of that one inverter is multiplied by fixed losses in the system and divided by the number of panels connected to the inverter, based on the DC/AC ratio, to arrive at the hourly WLF percentage. In Figure 6.4b, Figure 6.5b and Figure 6.6b the calculated WLF are shown for the same revenue models.

Considering the first week of January, shown in Figure 6.4, the WLF ranges from about five to 30% during the day. A clear day and night pattern can be seen. The south oriented farm reaches higher values compared to the east-west oriented farm for most days.

Since both DC/AC ratios are larger than one, the DC system is oversized with regards to the inverter input. This can lead to inverter clipping. At times of low irradiance, inverter clipping is not required. The PPA/ME and SDE++ revenue model have nearly the same WLF values at times of low irradiance since the WLF is scaled with the amount of modules connected to the inverter. The originally different inverter output values as seen in Figure 6.4a result in the same normalized WLF values.

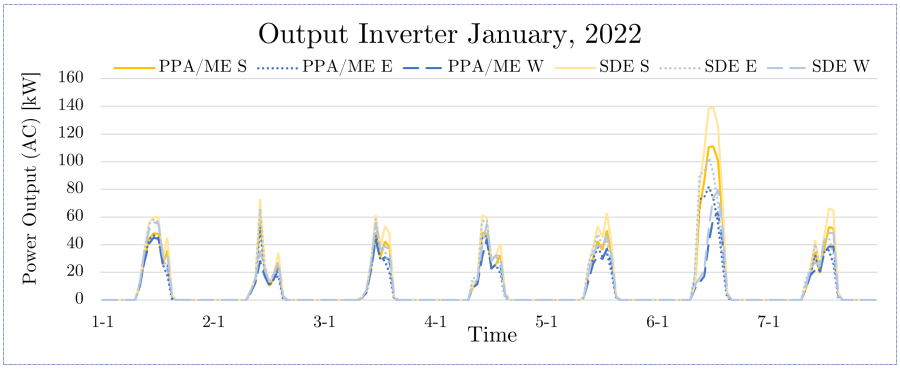

(a) AC output of inverter for January 2022 for the SDE++ and PPA/ME models, leading to DC/AC ratios of 2.0 and 1.6 respectively for east, west and south oriented modules.

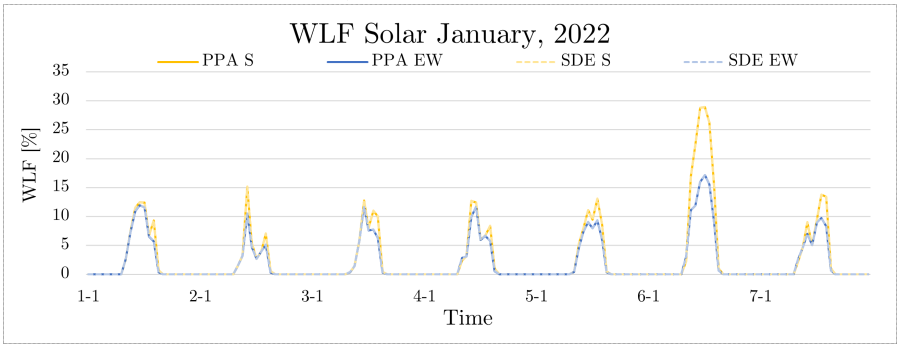

(b) WLF factor based on the inverter output in January 2022 for SDE++ and PPA/ME models which result in the same values for all revenue models.

Figure 6.4: AC output of inverter and WLF factor for all three revenue models for both EW and S oriented farms

The oversized system does require inverter clipping at times of high irradiance, visible as cut-offs in Figure 6.5a. The output is capped at the output power on the AC side of the inverter $P_{ac,0}$, as introduced in Table 5.7, for both east-west and south oriented farms and for both revenue models.

In Figure 6.5b, the difference between the DC/AC ratio used in the different revenue models can be seen in the WLF values. The SDE++ system contains more modules connected to one inverter on the DC side than the PPA or ME revenue model. This explains the higher WLF cut-off for the PPA/ME revenue model compared to the WLF cut-off for the SDE++ revenue model at times of high irradiance. The difference between the WLF of the east-west oriented and south oriented farm is marginal at times of high irradiance, since the produced energy is capped for both orientations at this maximum output power $P_{ac,0}$ value and the WLF is scaled with the number of modules connected to that inverter.

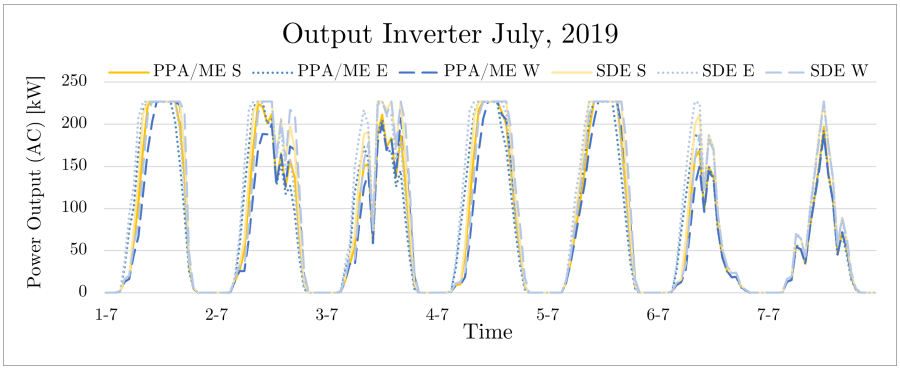

(a) AC output of inverter for July 2019 for the SDE++ and PPA/ME models, leading to DC/AC ratios of 2.0 and 1.6 respectively for east, west and south oriented modules.

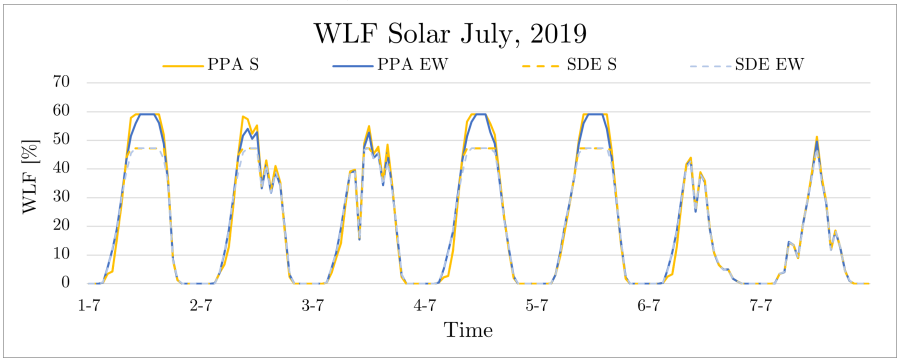

(b) WLF factor based on the inverter output in July 2019 for SDE++ and PPA/ME models which result in the same values for all revenue models.

Figure 6.5: AC output of inverter and WLF factor for all three revenue models for both EW and S oriented farms

In October no difference between the WLF of the different revenue models can be seen again given the low irradiance and no capping required. The WLF values are higher for the south oriented farm most of the times.

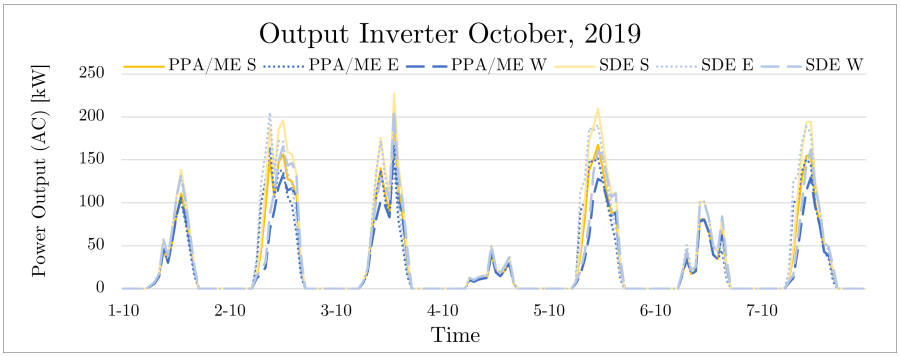

(a) AC output of inverter for October 2019 for the SDE++ and PPA/ME models, leading to DC/AC ratios of 2.0 and 1.6 respectively for east, west and south oriented modules.

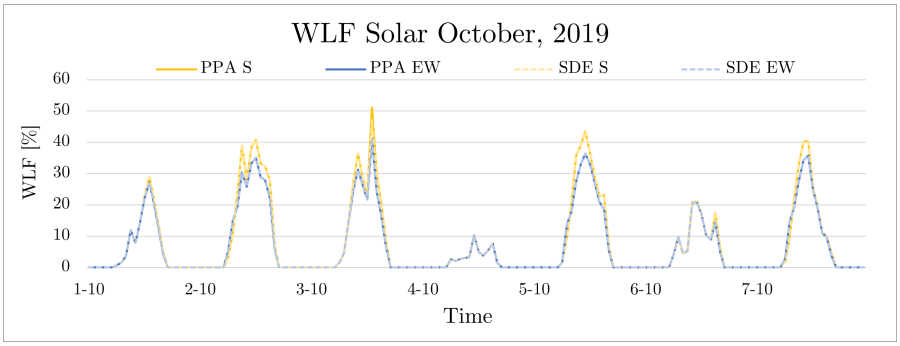

(b) WLF factor based on the inverter in October 2019 for SDE++ and PPA/ME models which result in the same values for all revenue models.

Figure 6.6: AC output of inverter and WLF factor for all three revenue models for both EW and S oriented farms

To better compare the WLF values for east-west and south oriented farms for all revenues models, the statistics of the data sets are considered, as shown in Table 6.2 and Table 6.3. The WLF factors for the ME and PPA revenue model show the same statistics for both years and both orientations, due to the similar DC/AC ratio. The SDE++ average and sample standard deviation are lower while the median shows higher values than the PPA and ME revenue model. Due to the larger number of modules connected to one inverter in the SDE++ revenue model, the inverter has an output of zero on the AC side less often, which can explain the higher median values.

The fact that average WLF is lower for the SDE++ revenue model can be attributed to the cut-off, resulting in lower values on average, which was already visible in Figure 6.5. The fact that the variability is lower for the SDE++ revenue model for both years and orientations, can be explained by the fact that the inverter has smaller fluctuations in the AC output due to a more uniform production profile of the accumulated output of the increased number of modules.

Table 6.2: Statistics of Weather and Losses Factors for different revenue models based on 2019 for a). East-West oriented farms and b). South oriented farms

(a) East-West

	ME	**PPA**	**SDE++**
Avg [%]	10.32	10.32	9.85
Med [%]	0.23	0.23	0.26
Std [%]	16.00	16.00	14.74

(b) South

	ME	**PPA**	**SDE++**
Avg [%]	10.98	10.98	10.37
Med [%]	0.25	0.25	0.28
Std [%]	17.22	17.22	15.63

Table 6.3: Statistics of Weather and Losses Factors for different revenue models based on 2022 for a). East-West Oriented Farms and b). South oriented farms

(a) East-West

	ME	PPA	SDE++
Avg [%]	11.02	11.03	10.49
Med [%]	0.24	0.24	0.27
Std [%]	16.75	16.75	15.39

(b) South

	ME	PPA	SDE++
Avg [%]	11.77	11.77	11.01
Med [%]	0.24	0.24	0.27
Std [%]	18.17	18.17	16.36

The average, median and standard deviation values are all lower for solar farms oriented to the east-west compared to the farms oriented to the south.

Wind

The weather and losses factor for wind in January and October based on input year 2019 and 2022 are shown in Figure 6.7. No clear pattern can be distinguished. The moments that the values for input year 2019 are higher than 2022 and vice versa correspond with the behaviour of the wind speeds during these periods. A clear cut-off can be seen at 87%, due to the internal losses in the system.

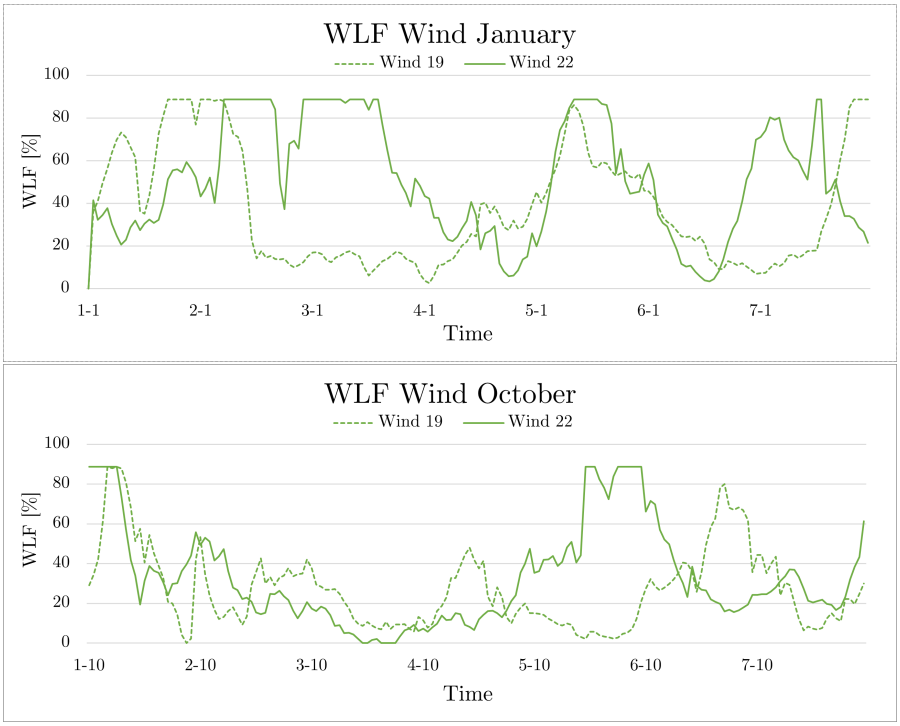

Figure 6.7: WLF of the potential wind farm in January and October.

6.2. Base Case Hybrid Farm Optimization Results

After the discussion of some time dependent input variables, the results of the optimization are presented and discussed. First, the behaviour of the hybrid farm is discussed. Afterwards, the results of each possible additions and input year are discussed for the different revenue models. Lastly, the results are presented in more detail using the yearly costs and revenues.

The behaviour of the total hybrid farm is illustrated using Figure 6.8, Figure 6.9 and Figure 6.10. The figures show the output of the existing farm and resulting residual cable capacity. The addition of wind or solar oriented to the east-west or south lead to new energy production, categorized in sold and curtailed energy. Adding the sold energy and the output of the existing farm, the combined energy output is found.

The first weeks of January, July and October are shown using 2022 data and the ME revenue model. The daily pattern of the existing farm is clearly seen in the output of the existing farm resulting in the residual cable capacity, with periods at night of no production and a fully available cable capacity.

In Figure 6.8, the addition of the wind farm increases the output of the total farms significantly, compared to both solar farms. Both solar farms oriented to the east-west and south have a similar production pattern to the existing farm and only produce at times when the existing farm also produces energy. The cable is still not used during the night, which is not the case for the wind farm. The wind farm curtails energy on the 3rd of January, while there is room available on the cable, as a result of negative market prices.

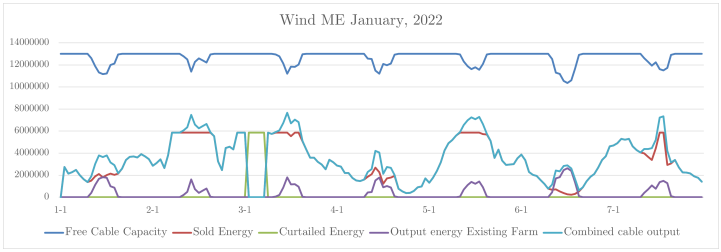

(a) Wind

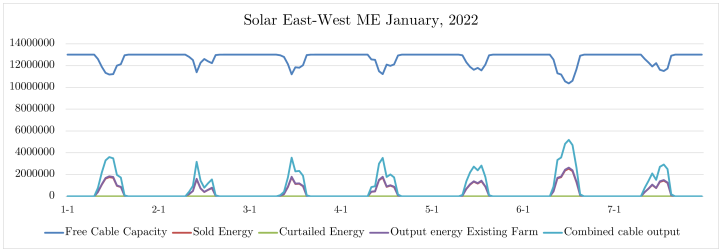

(b) Solar EW

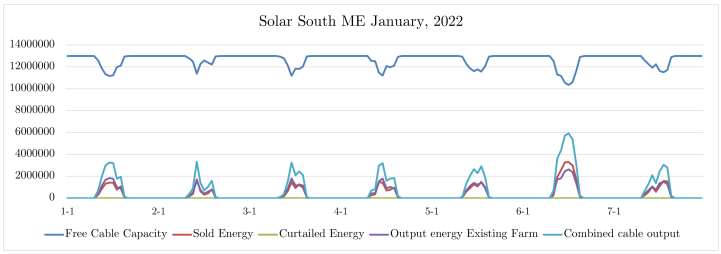

(c) Solar S

Figure 6.8: Free cable capacity, sold and curtailed energy, output energy of existing farm and combined cable output for the first week in January for Wind, Solar EW and Solar South using 2022 data and the ME revenue model.

In July, Figure 6.9, the impact of both solar farms on the total output of the farms is larger than the wind farm, as expected considering the seasonal behaviour. As mentioned before, both solar farms produce at the same time as the existing farm, resulting in periods of curtailment on one hand and periods of no usage of the cable on the other hand.

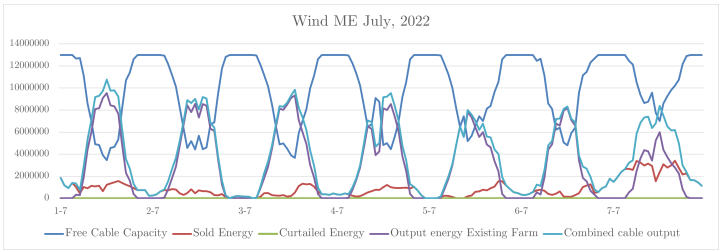

(a) Wind

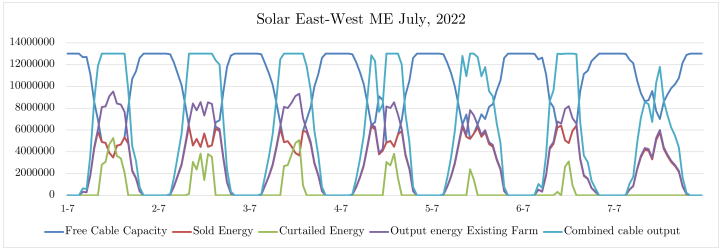

(b) Solar EW

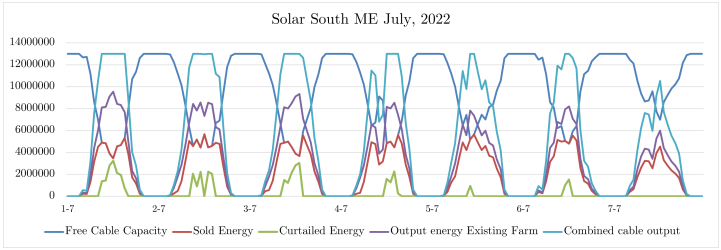

(c) Solar S

Figure 6.9: Free cable capacity, sold and curtailed energy, output energy of existing farm and combined cable output for the first week in July for Wind, Solar EW and Solar South using 2022 data and the ME revenue model.

On October 6th, Figure 6.10, a period of negative prices can be seen when solely the wind farm produces energy. No export constraint is active, but the energy is still curtailed, indicating negative prices. Later during the day, all three possible additions curtail energy, even with still some residual space on the cable. This is also due to a period of negative prices. On October 4th, the combined output of the existing farm and the added solar farms oriented either to the east-west or the south, is higher than the cable capacity. Therefore, albeit a small amount, energy is curtailed.

The results indicate that the energy is curtailed at times when the combined output is too high or when the prices are negative. It also shows that the export constraint is not violated in the current approach.

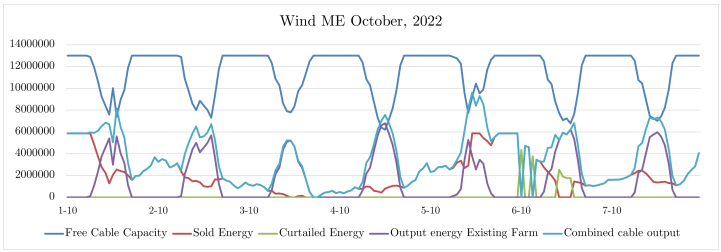

(a) Wind

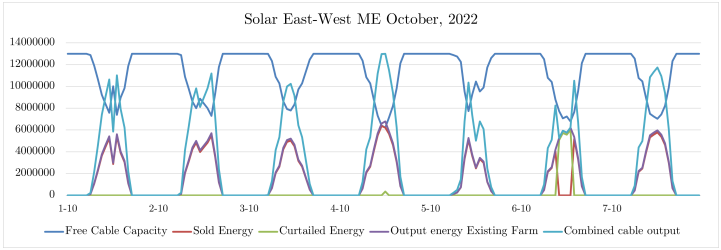

(b) Solar EW

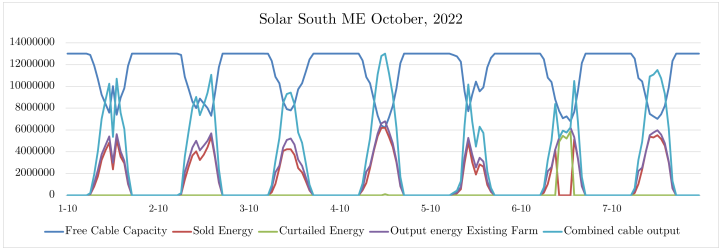

(c) Solar S

Figure 6.10: Free cable capacity, sold and curtailed energy, output energy of existing farm and combined cable output for the first week in October for Wind, Solar EW and Solar South using 2022 data and the ME revenue model.

In Table 6.5, Table 6.6 and Table 6.7 the results of the optimization are shown for SDE++, PPA and ME revenue models respectively. Each table shows the output of all three options for one weather- and spot market data input year. The economical indicators are the NPV and CAPEX. The different technical indicators are the installed capacity, capacity factor c_f of the new resource and the total generation $c_{f,tot}$, the cable capacity factor cc_f and the curtailment. The capacity factor of the farm before addition is 10.67% in 2019 and 11.60% in 2022. The cable capacity factor before addition of a new farm is 12.31 in 2019 and 13.38% respectively in 2022. An overview of the NPV and cable capacity factor cc_f values is shown in Table 6.4.

Table 6.4: Combined NPV and cable capacity factor for the three possible additions and both input years.

Year	model	Cable Capacity Factor (%)				NPV (€)		
		Before	Wind	Solar EW	Solar S	Wind	Solar EW	Solar S
2019	SDE++	12.31	25.17	22.33	20.91	7,835,431	3,636,107	3,607,003
	PPA	12.31	25.18	22.35	20.96	7,228,410	2,445,984	2,722,923
	ME	12.31	25.17	22.34	20.95	7,835,431	2,733,157	2,954,153
2022	SDE++	13.38	25.29	23.38	21.93	3,604,491	4,107,985	3,799,559
	PPA	13.38	25.32	23.76	22.35	4,905,470	3,033,529	3,166,238
	ME	13.38	25.29	23.54	22.16	3,604,491	3,113,634	3,093,212

The cable capacity factor cc_f, seen in either Table 6.4 or Table 6.5, Table 6.6 and Table 6.7, increases for all possible combinations, indicating a better usage of the grid connection point. The installed capacity, seen in Table 6.5, Table 6.6 and Table 6.7, in 2019 and 2022 is the same for all revenue models for each option, resulting in the same CAPEX. The installed capacity is equal to the upper limit of the

land boundary for all three additions for all revenue models and both input years, implying that the land area is an active constraint. The upper boundary of the solar farm oriented to the east-west farm (14.89 MW_p) is close to the value of the farm being developed by Vattenfall (approximately 15 MW_p). Due to the higher power density, more east-west installed capacity can be built compared to the south facing addition.

The capacity factor c_f and curtailment can be seen in Table 6.5, Table 6.6 and Table 6.7. The capacity factor of wind is higher using 2019 weather data than 2022 weather data and vice versa for solar, which can also be seen in the cable capacity factors before additions of the new resources and capacity factors of the existing farm. This corresponds with the weather and WLF statistics. The curtailment of all possible combinations is higher using 2022 data than 2019 data. This can be explained using the volatility of the electricity prices in both years, with 2022 spot market data showing more hours with negative prices, which leads to curtailment in the system.

Using the optimal installed capacity and the calculated WLF, the maximum produced energy by the added resource can be found. Illustrations of the maximum produced energy and the share that is sold can be found in Appendix A, combining the WLF and optimal installed capacity results.

The SDE++ model, shown in Table 6.5, leads to a positive NPV for all combinations in both years. The expected market value (MV) of wind energy, calculated using the the expected average spot market price in year t based on the LTMO and the value factor $LT_{f,j,t}$, does not drops below the wind SDE++ price of 62.4 €/MWh during the period the subsidy is awarded, as can be seen in Figure 5.10. Therefore, no subsidy is received for the added wind farm in the SDE++ revenue model, which is thus effectively the same as the ME revenue model for wind. The subsidy does impact the results of both solar farm additions, since the subsidy is awarded from 2028 until the subsidy ends in 2039.

In line with the higher capacity factor, the NPV for wind is higher using 2019 data than using 2022 data. Similarly, for solar farm oriented to the east-west and south the NPV is higher using 2022 data than 2019 data.

The solar farm oriented to the east-west generates a higher NPV than the farm oriented to the south based on both input years, despite the lower capacity factor. This is due to the higher installed capacity, based on two reasons. On the one hand, because of this, more energy can be produced and sold, if room available on the cable. On the other hand, more subsidy is awarded to the east-west oriented farm, which is dependent on installed capacity.

Table 6.5: SDE++ results for 2019 and 2022 for three possible additions

(a) 2019. The capacity factor of the existing farm is 10.67% and the cable capacity factor before the addition of the new resource is 12.31%.

	Wind	**Solar EW**	**Solar South**
NPV	€ 7,835,431	€ 3,636,107	€ 3,607,003
$P_{installed}$	6.60	14.80	11.38
CAPEX	€ 6,732,000	€ 7,424,463	€ 5,709,212
Capacity factor c_f	25.38%	10.32%	10.98%
Total capacity factor $c_{f,tot}$	15.16%	10.50%	10.80%
Cable capacity factor cc_f	25.17%	22.33%	20.91%
Curtailment	0.20%	10.64%	5.18%

(b) 2022. The capacity factor of the existing farm is 11.60% and the cable capacity factor before the addition of the new resource is 13.38%.

	Wind	**Solar EW**	**Solar South**
NPV	€ 3,604,491	€ 4,107,985	€ 3,799,559
$P_{installed}$	6.60	14.80	11.38
CAPEX	€ 6,732,000	€ 7,424,463	€ 5,709,212
Capacity factor c_f	23.97%	11.03%	11.76%
Total capacity factor $c_{f,tot}$	15.38%	11.32%	11.67%
Cable capacity factor cc_f	25.29%	23.38%	21.93%
Curtailment	2.13%	14.36%	8.91%

The PPA model, shown in Table 6.6, also results in a positive NPV for all combinations. The curtailment of the added wind farm is lower compared to the SDE++/ME model. The system curtails when there is no room on the cable or when the price is negative. For the PPA model, the hourly price used is the fixed PPA price, which is thus always positive. Therefore, no curtailment due to negative prices occurs leading to less curtailment for the wind farm compared to the other revenue models. The 0.06% curtailment is due to an export constraint. Due to the low curtailment and high capacity factor of wind, the cable capacity factor is largest with the PPA model using 2022 data for wind, reaching 25.32% compared to the 13.38% before addition of the wind farm.

For the solar farms the weather and losses factors differ between the SDE++ and PPA/ME model due to the different DC/AC ratios. So the curtailment in the PPA revenue model can only be compared to the ME revenue model curtailment. The curtailment in the PPA revenue model is indeed lower compared to the ME revenue model.

Despite the larger installed capacity, leading to more produced energy, and the higher cable capacity factor, the NPV for the solar farm oriented to the east-west is lower than the NPV for the solar farm oriented to the south. This can partially be explained by constant price for the energy reducing the value of the east-west oriented farm compared to the south oriented farm and partially by the higher WLF statistics and resulting capacity factor for the south oriented farm, resulting in more output per unit installed capacity. The farm oriented to the east-west does have higher net cash flows during operation than the south oriented farm, but also has higher investment costs. Therefore, the optimal NPV for the east-west oriented farm for this particular revenue model is lower compared to the south oriented farm.

Table 6.6: PPA results for 2019 and 2022 for three possible additions

(a) 2019. The capacity factor of the existing farm is 10.67% and the cable capacity factor before the addition of the new resource is 12.31%.

	Wind	**Solar EW**	**Solar South**
NPV	€ 7,228,410	€ 2,445,984	€ 2,722,923
$P_{installed}$	6.60	14.80	11.38
CAPEX	€ 6,732,000	€ 7,658,411	€ 5,889,112
Capacity factor c_f	25.38%	10.32%	10.98%
Total capacity factor $c_{f,tot}$	15.16%	10.50%	10.80%
Cable capacity factor cc_f	25.18%	22.35%	20.96%
Curtailment	0.06%	14.54%	9.98%

(b) 2022. The capacity factor of the existing farm is 11.60% and the cable capacity factor before the addition of the new resource is 13.38%.

	Wind	**Solar EW**	**Solar South**
NPV	€ 4,905,470	€ 3,033,529	€ 3,166,238
$P_{installed}$	6.60	14.80	11.38
CAPEX	€ 6,732,000	€ 7,658,411	€ 5,889,112
Capacity factor c_f	23.97%	11.03%	11.76%
Total capacity factor $c_{f,tot}$	15.38%	11.32%	11.67%
Cable capacity factor cc_f	25.32%	23.76%	22.35%
Curtailment	0.06%	15.50%	10.73%

The ME revenue model again results in positive NPV values for all three additions and both input years and is shown in Table 6.7. The NPV values for the wind farm are highest for both input years. The NPV values for the solar farm oriented to the south are higher with 2019 input data, but smaller with 2022 input data. This can be explained by the decreased value of the production of south oriented farms due to the higher south oriented solar penetration in 2022 compared to 2019, compared to a less decreased value for east-west oriented farms.

The average WLF for the ME and PPA model is higher than the SDE++ model, as seen Table 6.3 and Table 6.2, leading to more generated energy with the same input years and installed capacity and ultimately to more curtailment due to an active export constraint. The solar curtailment is higher in the ME revenue model compared to the PPA revenue model, due to negative prices in the ME revenue model. Using 2022 data, the curtailment values are highest for the ME revenue model, due to higher count of negative market prices compared to 2019 data.

Table 6.7: ME results for 2019 and 2022 for three possible additions

(a) 2019. The capacity factor of the existing farm is 10.67% and the cable capacity factor before the addition of the new resource is 12.31%.

	Wind	**Solar EW**	**Solar South**
NPV	€ 7,835,431	€ 2,733,157	€ 2,954,153
$P_{installed}$	6.60	14.80	11.38
CAPEX	€ 6,732,000	€ 7,658,411	€ 5,889,112
Capacity factor c_f	25.38%	10.32%	10.98%
Total capacity factor $c_{f,tot}$	15.16%	10.50%	10.80%
Cable capacity factor cc_f	25.17%	22.34%	20.95%
Curtailment	0.20%	14.60%	10.05%

(b) 2022. The capacity factor of the existing farm is 11.60% and the cable capacity factor before the addition of the new resource is 13.38%.

	Wind	**Solar EW**	**Solar South**
NPV	€ 3,604,491	€ 3,113,634	€ 3,093,212
$P_{installed}$	6.60	14.80	11.38
CAPEX	€ 6,732,000	€ 7,658,411	€ 5,889,112
Capacity factor c_f	23.97%	11.03%	11.76%
Total capacity factor $c_{f,tot}$	15.38%	11.32%	11.67%
Cable capacity factor cc_f	25.29%	23.54%	22.16%
Curtailment	2.13%	19.09%	14.74%

The curtailed energy data points for the ME revenue model using 2022 data are plotted against the corresponding spot prices at that time in Figure 6.11. The added solar farms have similar generation patterns to the existing resource, so for solar energy, curtailment due to export limitations occurs more often than for the added wind farm. At negative prices, the maximum produced output of the added solar farms is curtailed. At positive prices, a share of the maximum produced output of the added solar farms can also be curtailed due to a limited export capacity. For wind energy, the curtailment almost only occurs at negative price. This indicates the complementary behaviour of the generation patterns of the added wind farm and the existing solar farm oriented to the east-west.

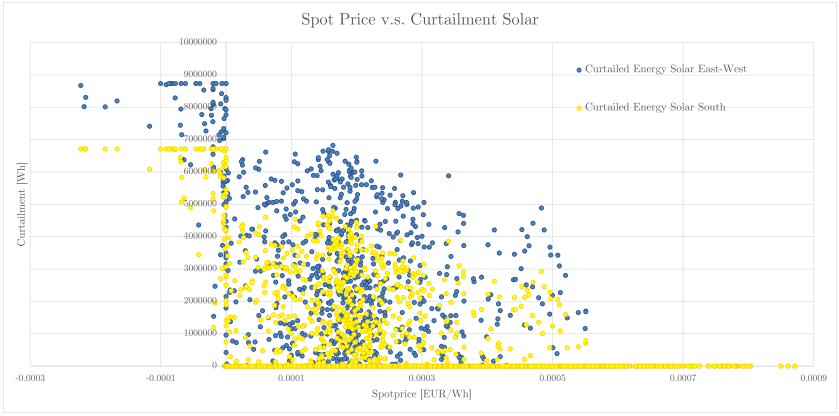

(a) Solar EW and S

(b) Wind

Figure 6.11: Scatterplot of curtailed energy and spot prices in 2022.

Based on the results presented above, it stands out that the differences between the NPV using 2019 and 2022 weather and spot market data are large for the added wind farm in all revenue models compared to the differences between the NPV using 2019 and 2022 weather data for the added solar farms. The wind NPV using 2019 data is more than double the NPV of wind based on 2022 data. The NPV of both solar farms is higher based on 2022 data compared to 2019 data, but with a smaller difference compared to wind.

The NPV is found by summing the yearly discounted net cash flows, which consist of yearly revenues and costs. The sold and curtailed energy indicate the behaviour of the system on hourly scale for one full year and the revenues earned by the sold energy are summed to find the yearly revenue. This is reproduced for the full lifetime of the project accounting for yearly factors based on the LTMO for years where the revenue model is exposed to market prices, inflation, degradation and discounting. The revenue side thus depends on the input spot market prices, input weather data and the correction factors used. The impact of these inputs and correction factors differs per revenue model.

First the impact of the weather data is discussed by considering the capacity factors and the yearly summed sold energy. The capacity factor for wind is 25.38% using 2019 data while it is 23.97% using 2022 data. In the SDE++ and ME case for example, the total sold wind energy in one year using 2019 data is 14.64 GWh, compared to 13.56 GWh using 2022 data. For the solar farms this difference is smaller, with for example a total sold energy of 12.28 GWh based on 2022 and 12.06 GWh based on 2019 data for the east-west oriented solar farm. These differences are in line with the weather and WLF statistics and partly explain that the 2022 values are higher for solar and 2019 values are higher for wind.

Another factor creating a larger difference between 2019 and 2022 input data for wind, is the fact that

the existing farm produces less output based on 2019 weather data resulting in more space on the cable compared to 2022 data. The residual cable capacity is thus higher based on 2019 data when the wind farm also produces more, while it is smaller based on 2022 data when the solar farm produces more.

The second factor impacting the difference between the two input years is the spot market prices. The hourly spot market prices influence the SDE++ and ME revenue values throughout the full lifetime of the project and the PPA revenue values after the duration of the PPA. The hourly spot market prices are on average higher for 2022 data than 2019 data. The yearly revenues are found by summing the hourly revenues consisting of a price and a volume.

For wind, the uncorrected summed revenue based on the 2019 spot market prices is lower than based on 2022 spot market prices. Using 2019 data, this revenue is €582,312, compared to €2,534,442 using the 2022 spot prices, despite the higher production and export capacity based on 2019 weather data. For the east-west oriented solar farm, the uncorrected summed revenue for base year 2022 was €2,919,283 and for base year 2019 €481,108 respectively.

The last factor impacting the revenue side are the correction factors used to find the value of the revenues for each year in the lifetime T_j. The uncorrected summed yearly revenues are corrected using the long-term market factor LT_t and technology dependent value factor $\mathrm{LT}_{\mathrm{f},j,t}$ when exposed to market prices and inflation, discount rate and degradation of the existing and added farm for all revenue models and years t considered.

In Figure 6.12, the yearly discounted revenues for all combinations can be seen. The hourly price is the market price for SDE++ and ME for all years in the lifetime of the project. The hourly price is the PPA price in the PPA model for the first ten years of the project. The hourly prices considered after the duration of the PPA are the market price. In the SDE++ model, a potential subsidy is awarded in the shape of a yearly addition to the earned revenue from the market, if the market value is indeed lower than the BB of the technology and until the duration of the SDE++ ends, which is 15 years after the start of the project.

As expected the SDE++ and ME trajectory for wind have the same values. The PPA revenues for the wind and both solar additions show a slight drop in the yearly revenues after the 10 year duration of the PPA. After the duration of the PPA the yearly revenues are market exposed and join the ME trajectory. The SDE++ and ME revenue models for both the solar farms and the wind farm start with the highest yearly revenues and quickly show a drop, following the trajectory of the expected average spot market prices, as seen in the LTMO in Figure 5.10. For the solar farms, the SDE++ helps to recover the yearly revenues compared to the ME revenues. After the duration of the SDE++, the revenues of the added solar farms based on the SDE++ revenue model drop and join the revenues based on the ME revenue model.

The yearly revenues based on 2019 input data are higher than the revenues based on the 2022 input data for the SDE++, PPA and ME revenue models for the added wind farm, in line with the NPV values. The yearly revenues based on 2022 input data are higher than the revenues based on the 2019 input data for the PPA revenue model for both added solar farms for the first 10 years of the project, after which the yearly revenues converge.

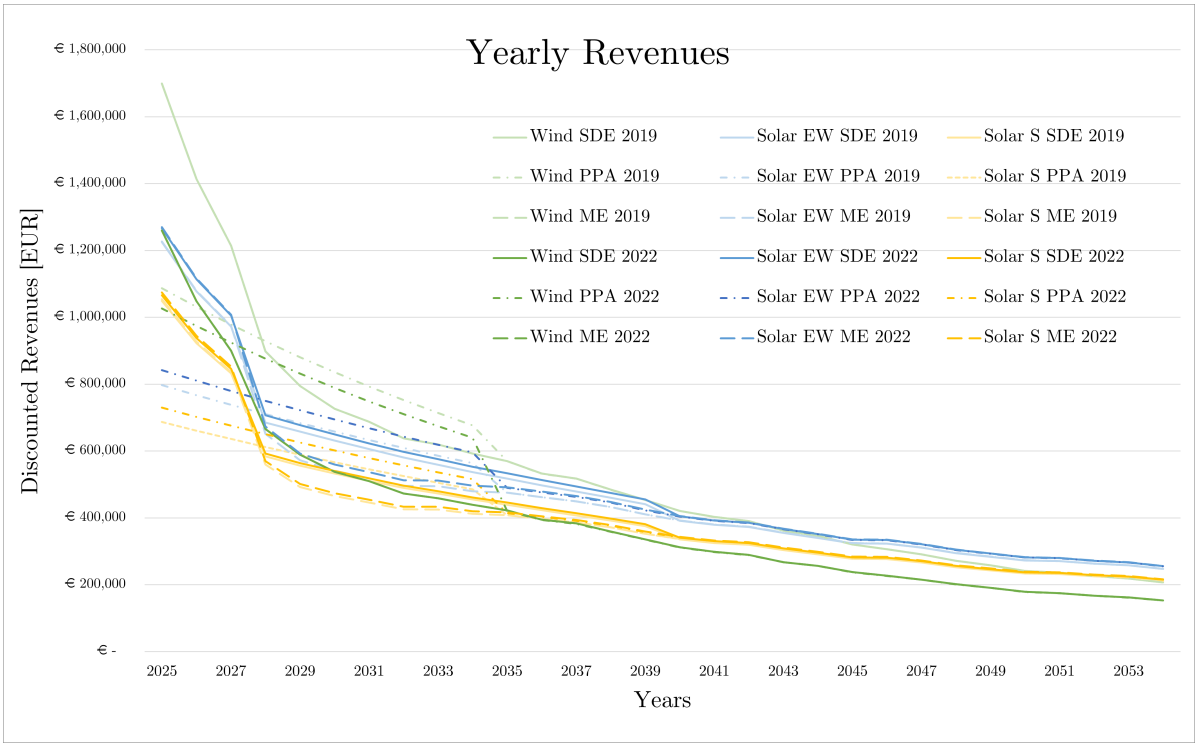

Figure 6.12: NPV for the different resources and models

In Figure 6.13, the yearly discounted costs for all combinations can be seen. The yearly discounted costs consist of both inflatable and non-inflatable costs and the land lease costs, corrected using the inflation and the discount factor. The wind OPEX are the same for all three revenue models and both input years, given the similar installed capacity.

The solar OPEX shape can be attributed to the inverter replacement costs. The inverter replacement costs are highest from year five to year 20, after which the costs decrease again, as also indicated in Table 5.9. From this graph and the table, it can be seen that the yearly OPEX are higher for PPA and ME revenue models than the SDE++ due to the lower DC/AC ratio of the PPA and ME models. Since the optimal installed capacity is the same using 2019 and 2022 data, the costs are the same for 2019 and 2022.

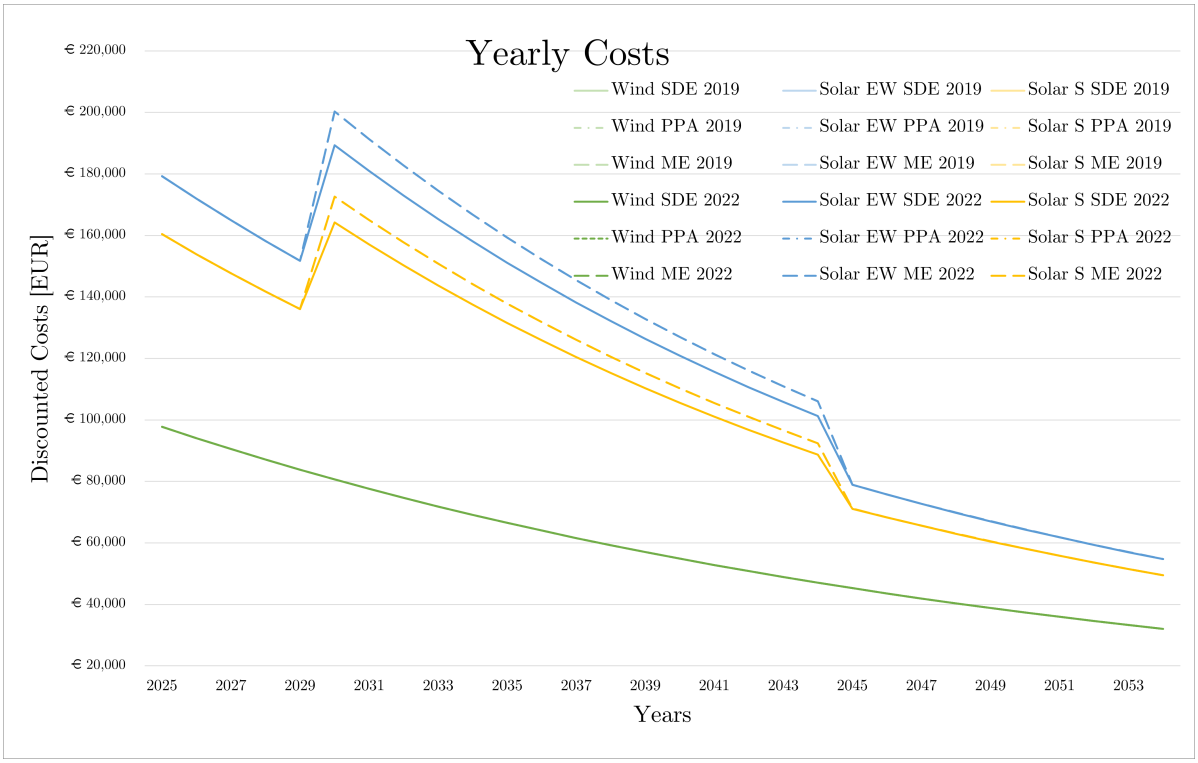

Figure 6.13: NPV for the different resources and revenue models

The inflation, degradation and discounting factors and the costs of a certain year $t \in T_j$ are the same for 2019 and 2022 weather and spot market input data. The difference between the NPV values based on input years 2019 or 2022 can therefore only be caused by the weather and spot market data, as discussed above, and the values based on the LTMO, if exposed to market prices.

As discussed above, the weather and spot market data do not create the difference seen in the yearly revenues and eventually NPV values of the SDE++ and ME business case between 2019 and 2022. For wind, the spot market prices of 2022 even result in a higher uncorrected yearly revenue than based on 2019 data, despite the NPV result. Since the value factor $\mathrm{LT}_{\mathrm{f},j,t}$ is independent of the input year used, 2019 or 2022, the long-term market factor LT_t, which does depend on the input year used, must play a role. Therefore, to better explain the difference in yearly revenue values for 2019 and 2022 for solar and wind, the long-term market factor LT_t is examined.

This yearly factor LT_t relates the average of the input year, 2019 or 2022, to the average expected value of the spot market price of the year in question, for example 2025, to account for expected value of energy in the future according to the LTMO. The calculation method can be found in Equation 5.1. An overview of the LTMO and LT_t values of the first ten years of operation of the added farm can be seen in Table 6.8.

Table 6.8: Expected average spot market values and corresponding long-term market values LT_t for base year 2019 or 2022.

Base year t_0		**2019**	**2022**
$price_{avg}$	[EUR/MWh]	41.9	242
Year	Expected $price_{avg}$ [EUR/MWh]	LT_t [-]	LT_t [-]
2025	136.0	3.25	0.56
2026	129.0	3.08	0.53
2027	121.0	2.89	0.50
2028	91.0	2.17	0.38
2029	88.0	2.10	0.36
2030	89.0	2.12	0.37
2031	90.0	2.15	0.37
2032	88.0	2.10	0.36
2033	90.0	2.15	0.37
2034	92.0	2.20	0.38

The summed hourly revenues based on 2022 or 2019 data are corrected to the expected revenue value of for example 2025 by considering the expected average price in 2025, which is 136 EUR/MWh and the average prices in the input years used. The yearly revenue based on 2022, with an average price of 242 EUR/MWh, will be reduced to 56% of the uncorrected value to account for the decreased expected average spot market price in 2025 compared to 2022 data. The yearly revenue based on 2019, with an average of 41.9 EUR/MWh, will be increased to 325% to account for the increased expected average price compared to 2019 data. So, the method to use the LTMO by effect of a long-term market values LT_t has a large impact on the output.

The PPA revenue model depends the least on the LTMO, since the first ten years, also with the higest impact on the NPV due to the discount rate, only depend on the PPA price. The PPA revenue model NPV values based on 2019 data are however also substantially higher for wind than the values based on 2022 data. To analyze this difference, the net cash flows are considered, by subtracting the yearly costs from the yearly revenues, and shown in Figure 6.14.

During the period that the PPA is active, the factors based on the LTMO are not used and the price considered is constant. Therefore, the only aspect influencing the yearly revenues is the weather input data. The sold energy for the added wind resource based on the hourly residual cable capacity and weather data is 13.85 GWh based on 2022 data and 14.66 GWh based 2019 data for the PPA revenue model. The sold energy and the fixed PPA price determine the yearly revenues, leading to higher revenues based on 2019 data for wind, translating into the yearly net cash flows and the NPV values. It can be seen that for solar farms the yearly net cash flows are higher based on 2022 data. Both show a drop after 10 years as a result from the end of the PPA duration.

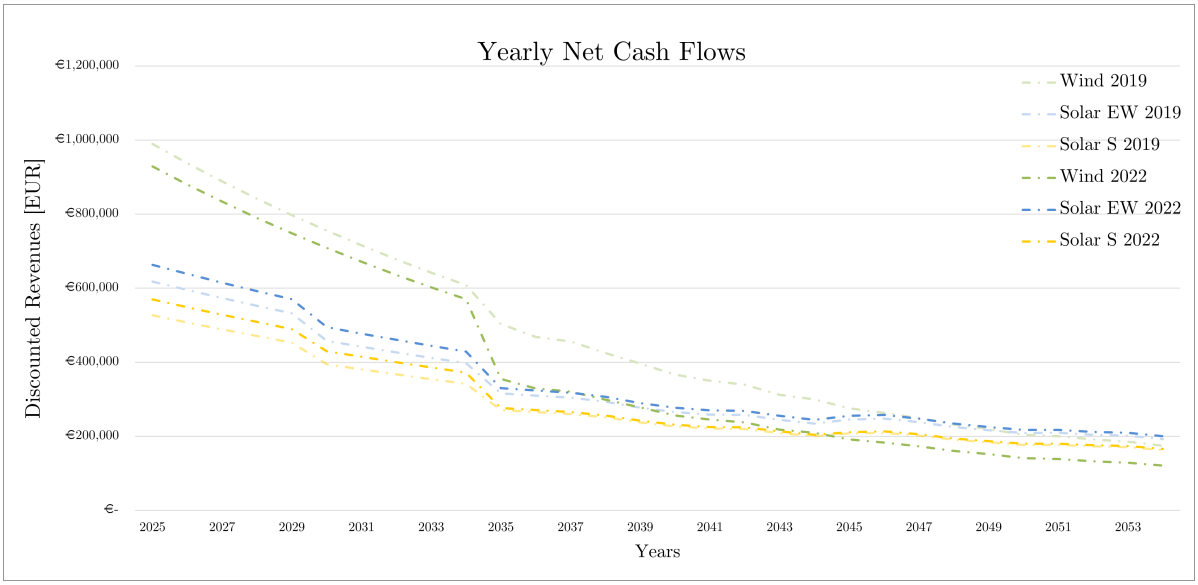

Figure 6.14: Yearly net cash flow for the PPA revenue model

To summarize, the 2019 and 2022 summed uncorrected revenue values are corrected with input year independent inflation, degradation of the existing and added farm and the discount rate. If exposed to the market prices in the year considered, the revenues earned that year are also corrected by the input year independent value factor $LT_{f,j,t}$ and by the input year dependent long-term market value LT_t. The yearly OPEX and one-time CAPEX are similar based on 2019 and 2022 input data.

The production for wind is higher and there is more residual cable capacity based on 2019 weather data, but the corresponding revenues are lower due to lower average prices for the 2019 spot market prices. The yearly revenues for the SDE++, PPA and ME revenue model based on 2019 data have higher values than the 2022 data. For the SDE++ and ME revenue model, this a combined result of the weather data impact and the long-term market value LT_t correction. The PPA revenue model is solely dependent on the weather statistics when the PPA is active and therefore results in higher NPV values based on 2019 than 2022 values for wind.

A similar analysis can be made for the solar farms. The solar production is higher based on 2022 weather data, but the difference between 2022 and 2019 input years is less compared to the wind addition due to the decreased residual cable capacity with the input year 2022 and the complementary behaviour of the existing and the added farm. For the SDE++ and ME scenario, the long-term market value LT_t reduces the yearly revenues based on 2019 data to lower values than the 2022 data. The PPA revenue model is solely dependent on the weather statistics when the PPA is active and therefore results in higher NPV values based on 2022 than 2019 values for solar.

This shows the impact of the input year used and the usage of the input year dependent long-term market value LT_t. Expanding the input years with more reference years would help smooth out these differences and find a more validated result. The current approach to use LTMO should be reevaluated to ensure a correct comparison between the average values of the input years and the year considered. Currently, the expected averages of the LTMO are assumed to have been calculated the same way as the average of the input year, but this might not be the case. Furthermore, the LTMO might be based on a certain use-case and is applied in this cable pooling case without any corrections to account for this difference.

An overview of the NPV of each revenue model and added technology are plotted together in Figure 6.15 and Figure 6.16 for 2019 and 2022 respectively. These figures and the discussed results are used to summarize the results of the base-case. All revenue models yield positive NPV values for both input years. The business case for a wind farm added to the existing east-west farm shows the most

potential of all three additions in all revenue models when considering 2019 data. This is due to the high capacity factor compared to solar and the complementary pattern of the generation, leading to few moments of curtailment. When considering 2022 data, the ME and PPA revenue model yield the highest NPV for the added wind farm, while the SDE++ model is highest for the east-west addition.

The solar south and east-west additions show very similar results, but some differences can be distinguished. First of all, considering the SDE++ revenue model, the east-west farm yields a higher NPV since the SDE++ is based on installed capacity. Secondly, the ME revenue model yields a higher NPV for the solar farm oriented to the south compared the farm oriented to the east-west using 2019 data, but vice versa using 2022 data. This can be partially be explained by the increased value of the production profile of the east-west oriented solar farm based on 2022 input data. Lastly, the PPA revenue model yields a higher NPV for both 2019 and 2022 for the added solar farm oriented to the south compared to the farm oriented to the east-west, due to a combination of higher output per installed capacity for the south oriented farm and less investment costs due to the smaller installed capacity. Due to the similar generation pattern as the existing resource, there is curtailment for the added solar farms.

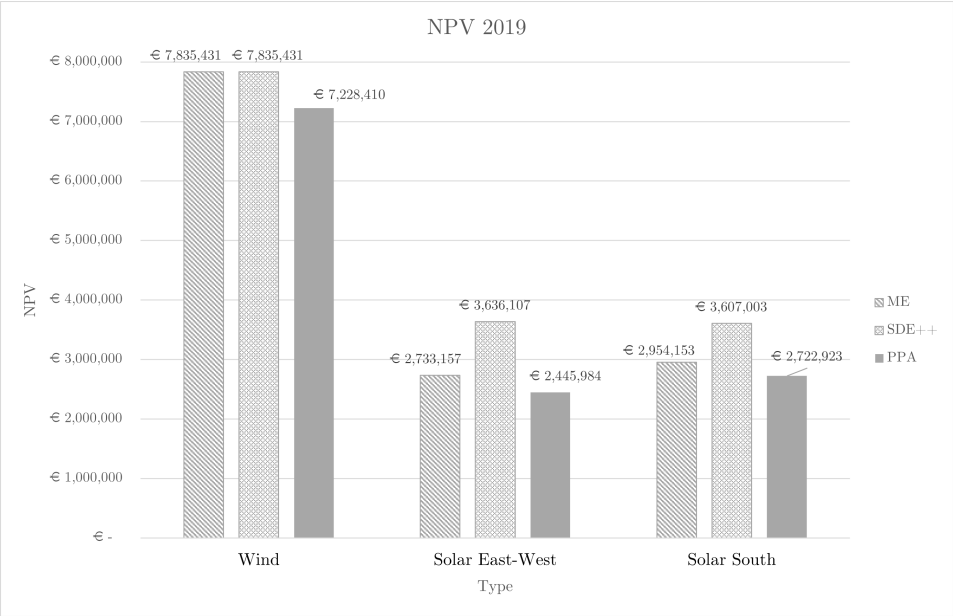

Figure 6.15: NPV for the different resources and revenue models

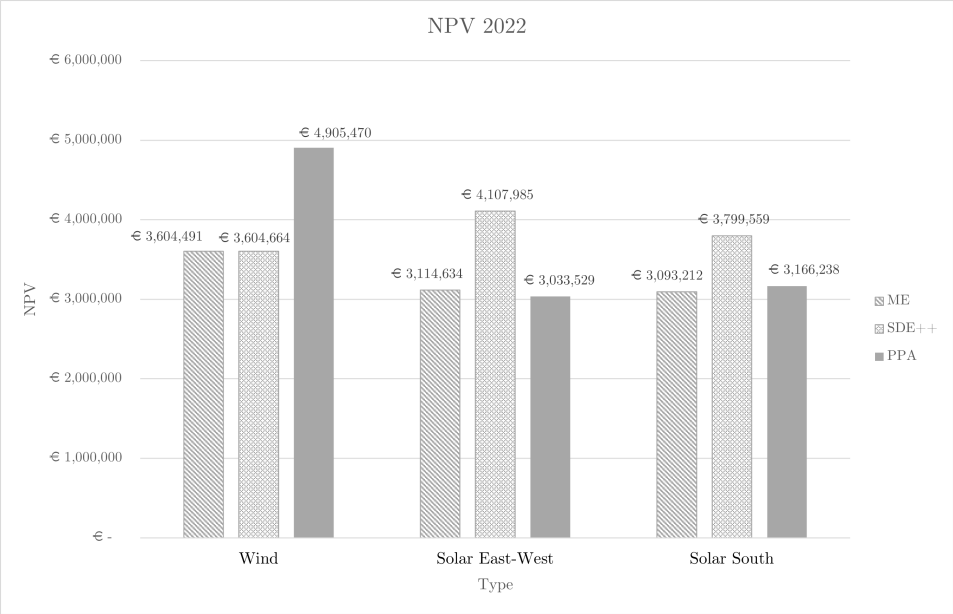

Figure 6.16: NPV for the different resources and revenue models

6.3. Sensitivities

As already indicated in the discussion of the results, the input clearly influences the results. Therefore, it is required to consider the sensitivity of the results. This section discusses different potentially sensitive inputs and the effects of changes thereof on the results to test the robustness of the base-case results. The sensitivity of some technical and economical inputs will first be discussed per resource type in subsection 6.3.1 and subsection 6.3.2 respectively. To generalize the results of the case study, some inputs are generalized in subsection 6.3.3.

6.3.1. Technical inputs

For wind energy, the technical inputs consist of turbine parameters and the wind speed. The impact of using a different turbine at the same hub height and the impact of the same turbine at a different hub height are considered by increasing and decreasing first the rated power and then the hub height by 10%. Furthermore, the impact of an increase and decrease of 10% of the wind speed is considered. The results can be seen in Table 6.9 for 2019 and 2022 input data.

Table 6.9: Sensitivity analysis of technical inputs for Wind

(a) 2019

	SDE++	PPA	ME
Prated +10%	12.20%	12.37%	12.20%
Prated -10%	-12.22%	-12.39%	-12.22%
Hub Height +10%	11.61%	12.03%	11.61%
Hub Height -10%	-12.49%	-12.95%	-12.49%
Wind speed at 100m +10%	48.62%	50.35%	48.62%
Wind speed at 100m -10%	-47.09%	-48.85%	-47.09%

(b) 2022

	SDE++	PPA	ME
Prated +10%	14.90%	13.58%	14.90%
Prated -10%	-14.90%	-13.59%	-14.90%
Hub Height +10%	20.39%	15.62%	20.39%
Hub Height -10%	-21.46%	-16.58%	-21.46%
Wind speed at 100m +10%	87.38%	66.11%	87.38%
Wind speed at 100m -10%	-79.62%	-62.23%	-79.62%

Since the results of the SDE++ and ME revenues are the same for wind, the impact of the changing input parameters is also the same. The impact of changing the rated power of the turbine by 10% results in approximately 12% change in the NPV using 2019 data and around 14-15% using 2022 data. More capacity is allowed to be installed, since at least one turbine is built, allowing more revenue to be made. The costs are scaled with the installed capacity and thus also increase. Since the impact on the NPV is positive, the additional revenues outweigh the extra costs.

Decreasing the hub height with 10% shows a larger impact on the NPV than the same percentage increase. The +10% and -10% change the NPV by around +12% and -13% using 2019 data, and a 16-20% increase and a 17-21% decrease using 2022 data. If the hub height changes, this influences the wind speed at the hub height and the output of the turbine. Considering the wind shear profile, a decrease of 10% in hub height leads to a larger decrease in the wind speed than an increase of the same size would lead to an increase of the wind speed. Since the wind speed directly determines the power output, a decrease of the hub height impacts the NPV more than an increase of the same percentage.

The third parameter was the wind speed at hub height. The wind speed was increased and decreased by 10% for all values in the year considered, leading to impacts on the NPV of 50% increase and decrease based on 2019 and a +70-90 increase and a -60-80% decrease based on 2022. The power output of a wind farm depends on the wind speed cubed. Therefore, the NPV is indeed very sensitive to the wind speed considered. The impact is larger in 2022 than 2019, which can be explained using comparison of the wind speed data in Table 5.2. The mean wind speed is higher in 2019 than 2022, but the maximum value and sample standard deviation are larger in 2022. The +/-10% impact is therefore more extreme on the results based on 2022 data.

For solar energy, the technical inputs consist of the DC/AC ratio and corresponding configuration, the tilt and orientation, the type of module and/or inverter and the irradiance. For the sensitivity analysis the DC/AC ratio, tilt and irradiance are considered. The results of increasing and decreasing these inputs by 10% are shown in Table 6.10 for the solar farm oriented to the east-west and Table 6.11 for the south oriented solar farm.

Table 6.10: Sensitivity analysis of technical inputs for solar farm oriented to the east-west case

(a) 2019

	SDE++	PPA	ME
DCAC +10%	+0.61%	+4.04%	+3.63%
DCAC -10%	-2.33%	-4.85%	-4.36%
Tilt +10%	-3.25%	-0.89%	-1.50%
Tilt -10%	+2.81%	-0.12%	+0.72%
Irradiance +10%	11.52%	14.88%	15.86%
Irradiance -10%	-17.34%	-23.86%	-23.72%

(b) 2022

	SDE++	PPA	ME
DCAC +10%	-0.03%	+3.29%	+3.11%
DCAC -10%	-1.75%	-3.91%	-3.70%
Tilt +10%	-2.94%	-0.79%	-1.28%
Tilt -10%	+2.57%	0.00%	+0.67%
Irradiance +10%	9.73%	10.43%	13.16%
Irradiance -10%	-15.56%	-18.77%	-20.83%

The increase of the DC/AC by 10% leads to a positive impact on the business case for the east-west oriented solar farm for the PPA and ME revenue models, with an original DC/AC ratio of 1.8. The impact of the DC/AC ratio increase on the SDE++ revenue model is close to zero, so the addition of extra modules on the DC side of the inverter does not positively or negatively impact the business case.

For the south oriented farm, as shown in Table 6.11, the impact on the PPA and ME revenue model is less positive and the impact on the SDE++ even becomes negative. This can be explained by the fact that the power density is smaller for south oriented farms. A higher DC/AC ratio leads to an increase in the number of modules built on the DC side and no increase in the maximum output on the inverter side. The costs for building more capacity increase, while the extra revenues are marginal. Increasing the DC/AC ratio of the PPA and ME revenue models would however be beneficial.

A decrease in the DC/AC ratio has a larger negative impact on the PPA and ME revenue model than on the SDE++ revenue model for both east-west and south oriented farms. Therefore, the DC/AC ratio range which is most profitable is between the PPA and ME and the SDE++ value, so between 1.8 and 2.0. Going below the PPA and ME value of 1.8 reduces the business case significantly and increasing the DC/AC ratio above the SDE++ value of 2.0 barely increases or even decreases the business case.

Increasing the tilt with 10% reduces the power density of the farms by 1-3%. Therefore, the allowed installed capacity decreases and the impact on the business case is slightly negative. The other way around, decreasing the tilt by 10% increases the power density and thus the allowed installed capacity, impacting the business case positively with about 1-2.5%. This indicates that the tilt selected is not ideal and that the impact of the power density on the business case is significant and building more capacity improves the business case for this change in the tilt.

Table 6.11: Sensitivity Analysis of Technical Inputs for Solar South Farm

(a) 2019

	SDE++	PPA	ME
DCAC +10%	-3.34%	2.84%	2.63%
DCAC -10%	-0.60%	-3.36%	-3.11%
Tilt +10%	-2.07%	-0.42%	-0.65%
Tilt -10%	1.96%	0.24%	0.50%
Irradiance +10%	11.57%	13.53%	14.51%
Irradiance -10%	-16.92%	-21.01%	-21.27%

(b) 2022

	SDE++	PPA	ME
DCAC +10%	-4.23%	2.40%	2.40%
DCAC -10%	0.15%	-2.89%	-2.89%
Tilt +10%	-2.57%	-0.52%	-0.89%
Tilt -10%	2.45%	0.36%	0.77%
Irradiance +10%	10.15%	9.69%	12.21%
Irradiance -10%	-16.02%	-17.19%	-19.40%

The solar farms oriented to the south and east-west are sensitive to the irradiance inputs. A change in irradiance influences the output of the existing resource and the output of the new resource, both impacting the business case. Increasing the irradiance with 10% results in 10-16% and 10-15% increase in the business case for east-west and south oriented farm respectively. Decreasing the irradiance with 10% results in an even larger decrease in the business case, ranging from a 16-24% and 16-21% decrease in the business case for east-west and south oriented farm respectively.

If the irradiance increases, the output of the existing farm and the new solar resource both increase. The increase in the output of the existing resource results in less export capacity and since the production patterns are similar, this limits the export capacity of the new resource. The business case does increase, indicating that there are many time instances at which residual space was available before the irradiance increase. The decrease of the irradiance might lead to more export capacity, but at times when the new resource also produces less, given the similar production patterns. Therefore, the business case decreases more significantly than it increases for the same percentage increase of the irradiance.

The results based on 2019 data are more sensitive to changes in the irradiance than the results based on 2022 data. The capacity factor of the existing resource and new resource c_f and therefore cable capacity factor cc_f based on 2019 weather data are lower than the c_f and cc_f based on 2022 data. The output of the new and existing resource based on 2022 data reaches the maximum grid connection capacity more and therefore increasing the 2022 irradiance data by 10% impacts the business case less than the same increase for 2019, since the business case has less space to improve compared to the 2019 situation. Therefore, the results based on 2019 data are more sensitive to changes in the irradiance.

All influences, except that of the irradiance, on the NPV were smaller than the change in the input, indicating that the solar farm NPV calculations are not very sensitive to the technical inputs that have been altered here.

Since the optimal installed capacity for all technologies reaches maximum, imposed by the power density and the available land area, for all models, the land area is increased by 150% and 200% to analyze the influence on the business case. The results are shown in Table 6.12, Table 6.13 and Table 6.14. For wind, Table 6.12, the increase in land size still does not allow more than one turbine to be built, so the business case only decreases since the land lease costs increase.

Table 6.12: Impact of increasing the land size on NPV of added wind farm

(a) 2019

	SDE++	PPA	ME
Land size 150%	-11.29%	-12.24%	-11.29%
Installed Capacity [MW]	6.60	6.60	6.60
Land size 200%	-22.58%	-24.48%	-22.58%
Installed Capacity [MW]	6.60	6.60	6.60

(b) 2022

	SDE++	PPA	ME
Land size 150%	-24.54%	-18.04%	-24.54%
Installed Capacity [MW]	6.60	6.60	6.60
Land size 200%	-49.09%	-36.07%	-49.09%
Installed Capacity [MW]	6.60	6.60	6.60

The impact on the business case for the solar farm oriented to the east-west is negative, but the installed capacity does increase compared to the base case. The land size does not form a constraint anymore, given that both 150% and 200% yield the same capacity and the different revenues also result in different installed capacities.

Table 6.13: Impact of increasing the land size on NPV of added solar farm oriented to the east-west

(a) 2019

	SDE++	PPA	ME
Land size 150%	-12.34%	-34.63%	-28.51%
Installed Capacity [MW]	21.41	16.54	17.84
Land size 200%	-36.68%	-70.80%	-60.88%
Installed Capacity [MW]	21.41	16.54	17.84

(b) 2022

	SDE++	PPA	ME
Land size 150%	-9.41%	-27.18%	-23.05%
Installed Capacity [MW]	21.60	16.80	17.87
Land size 200%	-30.94%	-56.35%	-50.54%
Installed Capacity [MW]	21.60	16.80	17.87

The south oriented solar farm, Table 6.14, shows that with increasing the land size with 150%, the land size still forms a constraint for the installed capacity for the SDE++ and ME case. The increased land size to 200% still leads to increases in the installed capacity compared to the 150% case. The installed capacity of the PPA revenue model is the same for 150% and 200%, so the land size does no longer form a constraint.

Table 6.14: Impact of increasing the land size on NPV of added solar farm oriented to the south

(a) 2019

	SDE++	**PPA**	**ME**
Land size 150%	4.30%	-16.65%	-9.30%
Installed Capacity [MW]	17.07	16.72	17.07
Land size 200%	-15.59%	-49.14%	-38.85%
Installed Capacity [MW]	21.16	16.72	18.17

(b) 2022

	SDE++	**PPA**	**ME**
Land size 150%	3.11%	-15.13%	-10.85%
Installed Capacity [MW]	17.07	16.29	17.07
Land size 200%	-17.61%	-43.07%	-38.67%
Installed Capacity [MW]	20.22	16.29	17.09

Even thought the land size forms an active constraint for all three additions, increasing the land size does not necessarily positively impact the business case compared to the base case.

Since the power density values used in the results are not the correct values, based on these results an indication of the impact of the change in the power density can be discussed. The change in the power density for the solar farms oriented to the south is minimal and will be ignored. The power density values of the east-west oriented solar farm used for the results are lower than the correct values. Therefore, more installed capacity can be fitted into the same land area.

Given the tendency of the optimization to build more capacity if the land area increases, despite both the higher land lease and higher installation costs, one can expect that the maximum allowed capacity will be built with a higher power density if no extra land-lease cost are considered. The NPV values however can still be lower than the original value, because the revenues made by the extra installed capacity do not outweigh the costs of installing more capacity.

The cable capacity factor is expected to improve for a higher power density value, since the east-west oriented solar farm produces more electricity and can export more on the cable. Due to the similar generation patterns, this reasoning also leads to more curtailment. The PPA and ME revenue model are calculated with the new power density values and compared to the old values in Table 6.15.

Table 6.15: Impact of new power density values for the solar farm oriented to the east-west based on 2022 input data for two revenue models.

(a) 2022, PPA. The capacity factor of the existing farm is 11.60% and the cable capacity factor before the addition of the new resource is 13.38%.

	Old	**New**
NPV	€ 3,033,529	€ 2,964,401
$P_{installed}$	14.80	16.54
CAPEX	€ 7,658,411	€ 8,558,640
Cable capacity factor cc_f	23.76%	24.72%
Curtailment	15.50%	19.17%

(b) 2022, ME. The capacity factor of the existing farm is 11.60% and the cable capacity factor before the addition of the new resource is 13.38%.

	Old	**New**
NPV	€ 3,114,634	€ 3,223,789
$P_{installed}$	14.80	16.82
CAPEX	€ 7,658,411	€ 8,706,224
Cable capacity factor cc_f	23.54%	24.48%
Curtailment	19.10%	22.23%

As expected, the installed capacity and corresponding CAPEX increase for both revenue models. The NPV value increases for the ME revenue model, further increasing the NPV relative to the south oriented farm, but decreases for the PPA revenue model, further decreasing relative to the south oriented farm. The revenues due to the installed capacity do not outweigh the additional costs of building the extra installed capacity in the PPA revenue model. Interesting to see is that the installed capacity values are not the same for both revenue models, indicating that the land size does not form a constraint at the PPA revenue model. The cable capacity factor and curtailment increase for both revenue models.

6.3.2. Economic Sensitivity

The economic sensitivities discussed are the increase or decrease of economical parameters by 10% and the impact on the business case. First of all, the impact of changing the CAPEX or OPEX are considered followed by the impact of the increase or decrease of the installed capacity independent land lease. As discussed before, the long-term market factor LT_t, comparing the average spot market price of the base year to the expected average spot market price in a future year, has a large impact on the NPV. Therefore, the impact of increasing and decreasing the LT_t by 10% is discussed. The impact of increasing and decreasing the technology dependent value factor $LT_{f,j,t}$, indicating the expected value of a technology in the expected future spot market, and the discount rate by 10% on the NPV are also discussed. In Table 6.16, Table 6.17 and Table 6.18 the impact of changing these parameters on the NPV is shown for the added wind and solar farms respectively.

The wind farm, Table 6.16, responds more to the CAPEX changes in the NPV based on the 2022 data compared to the 2019 data. Since the CAPEX is a fixed number, the impact on a lower NPV is larger than on a higher NPV. The impact of a change in the OPEX is marginal since a large part of the operational costs consists of the land lease.

As expected, the impact of the long-term market factor LT_t and the value factor $LT_{f,j,t}$ are large, especially on the business case that is fully dependent on the market prices, ME and SDE++ in the case of wind. A decrease of the value factor $LT_{f,j,t}$ by 10% results in a slightly less negative impact on the business case than a decrease of the long-term market factor LT_t for the SDE++ revenue model, which can be attributed to the fact that the market value for wind, which depends on this value factor $LT_{f,j,t}$, now drops below the BB for wind for a few years and the farm now receives a little subsidy.

The impact of changes in the inflation is smaller than the changes itself, so the output is not sensitive to changes in the inflation rate. The output is sensitive to changes in the discount rate. An increase in the discount rate requires are higher desired return on the investment resulting in a smaller dis-

count factor and reduced discounted cash flows and eventually a decrease in the NPV. The impact is larger using 2022 data instead of 2019 data, since the smaller NPV values are more sensitive to this change. This can be explained by the fact that the CAPEX remain constant, since the cash flow is not discounted, while the positive net cash flows during operation become smaller. Therefore, the NPV becomes smaller.

A change in the EPEX prices does not result in any change in the NPV, due to the definition of the long-term market factor LT_t, which corrects for this difference.

The impact of changes in the SDE++ BB are zero. An increase in the BB potentially results in more years where the market value gets below the required BB and thus more years where subsidy is awarded. However, the new BB value is still always higher than the expected market value based on the LTMO, so no subsidy is awarded and the NPV stays the same. A decrease in the BB results in even less years where the market value gets below the required BB, which was already zero.

The impact of changes in the PPA are significant since the PPA price is used in the first ten years of the lifetime, which weigh highest in the NPV calculations. Since the CAPEX remain constant and weighs more on the lowest NPV value, the impact of increasing the revenues for the first ten years is larger for the year with the lowest NPV value in the base-case, so 2022 for wind.

Table 6.16: Economic Sensitivities for Wind Farm

(a) 2019

	SDE++	**PPA**	**ME**
CAPEX +/-10%	-/+8.60%	-/+9.32%	-/+8.60%
OPEX +/-10%	0.00%	-/+0.01%	0.00%
Land Lease +10%	-/+2.26%	-/+2.45%	-/+2.26%
Long-Term Market Factor LT_t +/-10%	+/-20.86%	+/-9.76%	+/-20.86%
Value Factor $LT_{f,j,t}$ +10%	20.86%	9.76%	20.86%
Value Factor $LT_{f,j,t}$ -10%	-20.63%	-9.76%	-20.86%
Discount Rate +10%	-10.39%	-11.45%	-10.39%
Discount Rate -10%	11.49%	12.66%	11.49%
EPEX +/-10%	+/-0.00%	+/-0.00%	+/-0.00%
Inflation +10%	4.24%	4.63%	4.24%
Inflation -10%	-4.10%	-4.48%	-4.10%
SDE++ BB +/-10%	0.00%	-	-
PPA +/-10%	-	+/-12.01%	-

(b) 2022

	SDE++	**PPA**	**ME**
CAPEX +/-10%	-/+18.68%	-/+13.73%	-/+18.68%
OPEX +/-10%	-/+0.01%	-/+0.01%	-/+0.01%
Land Lease +10%	-/+4.91%	-/+3.61%	-/+4.91%
Long-Term Market Factor LT_t +/-10%	+/-33.60%	+/-10.64%	+/-33.60%
Value Factor $LT_{f,j,t}$ +10%	33.60%	10.64%	33.60%
Value Factor $LT_{f,j,t}$ -10%	-33.24%	-10.64%	-33.60%
Discount Rate +10%	-15.87%	-12.85%	-15.87%
Discount Rate -10%	17.55%	14.14%	17.55%
EPEX +/-10%	+/-0.00%	+/-0.00%	+/-0.00%
Inflation +10%	6.25%	5.12%	6.25%
Inflation -10%	-6.05%	-4.97%	-6.05%
SDE++ BB +/-10%	0.00%	-	-
PPA +/-10%	-	+/-16.71%	-

The solar farm oriented to the east-west, seen in Table 6.17, shows large responses to the change in CAPEX on the NPV based on data of 2019 and 2022 compared to wind, since the CAPEX relatively makes up a larger share of the NPV. The impact on the NPV values is less than the change in OPEX values, so the NPV is not sensitive to changes in the OPEX. The impact of both changes in CAPEX and OPEX are again largest for the input year and revenue model with the lowest NPV in the base case.

The impact of the long-term market factor LT_t is large compared the impact on the NPV of the wind farms. The impact of the value factor $LT_{f,j,t}$ is the same for the PPA and ME revenue models, but result in a different outcome for the SDE revenue models. This is due to the subsidy which depends on value factor $LT_{f,j,t}$. The same can be seen for a decrease in the value factor $LT_{f,j,t}$, which has a less negative impact compared to the same decrease in the long-term market factor LT_t, since the subsidy increases.

Overall, the impact of changes in the inflation are larger compared to the impact for wind, especially for the increase of the inflation. An increase in the inflation impacts the NPV more positively than a same decrease impacts the NPV negatively. The net cash flows each year are correct for inflation with a higher rate than before. Considering the net cash flows during operation are all positive, the impact of an increased inflation rate is higher on the positive cash flows than the one-time negative CAPEX before operation. It must be noted that this impact does not fully represent the real life scenario, where the discount rate and inflation are not independent. An increase in inflation would be accounted for in the discount rate, which is not the case in this approach.

The output is again sensitive to changes in the discount rate. The impact of increasing or decreasing the discount rate is larger than the impact on the wind NPV. The impact is again largest for the lowest NPV values of the base-case.

The impact of changes in the SDE++ BB are substantial. An increase in the BB potentially results in more years where the market value gets below the required BB, increasing the received subsidy. A decrease in the BB results in less years where the market value gets below the required BB, decreasing the received subsidy. However, if the BB is lower and the market value remains the same, a higher price difference occurs and therefore, a higher subsidy price is used. This explains the less negative impact due to a decrease in the SDE++ BB compared to the positive impact of the same increase.

The impact of changes in the PPA are again significant and larger than the impact for the added wind resource, especially on the NPV based on 2019 data. Overall, the east-west business case seems to be more sensitive to the economic inputs than the wind business case.

Table 6.17: Economic Sensitivities solar farm oriented to the east-west

(a) 2019

	SDE++	**PPA**	**ME**
CAPEX +/-10%	-/+20.30%	-/+30.72%	-/+27.49%
OPEX +/-10%	-/+5.04%	-/+7.95%	-/+7.11%
Land Lease +/-10%	-/+4.87%	-/+7.23%	-/+6.47%
Long-Term Market Factor LT_t +/-10%	+/-38.34%	+/-28.31%	+/-51.08%
Value Factor $LT_{f,j,t}$ +10%	24.76%	28.31%	51.08%
Value Factor $LT_{f,j,t}$ -10%	-23.36%	-28.31%	-51.08%
Discount Rate +10%	-18.68%	-26.92%	-23.47%
Discount Rate -10%	20.81%	30.03%	26.21%
EPEX +/-10%	+/-0.00%	+/-0.00%	+/-0.00%
Inflation +10%	7.76%	11.95%	10.44%
Inflation -10%	-7.49%	-11.53%	-10.07%
SDE++ BB +10%	17.29%	-	-
SDE++ BB -10%	-15.32%	-	-
PPA +/-10%	-	+/-28.58%	-

(b) 2022

	SDE++	**PPA**	**ME**
CAPEX +/-10%	-/+17.97%	-/+24.77%	-/+23.35%
OPEX +/-10%	-/+4.46%	-/+6.41%	-/+6.04%
Land Lease +/-10%	-/+4.31%	-/+5.83%	-/+5.50%
Long-Term Market Factor LT_t +/-10%	+/-35.09%	+/-23.52%	+/-44.89%
Value Factor $LT_{f,j,t}$ +10%	23.06%	23.53%	44.89%
Value Factor $LT_{f,j,t}$ -10%	-21.83%	-23.52%	-44.89%
Discount Rate +10%	-17.26%	-22.77%	-20.89%
Discount Rate -10%	19.23%	25.40%	23.33%
EPEX +/-10%	+/-0.00%	+/-0.00%	+/-0.00%
Inflation +10%	7.18%	10.07%	9.25%
Inflation -10%	-6.92%	-9.71%	-8.92%
SDE++ BB +10%	15.27%	-	-
SDE++ BB -10%	-13.52%	-	-
PPA +/-10%	-	+/-24.18%	-

For the solar farm oriented to the south, as seen in Table 6.18, the impact of changes in economic inputs are smaller than the impact of the east-west oriented farm and show similar behaviour. The input years with the lowest NPV for each revenue model in the base-case, are most impacted by a change in most inputs.

Table 6.18: Economic Sensitivities Solar South

(a) 2019

	SDE++	PPA	ME
CAPEX +/-10%	-/+15.74%	-/+21.22%	-/+19.56%
OPEX +10%	-/+3.90%	-/+5.49%	-/+5.06%
Land Lease +10%	-/+4.91%	-/+6.50%	-/+5.99%
Long-Term Market Factor LT_t +/-10%	+/-33.11%	+/-21.86%	+/-40.61%
Value Factor $LT_{f,j,t}$ +10%	22.57%	21.86%	40.61%
Value Factor $LT_{f,j,t}$ -10%	-21.49%	-21.86%	-40.61%
Discount Rate +10%	-15.86%	-20.59%	-18.47%
Discount Rate -10%	17.67%	22.97%	20.63%
EPEX +/-10%	+/-1.94%	+/-3.18%	+/-2.78%
Inflation +10%	6.50%	8.93%	8.04%
Inflation -10%	-6.27%	-8.62%	-7.76%
SDE++ BB +10%	13.32%	-	-
SDE++ BB -10%	-11.79%	-	-
PPA +/-10%	-	+/- 21.88%	-

(b) 2022

	SDE++	PPA	ME
CAPEX +/-10%	-/+14.94%	-/+18.25%	-/+18.17%
OPEX +10%	-/+3.71%	-/+4.72%	-/+4.70%
Land Lease +10%	-/+4.66%	-/+5.59%	-/+5.56%
Long-Term Market Factor LT_t +/-10%	+/-31.93%	+/-19.05%	+/-38.43%
Value Factor $LT_{f,j,t}$ +10%	21.94%	19.06%	38.43%
Value Factor $LT_{f,j,t}$ -10%	-20.91%	-19.05%	-38.43%
Discount Rate +10%	-15.38%	-18.30%	-17.61%
Discount Rate -10%	17.13%	20.40%	19.67%
EPEX +/-10%	+/-0.00%	+/-0.00%	+/-0.00%
Inflation +10%	6.31%	7.94%	7.67%
Inflation -10%	-6.09%	-7.67%	-7.40%
SDE++ BB +10%	12.62%	-	-
SDE++ BB -10%	-11.18%	-	-
PPA +/-10%	-	+/-19.94%	-

For all three added farms, the impact of the change in the OPEX, land lease, EPEX spot market prices is smaller than the change itself, so these are not sensitive inputs.

6.3.3. Generalization

So far, changes in constant inputs, such CAPEX, impact the originally lowest NPV values the most. Time varying inputs like the long-term market factor LT_t, value factor $LT_{f,j,t}$ and the discount rate influence all NPV values significantly. The outcome of the east-west farm is most sensitive to changes in the economical inputs, followed by the south oriented farm. The wind farm however is more sensitive to changes in technical inputs. Changing the land size available has a negative impact on all NPV values, even though more capacity is installed for both solar additions.

All negative impacts do however still result in a positive business case for all three technologies, so the business case for this case study specifically is robust. The case study considers a relatively large grid connection for a solar farm, which can be considered a case which will not occur often in real life. This section attempts to more generally discuss the addition of a renewable resource to an existing resource.

To analyse the impact of a smaller grid connection on the business case, the grid connection sized is reduced in steps of 10% to 60% of the original size. The results can be seen in Table 6.19, Table 6.20

and Table 6.21. The impact of reducing the grid connection size in steps of 10% does not impact the business case of the wind farm heavily. With a reduction to 60% of the original grid connection size, the NPV of the wind farm only reduces by 3.5-5%, as can be seen in Table 6.19, again indicating the complementary behaviour of the two resources.

Table 6.19: Impact of changing the grid connection size on the business case of the added wind farm

(a) 2019

	SDE++	PPA	ME
90% of grid connection	-0.31%	-0.38%	-0.31%
80% of grid connection	-1.00%	-1.20%	-1.00%
70% of grid connection	-2.18%	-2.57%	-2.18%
60% of grid connection	-4.53%	-5.17%	-4.53%

(b) 2022

	SDE++	PPA	ME
90% of grid connection	-0.06%	-0.16%	-0.06%
80% of grid connection	-0.28%	-0.57%	-0.28%
70% of grid connection	-1.27%	-1.85%	-1.27%
60% of grid connection	-3.53%	-4.59%	-3.53%

The impact on the solar farms is large. A 10% reduction in the grid connection size leads to approximately 30-50% and 20-40% decrease in the NPV for solar EW and S respectively. The NPV even becomes negative with 70% and 60% of the original grid connection size.

Table 6.20: Impact of changing the grid connection size on the business case of the added solar EW farm

(a) 2019

	SDE++	PPA	ME
90% of grid connection	-29.03%	-45.14%	-39.86%
80% of grid connection	-62.81%	-87.16%	-79.49%
70% of grid connection	-94.43%	-122.72%	-113.67%
60% of grid connection	-116.43%	-143.99%	-135.26%

(b) 2022

	SDE++	PPA	ME
90% of grid connection	-26.98%	-40.24%	-35.84%
80% of grid connection	-59.29%	-78.42%	-72.84%
70% of grid connection	-89.91%	-111.05%	-105.15%
60% of grid connection	-111.36%	-131.26%	-126.11%

Table 6.21: Impact of changing the grid connection size on the business case of the added solar S farm

(a) 2019

	SDE++	PPA	ME
90% of grid connection	-23.86%	-35.49%	-31.32%
80% of grid connection	-52.17%	-73.84%	-66.03%
70% of grid connection	-84.43%	-109.02%	-100.96%
60% of grid connection	-109.39%	-131.46%	-124.50%

(b) 2022

	SDE++	PPA	ME
90% of grid connection	-23.50%	-34.23%	-31.13%
80% of grid connection	-52.99%	-70.78%	-66.29%
70% of grid connection	-85.52%	-103.67%	-99.99%
60% of grid connection	-109.45%	-124.86%	-122.40%

The impact is largest on the PPA and ME revenue models for the solar cases, as the subsidy received depends on the installed capacity and fixed FLH rather than the actual exported energy. The impact for both solar and wind is largest in the PPA case, since the the price at which energy can be sold is positive for each hour and a limitation in the export cable, and thus not selling energy, results in a reduction in the NPV.

The difference in the impact levels for solar and wind are large and therefore the conclusion can be drawn that the complementary behaviour of the generation pattern does indeed play an important part in the potential of a cable pooling location where the export constraint is determined by the generation pattern of the existing resource.

Another generalisation considered, is to use a fixed part of the existing grid connection. The assumption used before, where only the residual cable capacity could be used, creates an export constraint that is time- and generation dependent. Another possible cable pooling agreement could have the shape of dividing the grid connection capacity. A fixed percentage of the grid connection is available for the new resource, resulting in a constant export constraint. The impact on the business case by allowing the new farm to export on a fixed part of the original grid connection size are examined.

The fixed grid connection sizes considered are 25%, 50% and 100% of the original grid connection size, leading to 3.25 MVA, 6.5 MVA or 13 MVA export capacity. Since a fixed percentage is used in these scenarios, the original costs of the grid connection will be shared accordingly, in contrast to the case where only the residual space is used and grid connection costs were assumed zero. The grid connection investment costs are subtracted from the NPV. The costs of the grid connection will not be shared due to confidentiality, but the impact on the business case will be discussed. No operational costs or possible additional compensation for the existing farm are considered. The impact on the business case outputs are shown in Table 6.22, Table 6.23 and Table 6.24 respectively.

For the wind farm, a fixed percentage of the grid connection does not yield a more positive business case than a time-varying grid connection. Given the complementary generation patterns of the new wind resource and the existing solar resource, a time-varying grid connection does not often form an export constraint for the wind farm.

A constant grid connection of 3.25 MVA and corresponding grid connection costs, decreases the business case by almost 40%. A constant grid connection of 6.5 MVA, comparable to the rated capacity of the turbine of 6.6 MW, also impacts the business case negatively compared to a time-varying grid connection without any grid connection costs. The same holds for the oversized 13 MVA scenario.

Table 6.22: Impact of a fixed cable capacity on the wind business case

(a) 2019

Grid capacity	% of Grid connection	SDE++	PPA	ME
3.25 MVA	25%	-36.20%	-38.33%	-36.20%
6.5 MVA	50%	-4.19%	-4.52%	-4.19%
13 MVA	100%	-8.49%	-9.18%	-8.49%

(b) 2022

Grid capacity	% of Grid connection	SDE++	PPA	ME
3.25 MVA	25%	-46.04%	-44.63%	-46.04%
6.5 MVA	50%	-9.29%	-6.74%	-9.29%
13 MVA	100%	-18.63%	-13.60%	-18.63%

For the solar farm oriented to the east-west with a size of almost 15 MWp, a fixed grid connection capacity of 3.25 MVA, does not positively impact the business case, since it would result in much curtailment. However, the business case improves if the solar farm oriented to the east-west would have a fixed 6.5 or 13 MVA grid connection, despite the additional grid connection fees. The new solar resource now has less export constraints compared to the situation where the residual grid connection space could be used to export energy.

For SDE++, a 6.5 MVA grid connection results in a higher NPV than a 13 MVA grid connection, so the optimum is somewhere between these two values. For PPA and ME revenue models, a 13 MVA grid connection leads to an even higher NPV than a 6.5 MVA grid connection and the optimum value might be even higher than 13 MVA.

Table 6.23: Impact of a fixed cable capacity on the solar farm oriented to the east-west business case

(a) 2019

Grid capacity	% of Grid connection	SDE++	PPA	ME
3.25 MVA	25%	-57.55%	-64.91%	-63.83%
6.5 MVA	50%	26.59%	44.37%	36.75%
13 MVA	100%	23.90%	68.24%	56.18%

(b) 2022

Grid capacity	% of Grid connection	SDE++	PPA	ME
3.25 MVA	25%	-56.67%	-60.59%	-62.00%
6.5 MVA	50%	22.43%	37.81%	29.70%
13 MVA	100%	19.86%	58.40%	45.39%

For the solar south farm with a size of almost 12 MWp, a fixed grid connection capacity of 3.25 MVA, again does not positively impact the business case, since it would result in much curtailment. However, the business cases for the PPA and ME revenue model improve considering a 6.5 or 13 MVA grid connection. The new solar resource now has less export constraints compared to the situation where the residual grid connection space could be used to export energy.

For SDE++, the NPV increases if 6.5 MVA was available, while 13 MVA does not positively impact the business case. A 13 MVA grid connection, can be considered oversized for this 12 MWp solar farm. For PPA and ME cases, the same trend can be seen: a 6.5 MVA or 13 MVA grid connection both improve the business case, but a 13 MVA business case is not the optimum.

Table 6.24: Impact of a fixed cable capacity on the solar south business case

(a) 2019

Grid capacity	% of Grid connection	SDE++	PPA	ME
3.25 MVA	25%	-49.04%	-57.33%	-55.62%
6.5 MVA	50%	7.87%	33.50%	28.36%
13 MVA	100%	-1.65%	23.63%	19.15%

(b) 2022

Grid capacity	% of Grid connection	SDE++	PPA	ME
3.25 MVA	25%	-50.32%	-55.55%	-56.72%
6.5 MVA	50%	5.84%	30.88%	25.14%
13 MVA	100%	-3.19%	22.65%	16.62%

The positive impact of using a fixed grid connection capacity of 6.5 or 13 MVA is largest for the PPA and ME revenue model and less for the SDE++ revenue in the solar south and east-west scenarios. This can be explained by the fact that the yearly revenues in the SDE++ revenue model contains the subsidy share which does not depend on the size of the export capacity.

It can be concluded that in case of similar generation patterns, arranging an agreement where the added resource is allowed to use a fixed share of the grid connection could improve the business case, despite of the additional grid connecting costs. It should be considered that using a fixed share of the grid connection capacity that was first fully available to the existing resource, requires an additional compensation for missed revenues for the existing farm on top of the shared costs of the grid connection.

6.4. Hybrid farm including Battery Optimization Results

This section discusses the impact of on-site storage on the cost-benefit framework. This section first identifies the curtailed energy in the base case either due to export constraints or negative prices. Secondly, the results of a hybrid farm with a battery added are discussed, solely focusing on the additional revenues a on-site storage system could earn. Lastly, costs are taken in to consideration and the added impact of on-site storage is further examined.

The results of ME revenue model based on 2022 data are considered to analyse the potential of the curtailed energy. It is the revenue model and input year resulting in the highest curtailment percentage and therefore there is potential in this specific case to consider peak shifting with a battery. To quantify the energy currently curtailed of each added resource for this revenue model, the curtailment is shown as a summed number of MWh and as a share of the total produced energy in Table 6.25.

Table 6.25: Curtailment Data

	Unit	Wind	Solar East-West	Solar South
Curtailment	%	2.13	19.1	14.7
Curtailment	MWh	2.95	27.3	17.3

As one can see, the curtailment is highest for the solar farm oriented to the east-west addition, as expected due to the similar generation pattern as the existing farm and the higher power density of the east-west oriented farm. Given that the grid connection in this case study is relatively large and the impact a smaller grid connection size has on the business case of a solar farm oriented to the east-west addition, it would be interesting to see if a battery added to this hybrid farm could improve the business case by peak shifting energy.

As mentioned in section 4.2 and section 5.3, the battery added to the hybrid farm has a predetermined

size. The behaviour of the battery is added to the optimization, which now aims to find the optimal size of the added east-west oriented solar farm and the energy flows by either selling energy directly or storing it in the battery and selling energy at a later time. The installation and operational costs of the battery are considered zero in the optimization.

The business case results of the hybrid farm consisting of a solar farm oriented to the east-west and a battery, are shown in Table 6.26 and Table 6.27. It shows the new NPV and the difference with the NPV without a battery, depicted as ∆NPV in M€. The table also shows the cable capacity factor cc_f, the curtailment and the expected CAPEX of the battery system. Since the costs are considered based on the NREL values per kWh, the costs scale with the energy of the battery and not the power. This is a simplification of the real-life situation, where power and energy both determine the costs of the battery.

The NPV of the hybrid farm including battery and the influence of subtracting the battery CAPEX are shown in Figure 6.20. The NPV of the original ME revenue model based on 2022 data and the added NPV due to the battery are visualized in Figure 6.17. The behaviour of a selection of battery configurations on a weekly level can be seen in Appendix B and an example is shown in Figure 6.18 and Figure 6.19.

Table 6.26: Hybrid Farm Optimization Results including Battery. For power ratings of 0.5 or 1 MW and C-rate of $\frac{1}{2}$ or $\frac{1}{4}$. Comparisons are drawn with base case ME model results for the solar farm oriented to the east-west results based on 2022 data.

	C-rate = 1/2		C-rate = 1/4		*No battery*
Power [MW]	0.5	1	0.5	1	
Energy [MWh]	1	2	2	4	
NPV [M€]	3.312	3.498	3.456	3.775	*3.115*
∆NPV [M€]	0.1976	0.3840	0.3414	0.6603	
cc_f	23.65%	23.74%	23.72%	23.89%	*23.54%*
Curtailment	18.09%	17.16%	17.36%	15.75%	*19.09%*
CAPEX battery [M€]	0.30	0.60	0.60	1.20	

Table 6.27: Hybrid Farm Optimization Results including Battery. For power ratings of 2 and 3 MW and C-rate of $\frac{1}{2}$ or $\frac{1}{4}$. Comparisons are drawn with base case ME model results for the solar farm oriented to the east-west results based on 2022 data.

	C-rate = 1/2		C-rate = 1/4		*No Battery*
Power [MW]	2	3	2	3	
Energy [MWh]	4	6	8	12	
NPV [M€]	3.847	4.168	4.361	4.879	*3.115*
∆NPV [M€]	0.7324	1.054	1.246	1.765	
cc_f	23.92%	24.08%	24.19%	24.44%	*23.54%*
Curtailment	15.43%	13.94%	12.87%	10.38%	*19.09%*
CAPEX battery [M€]	1.20	1.80	2.40	3.60	

As one can see in Table 6.26, Table 6.27 and Figure 6.17, the NPV of the hybrid system including a battery increases compared to a hybrid farm without a battery. The additional NPV increases with larger battery sizes. For the smaller batteries, shown in Table 6.26, doubling the original battery size in terms of power and energy, results in a higher added value than doubling the energy, while keeping the power constant, indicating that the power is an important factor. The curtailment decreases as the battery power and energy increase. The cable capacity factor cc_f increases as the battery power and energy increase.

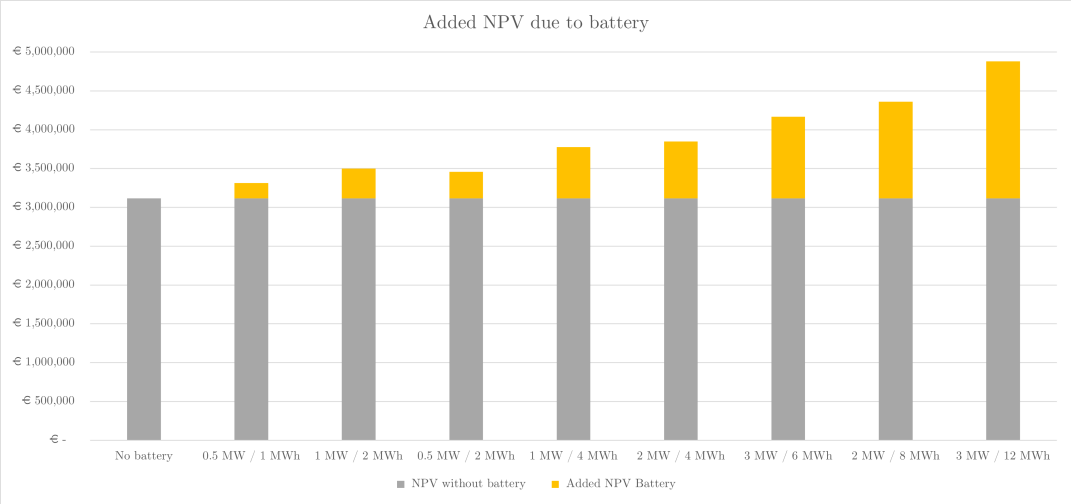

Figure 6.17: The added NPV $\triangle$NPV due to the battery system compared with the NPV before the battery addition.

The behaviour of the hybrid farm including a 3 MW / 12 MWh battery compared to the hybrid farm without a battery can be seen in Figure 6.18.

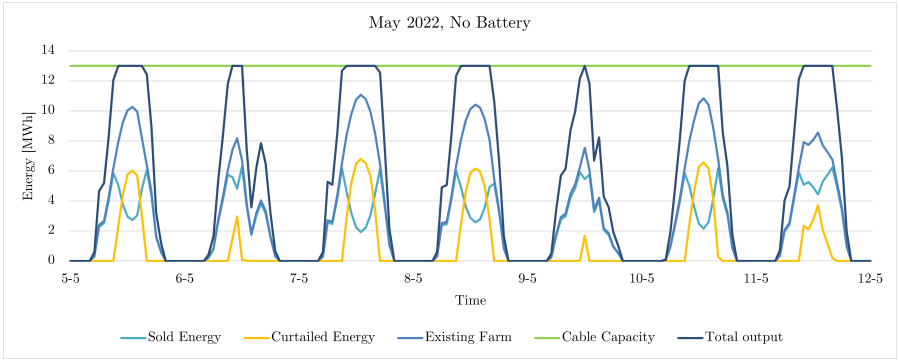

(a) Behaviour of the hybrid farm

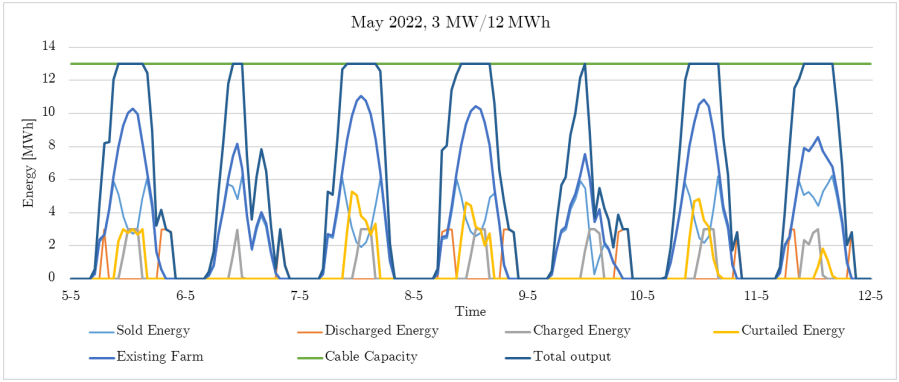

(b) Behaviour of the hybrid farm including a battery

Figure 6.18: Visualization of the impact of a battery on a hybrid farm for a week in May based on the ME revenue model and 2022 input data.

At times where the cable is limiting, the battery charges energy and decreases the curtailed energy. The battery mostly discharges at times when the solar farms produce little or no energy and thus increases the cable usage. To consider the battery behaviour in more detail, the SoC and the charge/discharge behaviour, curtailment and spot price are shown in Figure 6.19a and Figure 6.19b respectively.

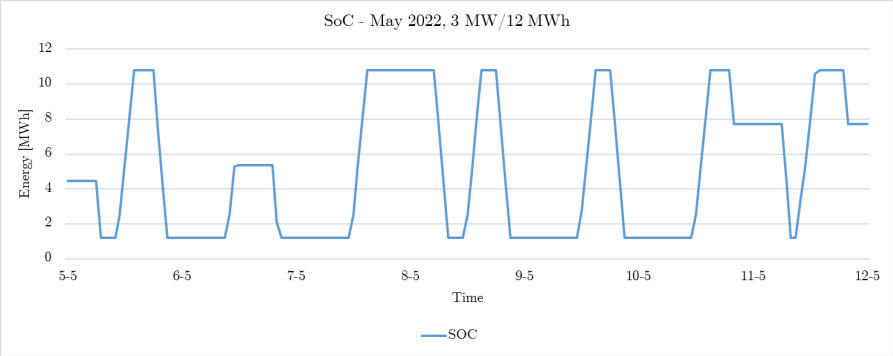

(a) State of Charge (SoC) of 3 MW / 12 MWh battery

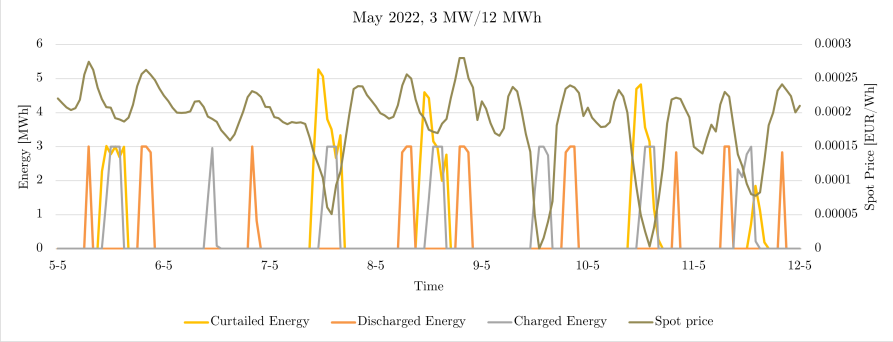

(b) Charge and discharge behaviour of 3 MW / 12 MWh considering the spot price. The residual curtailment is also shown.

Figure 6.19: A more detailed image of the battery behaviour in a hybrid farm in a week in May based on the ME revenue model and 2022 input data.

The SoC is limited between 10 and 90% of the battery energy, as can be seen in Figure 6.19a. The battery does not charge and discharge at the same time. The battery charges at times when there was curtailment in the situation without a battery, as shown in Figure 6.18a. The battery discharges at times of relatively high prices, as shown in Figure 6.19b. There is still some residual curtailment.

As discussed before, the costs of the battery considered are per unit of energy. It can be seen in Table 6.26 that the 1 MW/2 MWh and 0.5 MW/2 MWh yield the same battery CAPEX with this approach, but the NPV and cable capacity factor cc_f are higher and curtailment is lower for the 0.5 MW/2 MWh configuration. Doubling the battery size improves the added NPV ΔNPV with a factor a bit lower than two, while the CAPEX increase with a factor two.

The added NPV ΔNPV is always lower than the added CAPEX that needs to be paid in order to install the battery in the hybrid farm. This is also visualised in Figure 6.20. One can see that a the battery might improve the NPV, but has significant costs, resulting in a decrease in the NPV when considering the battery costs.

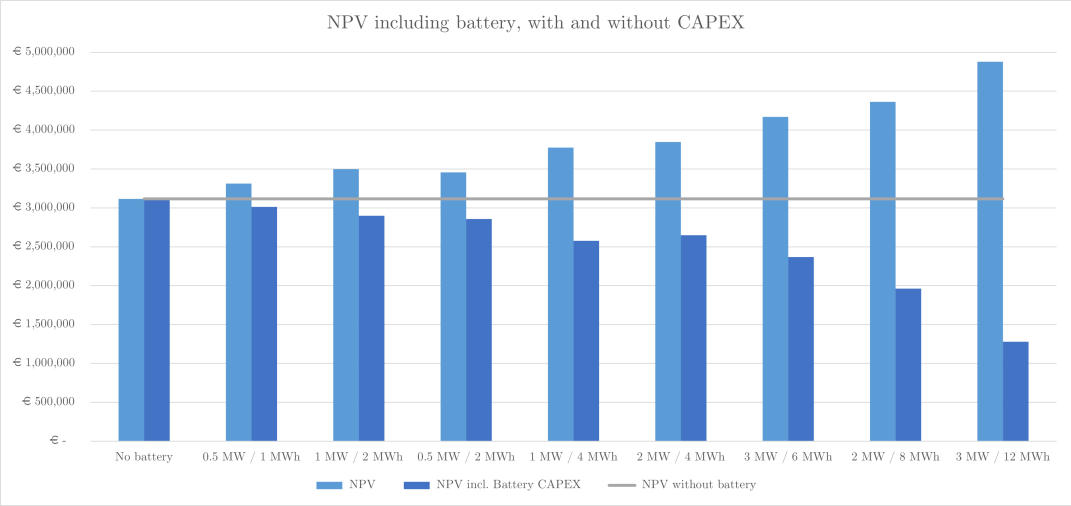

Figure 6.20: NPV of hybrid farm including battery, shown both excluding and including battery CAPEX. The grey line represents the NPV before battery addition.

This unprofitable part can be used to indicate the required additional revenue from potential other revenue streams or the required subsidy, considering the introduction of the subsidy per kWh of shifted solar energy, as discussed in chapter 2. The additional NPV due to the addition of the battery and the additional costs are combined to find the unprofitable part, as shown in Table 6.28 and Table 6.29. The unprofitable part is divided by the sum of the shifted energy to find the required subsidy to make up for the unprofitable part. The sum of the shifted energy is found by summing the discharged energy from the battery. It must be noted that the requirements for the upcoming subsidy are not specified yet, but will likely use a time-frame within which the total system may or may not export, to enforce peak-shifting. This has not been taken into account in this analysis yet, since the details still need to be presented.

Table 6.28: Hybrid Farm Optimization Results including Battery. For power ratings of 0.5 or 1 MW and C-rate of $\frac{1}{2}$ or $\frac{1}{4}$. Comparisons are drawn with base case ME model results for the solar farm oriented to the east-west results based on 2022 data.

	C-rate = 1/2		C-rate = 1/4	
Power [MW]	0.5	1	0.5	1
Energy [MWh]	1	2	2	4
ΔNPV [M€]	0.1976	0.3840	0.3414	0.6603
CAPEX battery [M€]	0.30	0.60	0.60	1.20
Sum of shifted energy [MWh]	151.8	295.5	264.0	512.4
Unprofitable part [M€]	0.1024	0.2160	0.2586	0.5397
Required subsidy [€/kWh]	0.6750	0.7310	0.9797	1.053

Table 6.29: Hybrid Farm Optimization Results including Battery. For power ratings of 2 and 3 MW and C-rate of $\frac{1}{2}$ or $\frac{1}{4}$. Comparisons are drawn with base case ME model results for the solar farm oriented to the east-west results based on 2022 data.

	C-rate = 1/2		C-rate = 1/4	
Power [MW]	2	3	2	3
Energy [MWh]	4	6	8	12
ΔNPV [M€]	0.7324	1.054	1.246	1.765
CAPEX battery [M€]	1.20	1.80	2.40	3.60
Sum of shifted energy [MWh]	566.6	812.2	970.1	1386.7
Unprofitable part [M€]	0.4676	0.7463	1.154	1.835
Required subsidy [€/kWh]	0.8523	0.9189	1.1893	1.3234

The lowest required subsidy is found for the smallest battery with a C-rate of 1/2. Higher subsidies are required for the batteries with a C-rate of 1/4 than a C-rate of 1/2 due to the higher required costs, despite the higher added NPV.

Making a battery twice as deep by going from C-rate of 1/2 to 1/4, results in less added value to the NPV than making a battery twice as large, by keeping the C-rate constant and going from 0.5 to 1 MW for example. This is also a result of only allowing the battery to charge from the energy produced by the added resource and not from the grid, which would induce grid fees for the grid connected power, creating more value for a C-rate of 1/4.

A C-rate of 1/2 also leads to a lower unprofitable part and thus required subsidy or alternative revenues, so the costs of the battery are better covered by the earned revenues. Therefore, it can be concluded that a C-rate of 1/2 is most optimal in this battery trading application.

Which battery configuration is optimal as an addition of the hybrid farm will depend on the height of the subsidy awarded or the earning from alternative revenue streams and other preferences. The larger the battery, the higher unprofitable top and the need for a subsidy or alternative revenue streams, but it also yields a higher cable capacity factor cc_f and lower curtailment.

The results discussed here use the old power density values. The new power density values increase the power density of the east-west oriented solar farm, resulting in higher installed capacity values and more curtailed energy. The amount of energy that could be shifted increases, which could increase the added value of the battery.

7

Conclusions and Recommendations

The potential of cable pooling in the Dutch context is considered in this thesis as a possible solution to congestion for developers. Cable pooling is defined as a (existing) renewable resource that shares its grid connection with another (new) renewable resource. The combined generation is considered a hybrid farm and the joined output is delivered to the grid. According to various industry parties, cable pooling shows potential in the Netherlands and could provide new development locations in congested areas. The urgency to investigate alternative grid connecting possibilities will stay present until the grid congestion status is solved, which can take up to 10 years.

Cable pooling is considered a multi faced challenge, dealing with regulatory, legal, technical and financial parameters. This research therefore aims to create a calculation framework for developers with a potential cable pooling location to make a preliminary analysis of the economical potential of the location, which can be used as a decision tool on whether or not to continue the cable pooling development there.

The focus in literature on hybrid farms is mostly on stand-alone applications and there are few papers focused on sharing a grid connection with a hybrid farm. The current grid-connected research does not consider the influence of the market prices on the business case of a technology. A contribution of this research is therefore considering an hourly time scale to show the influence of the energy production of a technology and the prices at that time. Furthermore, the prior research usually did not consider the long-term market developments. The focus was often on optimally sizing one total hybrid farm and not analysing the potential of adding different technologies to an existing technology. Therefore, this research considers different generation types to add to one existing resource to form different hybrid farms configurations.

The current and future Dutch context shape the regulatory and legal context for cable pooling. Currently, two generating resources in close proximity are allowed to share one grid connection and operate as two separate generating resources, with an upcoming expansion to four generating resources and the inclusion of energy conversion and storage installations. Therefore, a hybrid farm consisting of generation resources is considered using combinations of solar and wind, with a battery expansion.

An important future development to monitor is the Use-it-or-lose-it (”UIOLI”) principle, which could cause that the size of oversized grid connections will be decreased to the required amount if the full grid connection capacity is not used. It could also incentivise cable pooling as more oversized grid connection owners will look for a purpose for this oversized part. Furthermore, different mechanisms are in development to use the current grid-infrastructure better, like usage of fault reserves, congestion management and non-firm ATO.

The Dutch context also yields different revenue streams. Generating resources earn revenue by trading on the spot market. Three different revenue models are considered. One revenue model considers yearly additions to the revenues earned on the spot market based on the SDE++ subsidy, present to

make up for the unprofitable part of the business case. Another revenue model considers a Power Purchase Agreement (”PPA”), an agreement between consumer and producer with a fixed price. The last revenue model solely considers the market earned revenues and is market exposed (”ME”). The revenue models based on the Dutch context are also a contribution to the current literature.

Combining the Dutch context and the literature, a problem definition was formulated to identify and optimize the potential of a cable pooling location using an hourly analysis and long-term economics to find the maximum Net Present Value (”NPV”) of the installed capacity of the added farm, taking into account all the technical and financial parameters. The NPV can be found for different revenue models and different possible additions.

A cable pooling location is contains a renewable generation project with a secured grid connection, called the existing renewable resource. The existing renewable resource can be one of two types of renewable generation: solar or wind. The new renewable resource is either a wind farm or a solar farm, possibly in combination with a battery. The focus for cable pooling has been mostly on combining solar energy oriented to the south and wind energy, due to the complementary generation patterns. Due to the low and sometimes even negative prices during the solar peak, interest in solar panels oriented to the east and west is growing. The three possible additions to form a hybrid farm considered are therefore wind or solar oriented to either the south or east-west.

The residual space on the connection after export of the existing farm forms an export constraint for the added farm and is considered for each hour. Each type of new renewable resource has its own typical generation profile with correlation to the existing renewable resource and thus the hourly residual cable capacity . A technology dependent hourly weather and losses factor (”WLF”) is introduced to find the hourly maximum produced energy based on a weather and internal losses dependent reduction factor for the installed capacity. For solar energy, this also depends on the DC/AC ratio, which is revenue model dependent. This maximum produced energy is divided into hourly sold and curtailed energy.

Furthermore, the optimal installed capacity is bounded by the available land area to develop the new resource. This is enforced by use of a technology specific power density function. The highest power density is found for solar farms oriented to the east and west, followed by solar farms oriented to the south. Wind farms have the lowest power density.

The optimization method is tested using a case study. A location is selected with a grid connection size of 13 MVA and an existing solar farm with east-west orientation with a size of 15 MWp. The size of the land area that can be used for the new farm is 12 ha. Hourly weather and spot market data are used from the years 2019 and 2022. The base year 2019 is selected given the least external influences on the market prices and 2022 as being the most representative for the future given the increased share of renewable energy and its influence on the spot market prices.

Results of the optimization of the hybrid farm are generated using a base case and different sensitivities. Furthermore, results of the optimization of the hybrid farm including a battery are generated. The addition of either of the three possible additions to form a hybrid farm with the existing resource, result in positive NPV values and an increased usage of the grid connection, defined as the cable capacity factor.

The wind addition generates the highest NPV values for nearly all revenue models and both years, caused by the complementary behaviour of the wind generation and the generation of the existing solar farm oriented to the east-west. Therefore, curtailment of the added wind resource is limited and occurs almost only at negative prices. For both solar additions, oriented to the south or east-west, curtailment also occurs at positive prices if the export constraint is active.

The results of the two solar farms are similar, but some results can be distinguished. The SDE++ revenue model results in a higher NPV for the solar farm oriented to the east-west due to a higher installed capacity. The NPV based on 2022 input data for the SDE++ model is higher for the solar farm oriented to the east-west than the wind farm. For the PPA revenue model, the yearly net cash flows are higher

for the east-west oriented solar farm for both input years, but the high investment costs and the lower capacity factor, leading to less output per installed capacity, cause the optimal NPV to be lower than the NPV for the south oriented farm. For the ME revenue model shows the increased value of the slightly shifted output of a east-west oriented farm compared to a south oriented farm, resulting in a higher NPV based in 2022 spot market data.

The results are tested for robustness by varying some of the inputs. Different technical and economical inputs are varied by + or -10% and the impact on the NPV is considered. The results of the wind addition are very sensitive to the wind speed inputs and the hub height selected. The results of the solar addition, both south and east-west oriented, are sensitive to the irradiance inputs. Changing the tilt shows a small impact on the business case, but indicate that the tilt value used is not optimal. For follow-up studies, it is recommended to more carefully select one or multiple tilt values at the start of the analysis or even add the tilt as a decision variable in the optimization.

The long-term developments are considered using a long-term market outlook ("LTMO"), divided into the market factor LT_t to indicate the yearly expected price of the spot market in the future and value factor $LT_{f,j,t}$ to indicate the yearly expected value of solar and wind energy in the future. The results of all additions are very sensitive to the usage of the LTMO and to changes in the discount rate and investment costs.

Even with large changes in the NPV, all additions and all revenue scenarios for both input years result in a positive NPV for all technologies. Adding a resource with a similar generation profile thus results in a positive NPV in this particular case study. The grid connection size of 13 MVA is relatively large for a 15 MWp east-west oriented solar farm. Therefore, a generalization is made by decreasing the grid connection size in steps of 10% and the impact on the business case for each addition is considered. This quickly shows that the influence is negligible for the wind addition, while substantial for both solar additions.

A reduction to 70% and 60% of the original grid connection size results in negative NPV values for the PPA and ME revenue models and SDE++ revenue model respectively for both base years and both solar additions. Therefore, it can be concluded that in this particular case study, there is ample space on the grid connection and the results are robust, but generally speaking, a complementary production pattern is preferred when considering a cable pooling hybrid farm where only the residual space on the cable can be used by the added resource.

A cable pooling agreement where the addition can use a fixed grid capacity share instead of the residual energy after export of the existing farm is also considered. From about 6.5 MVA (50% of the grid connection capacity) and higher fixed grid capacity values, this shows promise for both solar additions due to the similar production pattern, despite of the costs associated with the grid connection. The existing farm is however likely to want a compensation for this usage, which is currently not taken into account.

The base case results show that the ME revenue model based on 2022 data yields the highest curtailment for all additions. The highest curtailment is seen for the solar addition oriented to the east-west, explained by the similar production pattern as the existing resource. The curtailed energy could temporarily be stored and sold at a later time using a battery, defined as energy shifting. The optimization is performed to find the optimal solar east-west addition to the existing east-west farm including a battery. The behaviour of the battery shows that the excess energy is stored and sold at a later time, increasing the revenues and cable capacity factor, while also reducing the curtailment.

Different battery configurations are considered. Not considering the costs of installing and maintaining the battery per unit energy, a battery added to the hybrid farm yields a higher NPV than the base case hybrid farm scenario. The NPV increases as the power rating and energy of the battery increase. Considering the battery costs per unit energy however leads to a decrease in the NPV compared to the base case scenario. The upcoming peak-shifting subsidy for a battery added to a solar farm per kWh or alternative revenue streams could make up for this unprofitable part. A battery with a C-rate of 1/2

seems more fit for the energy shifting revenue stream than the C-rate of 1/4 based on the approach used in this thesis.

Based on these results, there are take-aways and conclusions on three levels. The levels are, from small to large: the case study, the optimization tool, consisting of the methodology applied in python, and cable pooling in the Dutch context. The relation is shown using an onion diagram in Figure 7.1. The same levels are used to give the main recommendations.

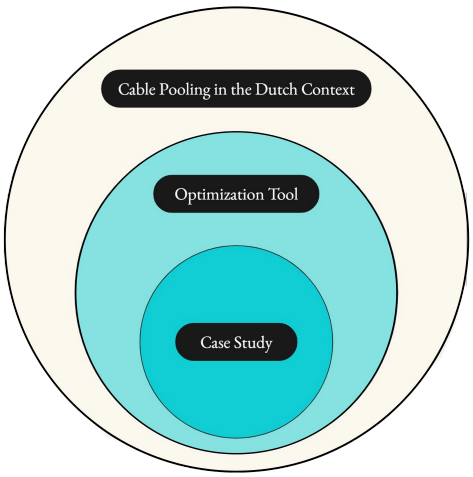

Figure 7.1: Onion diagram depicting the different levels for the take-aways and conclusions

The case study shows potential for a cable pooling hybrid farm consisting of either a wind or solar addition, with both orientations. The results of this case study are robust to changes in the input, despite large impact of certain technical and economical inputs. The case study considered has a relatively large grid connection and generalizing the results shows that complementary resources result in a better fit for a cable pooling hybrid farm if the residual space is used than resources with similar production patterns. For similar production patterns, sharing the grid connection based on a fixed share is more interesting. This matches the approach used for the east-west oriented farm in development, where Vattenfall will share the grid connection with the other solar farm oriented to the east-west based on a 50/50 share.

The solar power density values used to obtain the results differ from the values that result from the approach used in this research for the east-west oriented farm. This impacts the results, leading to higher installed capacities and corresponding CAPEX and an increased cable capacity factor and curtailment. The PPA and ME revenue models have been recalculated using 2022 data and the PPA NPV decreases, while the ME NPV increases. Using the PPA revenue model, the land boundary no longer forms a constraint.

The tool is thus able to find the NPV for three different additions, each for three different revenue models and based on two input years. The tool can be tailored to the specific case study and quickly gains insides into the potential of a cable pooling location and the robustness of this potential by varying different inputs and can prove useful in the preliminary analysis of the potential of a cable pooling location for Vattenfall.

A recommendation would be to expand the tool with more revenue streams for the battery to make up for the unprofitable part. The battery could also be considered as a separate cable pooling resource in the future instead of a behind-the-meter addition. Another expansion could be to add more decision variables in the optimization, such as the tilt or orientation of the solar farm or the hub height of the turbine. It would also be interesting to consider an addition to the existing farm consisting of multiple resources combined.

The tool currently uses two different input years, each impacting the results. The impact of the input year selected is largest for the added wind resource. It would be valuable to expand the input years by adding more representative or more recent years to the base years in the future to create a more validated result.

Furthermore, as the tool showed to be sensitive to certain weather related and economical inputs, it is recommended to carefully consider the wind speed and irradiation inputs and the usage of the LTMO. The LTMO is used by introducing two factors, yearly long-term market factor LT_t and yearly technology dependent value factors $LT_{f,j,t}$. This approach aims to correct the summed yearly revenue values to account for the future value of electricity in general and for a specific technology in the future, but the current usage might not fully exploit this characteristic.

The expected average spot market values might be calculated in a different way than the average spot market values to which they are compared, resulting in the yearly long-term market factor LT_t. Additionally, the LTMO values might be tailored to a grid-connected resource with no export constraints, potentially leading to different yearly long-term market factors LT_t and value factors $LT_{f,j,t}$. Since a change of 10% in the long-term market factor LT_t, already impacts the NPV with values up to 50%, an improved approach for the LTMO should be considered in the future.

The tool consists of assumptions and simplifications which should be analysed in more detail based on more case-studies and a further deep dive into different topics. For example, the degradation of the existing farm and the impact thereof on the business case of the added resource, the costs of the grid connection usage when cable pooling, the impact of the LTMO and the tilt of the added solar farms.

Considering cable pooling in the Dutch context, congestion causes a need for alternative grid connecting possibilities for at least 10 more years, given the higher pace of the renewable development than the expansions and reinforcements of the grid. Based on the Dutch context and case study results, cable pooling shows potential the different revenue models (SDE++, PPA and ME) and additions (wind, solar oriented to the south and east-west), based on two input years (2019 and 2022). A possible expansion to four generating resources and conversion units sharing one grid connection is in the pipeline. The usage of the fault reserves as a grid connection possibility is not considered in this research but could present an interesting opportunity. These alternatives provide opportunities in congested areas, allowing parties like Vattenfall to continue the development of renewable energy while awaiting the grid expansions.

It must be noted that currently there are not many cable pooling projects present in the Netherlands, despite the regulatory and legal context allowing it. This is potentially due to legal hurdles and uncertainties, for example to which extent the grid connection capacity can be used by a hybrid farm instead of the existing resource. Therefore, it is recommended to create transparency in cable carrying capability calculation methods by DSOs to limit this uncertainty. Furthermore, to create a larger incentive to cable pool, it is recommended to create a separate subsidy for cable pooling projects. It would be interesting to gain insights into why cable pooling would or would not be used by industry parties and if not, what incentives would allow them to use it.

Bibliography

Abdul Aziz, N. I., Sulaiman, S. I., Shaari, S., Musirin, I., & Sopian, K. (2017). Optimal sizing of standalone photovoltaic system by minimizing the loss of power supply probability. *Solar Energy*, *150*, 220–228. https://doi.org/10.1016/j.solener.2017.04.021

Abedi, S., Alimardani, A., Gharehpetian, G. B., Riahy, G. H., & Hosseinian, S. H. (2012). A comprehensive method for optimal power management and design of hybrid RES-based autonomous energy systems. *Renewable and Sustainable Energy Reviews*, *16*(3), 1577–1587. https://doi.org/10.1016/j.rser.2011.11.030

ACM. (2022a). *Acm stimuleert netbeheerders slimmer gebruik te maken van bestaande netten*. Retrieved June 20, 2023, from https://www.acm.nl/nl/publicaties/acm-stimuleert-netbeheerders-slimmer-gebruik-te-maken-van-bestaande-netten

ACM. (2022b). *Codebesluit enkelvoudige storingsreserve*. Retrieved June 20, 2023, from https://www.acm.nl/nl/publicaties/codebesluit-enkelvoudige-storingsreserve

ACM. (2022c). *Consultatie alternatieve transportrechten en use it or lose it*. Retrieved June 20, 2023, from https://www.acm.nl/nl/publicaties/consultatie-alternatieve-transportrechten-en-use-it-or-lose-it

ACM. (2022d). *Onwerpcodebesluit enkelvoudige storingsreserve*. Retrieved June 20, 2023, from https://www.acm.nl/nl/publicaties/ontwerpcodebesluit-enkelvoudige-storingsreserve

ACM. (2022e). *Voorstel codewijziging variabel recht op transport non-firm ato*. Retrieved June 20, 2023, from https://www.acm.nl/nl/publicaties/voorstel-codewijziging-variabel-recht-op-transport-non-firm-ato

ACM. (2023a). *Acm maakt maatschappelijk prioriteren door netbeheerders mogelijk*. Retrieved June 20, 2023, from https://www.acm.nl/nl/publicaties/acm-maakt-maatschappelijk-prioriteren-door-netbeheerders-mogelijk

ACM. (2023b). *Brede steun voor maatschappelijk prioriteren, acm roept netbeheerders op aan de slag te gaan*. Retrieved November 3, 2023, from https://www.acm.nl/nl/publicaties/brede-steun-voor-maatschappelijk-prioriteren-acm-roept-netbeheerders-op-aan-de-slag-te-gaan

ACM. (2023c). *Ontwerp codebesluit non-firm ato*. Retrieved October 20, 2023, from https://www.acm.nl/system/files/documents/ontwerp-codebesluit-non-firm-ATO-2023-09-28.pdf

ACM. (2023d). *Publicatie eindnotitie consultatie atr en uioli (gotork)*. Retrieved October 20, 2023, from https://www.acm.nl/system/files/documents/publicatie-eindnotitie-consultatie-atr-en-uioli-gotork.pdf

Al-Sharafi, A., Yilbas, B. S., Sahin, A. Z., & Ayar, T. (2017). Performance assessment of hybrid power generation systems: Economic and environmental impacts. *Energy Conversion and Management*, *132*, 418–431. https://doi.org/10.1016/j.enconman.2016.11.047

Andergie. (2023). *Congestiemanagement*. Retrieved May 27, 2023, from https://andergie.nl/congestie management/

Anoune, K., Ghazi, M., Bouya, M., Laknizi, A., Ghazouani, M., Abdellah, A. B., & Astito, A. (2020). Optimization and techno-economic analysis of photovoltaic-wind-battery based hybrid system. *Journal of Energy Storage*, *32*. https://doi.org/10.1016/j.est.2020.101878

Astariz, S., & Iglesias, G. (2016). Output power smoothing and reduced downtime period by combined wind and wave energy farms. *Energy*, *97*, 69–81. https://doi.org/10.1016/j.energy.2015.12.108

Astariz, S., & Iglesias, G. (2017). The collocation feasibility index – A method for selecting sites for co-located wave and wind farms. *Renewable Energy*, *103*, 811–824. https://doi.org/10.1016/j.renene.2016.11.014

Astariz, S., Perez-Collazo, C., Abanades, J., & Iglesias, G. (2015). Co-located wave-wind farms: Economic assessment as a function of layout. *Renewable Energy*, *83*, 837–849. https://doi.org/10.1016/j.renene.2015.05.028

Bakos, G. C., & Tsagas, N. F. (2018). *Technoeconomic assessment of a hybrid solar/wind installation for electrical energy saving* (tech. rep.).

Barakat, S., Ibrahim, H., & Elbaset, A. A. (2020). Multi-objective optimization of grid-connected PV-wind hybrid system considering reliability, cost, and environmental aspects. *Sustainable Cities and Society*, *60*. https://doi.org/10.1016/j.scs.2020.102178

BCG. (2023). *Free electricity unlikely when needed*. Retrieved May 30, 2023, from https://www.bcg.com/publications/2022/free-electricity-unlikely-when-needed

Bloomberg. (2022). *Renewable energy burst sends dutch power prices to lowest ever*. Retrieved July 17, 2023, from https://www.bloomberg.com/news/articles/2022-04-25/renewable-energy-burst-sends-dutch-power-prices-to-lowest-ever#xj4y7vzkg

Centraal Bureau voor Statistiek. (2022). *Meer elektriciteit uit hernieuwbare bronnen, minder uit fossiele bronnen*. Retrieved September 11, 2023, from https://www.cbs.nl/nl-nl/nieuws/2022/10/meer-elektriciteit-uit-hernieuwbare-bronnen-minder-uit-fossiele-bronnen

Centraal Bureau voor Statistiek. (2023). *Aandeel hernieuwbare elektriciteit met 20 procent gestegen in 2022*. Retrieved September 11, 2023, from https://www.cbs.nl/nl-nl/nieuws/2023/10/aandeel-hernieuwbare-elektriciteit-met-20-procent-gestegen-in-2022

Chen, H. H., Kang, H. Y., & Lee, A. H. (2010). Strategic selection of suitable projects for hybrid solar-wind power generation systems. https://doi.org/10.1016/j.rser.2009.08.004

Cole, W., Frazier, A., & Augustin, C. (2021). *Cost projections for utility-scale battery storage: 2021 updat*. Retrieved September 8, 2023, from https://www.nrel.gov/docs/fy21osti/79236.pdf

Copernicus. (2023). *Era5 hourly data on single levels from 1940 to present*. Retrieved September 11, 2023, from https://cds.climate.copernicus.eu/cdsapp#!/dataset/reanalysis-era5-single-levels?tab=overview

Copernicus Atmosphere Monitoring Service. (2023). *Cams solar radiation time-series*. Retrieved September 8, 2023, from https://ads.atmosphere.copernicus.eu/cdsapp#!/dataset/cams-solar-radiation-timeseries?tab=overview

de Souza Nascimento, M. M., Shadman, M., Silva, C., de Freitas Assad, L. P., Estefen, S. F., & Landau, L. (2022). Offshore wind and solar complementarity in Brazil: A theoretical and technical potential assessment. *Energy Conversion and Management*, *270*. https://doi.org/10.1016/j.enconman.2022.116194

Diab, I., Scheurwater, B., Saffirio, A., Chandra-Mouli, G. R., & Bauer, P. (2022). Placement and sizing of solar PV and Wind systems in trolleybus grids. *Journal of Cleaner Production*, *352*. https://doi.org/10.1016/j.jclepro.2022.131533

Diaf, S., Diaf, D., Belhamel, M., Haddadi, M., & Louche, A. (2007). A methodology for optimal sizing of autonomous hybrid PV/wind system. *Energy Policy*, *35*(11), 5708–5718. https://doi.org/10.1016/j.enpol.2007.06.020

Diaf, S., Notton, G., Belhamel, M., Haddadi, M., & Louche, A. (2008). Design and techno-economical optimization for hybrid PV/wind system under various meteorological conditions. *Applied Energy*, *85*(10), 968–987. https://doi.org/10.1016/j.apenergy.2008.02.012

Dufo-López, R., Bernal-Agustín, J. L., Yusta-Loyo, J. M., Domínguez-Navarro, J. A., Ramírez-Rosado, I. J., Lujano, J., & Aso, I. (2011). Multi-objective optimization minimizing cost and life cycle emissions of stand-alone PV-wind-diesel systems with batteries storage. *Applied Energy*, *88*(11), 4033–4041. https://doi.org/10.1016/j.apenergy.2011.04.019

Duurzaam ondernemen. (2022). *Plaatsing batterij bij zonnepark en windturbine betekent primeur*. Retrieved May 27, 2023, from https://www.duurzaam-ondernemen.nl/plaatsing-batterij-bij-zonnepark-en-windturbine-betekent-primeur/#:~:text=Plaatsing%5C%20batterij%5C%20bij%5C%20zonnepark%5C%20en%5C%20windturbine%5C%20betekent%5C%20primeur,een%5C%20overschot%5C%20aan%5C%20elektriciteit.%5C%20Dit%5C%20stabiliseert%5C%20het%5C%20net.

Ekren, B. Y., & Ekren, O. (2009). Simulation based size optimization of a PV/wind hybrid energy conversion system with battery storage under various load and auxiliary energy conditions. *Applied Energy*, *86*(9), 1387–1394. https://doi.org/10.1016/j.apenergy.2008.12.015

Energiesamen. (2022). *Benutting storingsreserve wettelijk geregeld*. Retrieved June 20, 2023, from https://energiesamen.nu/nieuws/153/benutting-storingsreserve-wettelijk-geregeld

Energy Storage NL. (2023). *Kabinet overweegt verplichting batterijen bij zonneparken*. Retrieved May 27, 2023, from https://www.energystoragenl.nl/kabinet-overweegt-verplichting-batterijen-bij-zonneparken/

EnergyStorageNL. (2021). *Cable pooling met energieopslag*. Retrieved May 27, 2023, from https://www.energystoragenl.nl/wp-content/uploads/2021/11/20211125-Cable-Pooling-met-Energieopslag-ESNL-bijeenkomst-25-nov.pdf

Engie. (2022). *Energieprijzen 2023*. Retrieved September 8, 2023, from https://www.engie.nl/over-ons/kennisbank/artikel/energieprijzen-2023#:~:text=De%20hogere%20prijzen%20in%202021%20waren%20te%20wijten,het%20aanbod%2C%20wat%20resulteerde%20in%20een%20stijgende%20energieprijs.

Engin, M. (2013). Sizing and simulation of PV-wind hybrid power system. *International Journal of Photoenergy*, *2013*. https://doi.org/10.1155/2013/217526

Entso-E. (2023). *Requirements for generators*. Retrieved April 20, 2023, from https://www.entsoe.eu/network_codes/rfg/

Farfan, J., & Breyer, C. (2018). Combining Floating Solar Photovoltaic Power Plants and Hydropower Reservoirs: A Virtual Battery of Great Global Potential. *Energy Procedia*, *155*, 403–411. https://doi.org/10.1016/j.egypro.2018.11.038

Financiering Zonnepanelendelen. (n.d.). *Ppa voor zonne-energie*. Retrieved May 27, 2023, from https://financiering.zonnepanelendelen.nl/nl/blog/ppa-voor-zonne-energie/

Firan. (2023). *Cable pooling*. Retrieved March 20, 2023, from https://www.firan.nl/cable-pooling/

Gajewski, P., & Pieńkowski, K. (2021). Control of the hybrid renewable energy system with wind turbine, photovoltaic panels and battery energy storage. *Energies*, *14*(6). https://doi.org/10.3390/en14061595

Geocontent RVO. (2023). *Windviewer*. Retrieved September 11, 2023, from https://geocontent.rvo.nl/windviewer/

Golroodbari, S. Z., Vaartjes, D. F., Meit, J. B., van Hoeken, A. P., Eberveld, M., Jonker, H., & van Sark, W. G. (2021). Pooling the cable: A techno-economic feasibility study of integrating offshore floating photovoltaic solar technology within an offshore wind park. *Solar Energy*, *219*, 65–74. https://doi.org/10.1016/j.solener.2020.12.062

González, A., Riba, J. R., Rius, A., & Puig, R. (2015). Optimal sizing of a hybrid grid-connected photovoltaic and wind power system. *Applied Energy*, *154*, 752–762. https://doi.org/10.1016/j.apenergy.2015.04.105

GOPACS. (2023). *Producten*. Retrieved June 20, 2023, from https://www.gopacs.eu/biedplichtcontract-intraday/

Green Tech Renewables. (2020). *Determining module inter-row spacing*. Retrieved June 27, 2023, from https://www.greentechrenewables.com/article/determining-module-inter-row-spacing

Hezelaer Energy. (2019). *Liander over vrijgave storingsreserve: 'het gaat echt heel veel extra ruimte geven'*. Retrieved March 20, 2023, from https://www.hezelaer.nl/2020/12/11/hezelaer-energy-gaat-cable-poolen-uniek-in-nederland/

Hiendro, A., Kurnianto, R., Rajagukguk, M., Simanjuntak, Y. M., & Junaidi. (2013). Techno-economic analysis of photovoltaic/wind hybrid system for onshore/remote area in Indonesia. *Energy*, *59*, 652–657. https://doi.org/10.1016/j.energy.2013.06.005

Hier Opgewekt. (2021). *Kennisdossiers - cable pooling: Wat is het en wanneer is het interessant*. Retrieved May 17, 2023, from https://www.hieropgewekt.nl/kennisdossiers/cable-pooling-wat-is-het-en-wanneer-is-het-interessant

Holmgren, W. F., Hansen, C. W., & Mikofski, M. A. (2018). Pvlib python: A python package for modeling solar energy systems. [https://doi.org/10.21105/joss.00884]. *Journal of Open Source Software*, *3*(29), 884.

IEA-Wind. (2021). *Wind energy in the netherlands*. Retrieved March 20, 2023, from https://iea-wind.org/about-iea-wind-tcp/members/the-netherlands/

International Energy Agency. (2021). *The cost of capital in clean energy transitions*. Retrieved September 11, 2023, from https://www.iea.org/articles/the-cost-of-capital-in-clean-energy-transitions

Inverter.com. (2020). *What is solar inverter clipping?* Retrieved September 11, 2023, from https://www.inverter.com/what-is-solar-inverter-clipping#:~:text=When%20DC%20power%20generated%20from%20the%20solar%20panels,panels%20over%20the%20inverter%20capacity%20%28above%20one%20ratio%29.

Javed, M. S., Song, A., & Ma, T. (2019). Techno-economic assessment of a stand-alone hybrid solar-wind-battery system for a remote island using genetic algorithm. *Energy*, *176*, 704–717. https://doi.org/10.1016/j.energy.2019.03.131

Jongsma, C., Van Cappellen, L., & Vendrik, J. (2021). *Omslagpunt grootschalige batterijopslag Achtergrondrapport Dit rapport is geschreven door* (tech. rep.). CE Delft. Delft. www.ce.nl

Jongsma, C., van Cappellen, L., & Vendrik, J. (2021). *Omslagpunt grootschalige batterijopslag* (tech. rep.). CE Delft. Delft. www.ce.nl

K. Zipp. (2018). *Solar power world - why array oversizing makes financial sense*. Retrieved September 8, 2023, from https://new.abb.com/docs/librariesprovider117/default-document-library/solar-inverters/solar_power_world-article.pdf?sfvrsn=80a7614_4

Kaabeche, A., Belhamel, M., & Ibtiouen, R. (2011a). Sizing optimization of grid-independent hybrid photovoltaic/wind power generation system. *Energy*, *36*(2), 1214–1222. https://doi.org/10.1016/j.energy.2010.11.024

Kaabeche, A., Belhamel, M., & Ibtiouen, R. (2011b). Techno-economic valuation and optimization of integrated photovoltaic/wind energy conversion system. *Solar Energy*, *85*(10), 2407–2420. https://doi.org/10.1016/j.solener.2011.06.032

Kaldellis, J. K., Zafirakis, D., & Kondili, E. (2009). Optimum autonomous stand-alone photovoltaic system design on the basis of energy pay-back analysis. *Energy*, *34*(9), 1187–1198. https://doi.org/10.1016/j.energy.2009.05.003

Kaldellis, J. K., Zafirakis, D., & Kondili, E. (2010). Optimum sizing of photovoltaic-energy storage systems for autonomous small islands. *International Journal of Electrical Power and Energy Systems*, *32*(1), 24–36. https://doi.org/10.1016/j.ijepes.2009.06.013

Klimaatfeiten. (2020). *De schaalbaarheid van zonne- en windenergie*. Retrieved March 20, 2023, from https://www.klimaatfeiten.nl/maatregelen/energie/schaalbaarheid

Ma, T., Yang, H., & Lu, L. (2014). A feasibility study of a stand-alone hybrid solar-wind-battery system for a remote island. *Applied Energy*, *121*, 149–158. https://doi.org/10.1016/j.apenergy.2014.01.090

Ma, T., Yang, H., Lu, L., & Peng, J. (2014). Technical feasibility study on a standalone hybrid solar-wind system with pumped hydro storage for a remote island in Hong Kong. *Renewable Energy*, *69*, 7–15. https://doi.org/10.1016/j.renene.2014.03.028

Mertens, S. (2022). Design of wind and solar energy supply, to match energy demand. *Cleaner Engineering and Technology*, *6*. https://doi.org/10.1016/j.clet.2022.100402

Mousa, K., Alzu'bi, H., & Diabat, A. (2010). *Design of a Hybrid Solar-Wind Power Plant Using Optimization* (tech. rep.).

Najafi Ashtiani, M., Toopshekan, A., Razi Astaraei, F., Yousefi, H., & Maleki, A. (2020). Techno-economic analysis of a grid-connected PV/battery system using the teaching-learning-based optimization algorithm. *Solar Energy*, *203*, 69–82. https://doi.org/10.1016/j.solener.2020.04.007

Netbeheer Nederland. (2019). *Basisdocument over energie-infrastructuur*. Retrieved May 27, 2023, from https://www.netbeheernederland.nl/_upload/Files/Basisdocument_over_energie-infrastructuur_143.pdf

Netbeheer Nederland. (2020). *Cable pooling*. Retrieved May 27, 2023, from https://www.netbeheernederland.nl/_upload/Files/Netcapaciteit_60_5de4ca08ea.pdf

Next-Kraftwerke. (n.d.). *Power purchase agreement ppa*. Retrieved May 27, 2023, from https://www.next-kraftwerke.nl/kennis/power-purchase-agreement-ppa

Ngan, M. S., & Tan, C. W. (2012). Assessment of economic viability for PV/wind/diesel hybrid energy system in southern Peninsular Malaysia. *Renewable and Sustainable Energy Reviews*, *16*(1), 634–647. https://doi.org/10.1016/j.rser.2011.08.028

NREL SAM. (2020). *National renewable energy laboratory system advisory model - pv cost and component data*. Retrieved September 8, 2023, from https://sam.nrel.gov/photovoltaic/pv-cost-component.html

Ould Bilal, B., Sambou, V., Ndiaye, P. A., Kébé, C. M., & Ndongo, M. (2010). Optimal design of a hybrid solar-wind-battery system using the minimization of the annualized cost system and the minimization of the loss of power supply probability (LPSP). *Renewable Energy*, *35*(10), 2388–2390. https://doi.org/10.1016/j.renene.2010.03.004

PBL. (2022). *Pbl 2022 - zon pv op een kleinere netaansluiting*. Retrieved June 20, 2023, from https://www.pbl.nl/sites/default/files/downloads/pbl-2022-zon-pv-op-een-kleinere-netaansluiting-4909.pdf

Perera, A. T., Attalage, R. A., Perera, K. K., & Dassanayake, V. P. (2013). Designing standalone hybrid energy systems minimizing initial investment, life cycle cost and pollutant emission. *Energy*, *54*, 220–230. https://doi.org/10.1016/j.energy.2013.03.028

Public Domain Pictures. (2023). *Renewable energy*. Retrieved May 27, 2023, from https://www.publicdomainpictures.net/en/view-image.php?image=131043&picture=renewable-energy

Rabobank. (2023). *Dit zijn de gevolgenvan van een overbelast elektriciteitsnet*. Retrieved May 27, 2023, from https://www.rabobank.nl/bedrijven/groei/duurzaamheid/elektrische-bedrijfsmiddelen/netcongestie-overbelast-stroomnet

Rajkumar, R. K., Ramachandaramurthy, V. K., Yong, B. L., & Chia, D. B. (2011). Techno-economical optimization of hybrid pv/wind/battery system using Neuro-Fuzzy. *Energy*, *36*(8), 5148–5153. https://doi.org/10.1016/j.energy.2011.06.017

Rijksoverheid. (2023). *Klimaatbeleid*. Retrieved May 27, 2023, from https://www.rijksoverheid.nl/onderwerpen/klimaatverandering/klimaatbeleid

Royal HaskoningDNV. (2021). *Verbeteren netinpassing zonne-energieprojecten*. Retrieved May 27, 2023, from https://www.rvo.nl/sites/default/files/2022/02/Verbeteren-netinpassing-zonne-energieprojecten-10-toepassingen-in-kaart-gebracht.pdf

RVO. (2022). *Brochure sde++ 2022*. Retrieved May 30, 2023, from https://www.rvo.nl/sites/default/files/2022-06/Brochure_SDE_plus_plus_2022_versie_27_06_2022.pdf

RVO. (2023a). *Hoe de sde++ werkt*. Retrieved May 27, 2023, from https://www.rvo.nl/subsidies-financiering/sde/orienteren#hoe-de-sde%5C%2B%5C%2B-werkt

RVO. (2023b). *Netcapaciteit en netcongestie*. Retrieved May 27, 2023, from https://www.rvo.nl/onderwerpen/zonne-energie/netcapaciteit

RVO. (2023c). *Sde*. Retrieved May 30, 2023, from https://www.rvo.nl/subsidies-financiering/sde

RVO. (2023d). *Sde++ : Aanvragen*. Retrieved September 11, 2023, from https://www.rvo.nl/subsidies-financiering/sde/aanvragen

Sheffield Solar. (2023). *Comparison of east-west arrays*. Retrieved September 7, 2023, from https://www.solar.sheffield.ac.uk/panel-data/comparison-of-east-west-arrays/

Siemens Gamesa. (2021). *Onshore wind turbine sg 6.6-1*. Retrieved September 11, 2023, from https://www.siemensgamesa.com/products-and-services/onshore/wind-turbine-sg-5-8-170

Sioshansi, R., & Denholm, P. (2013). Benefits of colocating concentrating solar power and wind. *IEEE Transactions on Sustainable Energy*, *4*(4), 877–885. https://doi.org/10.1109/TSTE.2013.2253619

Smets, A., Jäger, K., Isabella, O., van Swaaij, R., & Zeman, M. (2016). *Solar energy: The physics and engineering of photovoltaic conversion, technologies and systems*. UIT Cambridge Limited.

Solar Dat. (2023). *Sun chart program*. Retrieved June 20, 2023, from http://solardat.uoregon.edu/SunChartProgram.php

Solar Magazine. (2023a). *Definitief 416.6 miljoen euro subsidie batterijen bij grote zonneparken en zonnedaken*. Retrieved October 20, 2023, from https://solarmagazine.nl/nieuws-zonne-energie/i35483/definitief-416-6-miljoen-euro-subsidie-batterijen-bij-grote-zonneparken-en-zonnedaken

Solar Magazine. (2023b). *Kabinet nieuwe verplichting voor batterijen bij zonneparken*. Retrieved May 27, 2023, from https://solarmagazine.nl/nieuws-zonne-energie/i34118/kabinet-nieuwe-verplichting-voor-batterijen-bij-zonneparken

Spotmarkt. (2023). *Apx-epex*. Retrieved June 10, 2023, from https://www.spotmarkt.nl/apx-epex/

Staffell, I., & Green, R. (2014). How does wind farm performance decline with age? *Renewable Energy*, *66*, 775–786. https://doi.org/10.1016/j.renene.2013.10.041

Stanley, A. P., & King, J. (2022). Optimizing the physical design and layout of a resilient wind, solar, and storage hybrid power plant. *Applied Energy*, *317*. https://doi.org/10.1016/j.apenergy.2022.119139

Statista. (2023). *Inflation rate in the european union and the euro area from 2018 to 2028(compared to the previous year)*. Retrieved September 11, 2023, from https://www.statista.com/statistics/267908/inflation-rate-in-eu-and-euro-area/

Stoutenburg, E. D., Jenkins, N., & Jacobson, M. Z. (2010). Power output variations of co-located offshore wind turbines and wave energy converters in California. *Renewable Energy*, *35*(12), 2781–2791. https://doi.org/10.1016/j.renene.2010.04.033

TenneT. (2022). *Investeringsplan net op land 2022*. Retrieved May 27, 2023, from https://tennet-drupal.s3.eu-central-1.amazonaws.com/default/2022-09/IP2022_Netopland_12-9-2022.pdf

TenneT. (2023). *Dutch ancillary services*. Retrieved June 10, 2023, from https://www.tennet.eu/markets/dutch-ancillary-services

The Solar Labs. (2021). *Inter-row spacing rooftop solar*. Retrieved June 20, 2023, from https://thesolarlabs.com/ros/inter-row-spacing-rooftop-solar/

Tito, S. R., Lie, T. T., & Anderson, T. N. (2016). Optimal sizing of a wind-photovoltaic-battery hybrid renewable energy system considering socio-demographic factors. *Solar Energy*, *136*, 525–532. https://doi.org/10.1016/j.solener.2016.07.036

Trikalitis, S., Lavidas, G., & Kaldellis, J. K. (2021). *Energy analysis of a Hybrid Wind-Wave Solution for Remote Islands* (tech. rep.). World Renewable Energy Congress.

Tweede Kamer. (2020). *Gewijzigd amendement van de leden van der lee en sienot ter vervanging van nr. 11 over een vorm van cablepooling*. Retrieved May 27, 2023, from https://www.tweedekamer.nl/kamerstukken/amendementen/detail?id=2020Z02659&did=2020D05592

Tweede Kamer. (2023). *Amendement van het lid boucke ter vervanging van nr. 23 over dat opslag- en conversie-installaties ook een aansluiting kunnen delen met een zon- of windpark*. Retrieved May 27, 2023, from https://www.tweedekamer.nl/kamerstukken/amendementen/detail?id=2023Z00428&did=2023D01069

van Aken, B., Binani, A., & Cesar, K. (2021). Towards nature inclusive east-west orientated solar parks.

van Cappellen, L., Jongsma, C., Rooijers, F., & Vendrik, J. (2023). Beleid voor grootschalige batterijsystemen en afnamenetcongestie. *CE Delft*. www.cedelft.nl

van Gastel, E., & de Jonge Baas, M. (2019). *Requirements for generators vanaf 27 april van kracht: Nieuwe technische eisen aan zonnepanelen en omvormers, handhaving uitgesteld*. Retrieved March 20, 2023, from https://solarmagazine.nl/nieuws-zonne-energie/i18180/requirements-for-generators-vanaf-27-april-van-kracht-nieuwe-technische-eisen-aan-zonnepanelen-en-omvormers-handhaving-uitgesteld

Venkataraman, S., Ziesler, C., Johnson, P., & Van Kempen, S. (2018). Integrated Wind, Solar, and Energy Storage: Designing Plants with a Better Generation Profile and Lower Overall Cost. *IEEE Power and Energy Magazine*, *16*(3), 74–83. https://doi.org/10.1109/MPE.2018.2793478

Ventolines. (2021). *Model Cable Pooling Overeenkomst Opslag* (tech. rep.).

Yang, H., Lu, L., & Zhou, W. (2007). A novel optimization sizing model for hybrid solar-wind power generation system. *Solar Energy*, *81*(1), 76–84. https://doi.org/10.1016/j.solener.2006.06.010

Yang, H., Wei, Z., & Chengzhi, L. (2009). Optimal design and techno-economic analysis of a hybrid solar-wind power generation system. *Applied Energy*, *86*(2), 163–169. https://doi.org/10.1016/j.apenergy.2008.03.008

Yang, H., Zhou, W., Lu, L., & Fang, Z. (2008). Optimal sizing method for stand-alone hybrid solar-wind system with LPSP technology by using genetic algorithm. *Solar Energy*, *82*(4), 354–367. https://doi.org/10.1016/j.solener.2007.08.005

Zaaijer, M., & Viré, A. (2021). *Introduction to wind turbines: Physics and technology* (Version 01/10/2021). TU Delft.

Zhou, W., Lou, C., Li, Z., Lu, L., & Yang, H. (2010). Current status of research on optimum sizing of stand-alone hybrid solar-wind power generation systems. https://doi.org/10.1016/j.apenergy.2009.08.012

Zonnepark de Grift. (n.d.). *Kansen voor cable pooling op de grift*. Retrieved May 17, 2023, from https://www.zonneparkdegrift.nl/techniek/kansen-voor-cablepooling-op-de-grift/

Zwager, D. (2020). *Cable pooling zon en wind*. Retrieved March 20, 2023, from https://www.dirkzwager.nl/kennis/artikelen/cable-pooling-zon-en-wind-1/

A

Output of added farms

This appendix shows the behaviour of added solar or wind resource in the hybrid farm.

The maximum energy output in MWh is found by multiplying the installed capacity with the WLF. The part that is sold is depicted as the colored graph below the maximum energy that can be produced.

For the solar farms both the SDE++ and PPA revenue streams are considered to also show the difference due to the DC/AC ratios, while the wind farm is only shown for the SDE++ revenue stream, which effectively is ME, given there is no subsidy awarded throughout the lifetime of the farm.
The base case AC output of the south and east-west oriented farm and the output of the wind turbine based on January 2022 can be found in Figure A.1.

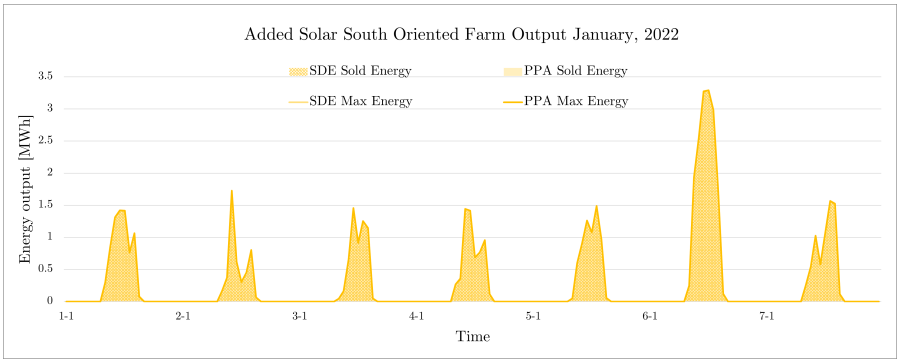

(a) AC output of added solar farm oriented to the south for the SDE++ and PPA scenarios, leading to DC/AC ratios of 2.0 and 1.6 respectively.

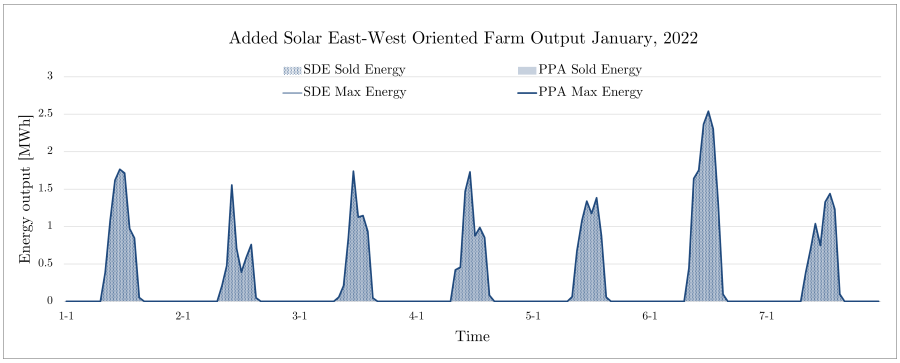

(b) AC output of added solar farm oriented to the east and west for the SDE++ and PPA scenarios, leading to DC/AC ratios of 2.0 and 1.6 respectively.

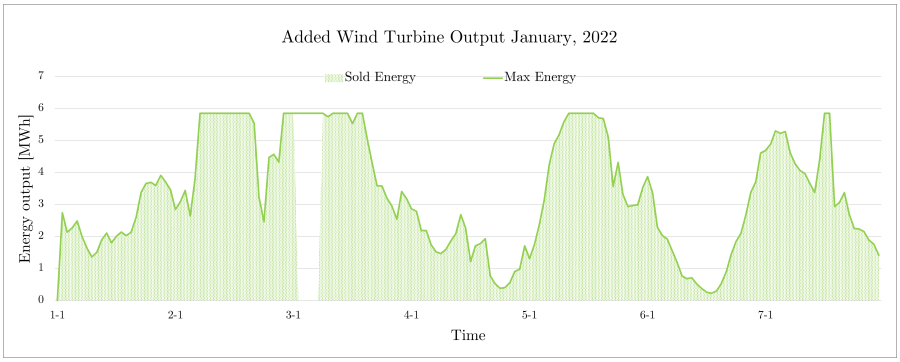

(c) Output of added wind farm

Figure A.1: AC output of added solar farms for both east-west and south oriented farms and output of the added wind turbine based on January 2022 data.

In January, the difference between the different DC/AC ratios is not visible and the farms sized based on SDE++ and PPA can export the same amount of energy.

On the 5th, 6th and 7th of January, the maximum produced energy of the east-west farms is not higher than the south oriented farm, despite the larger installed capacity.

The wind output shows a dip on the 5th of January, due to negative prices. The pattern of the WLF can be clearly seen for both solar farms and the wind farm.

The base case AC output of the south and east-west oriented farm and the output of the wind turbine based on July 2019 can be found in Figure A.2.

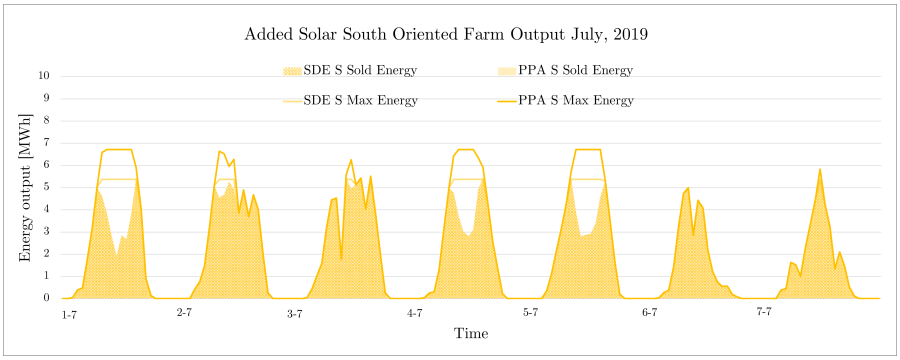

(a) AC output of added solar farm oriented to the south for the SDE++ and PPA/ME scenarios, leading to DC/AC ratios of 2.0 and 1.6 respectively.

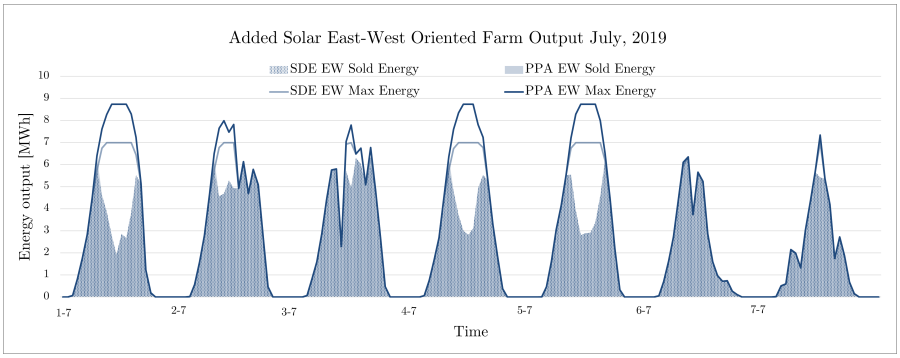

(b) AC output of added solar farm oriented to the east and west for the SDE++ and PPA/ME scenarios, leading to DC/AC ratios of 2.0 and 1.6 respectively.

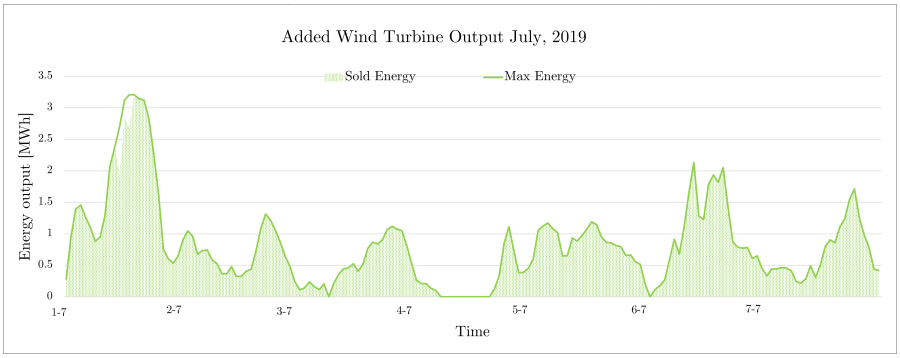

(c) Output of added wind farm

Figure A.2: AC output of added solar farms for both east-west and south oriented farms and output of the added wind turbine based on July 2019 data.

In July, the difference between the different DC/AC ratios is visible and the farms sized based on SDE++ and PPA do not export the same amount of energy. The farms sized based on the DC/AC ratio of SDE++ can export less energy per installed capacity than the farms sized based on the PPA revenue stream.

The maximum produced of the east-west farms are higher south oriented farms, due to the larger installed capacity. However, the sold energy is limited by either negative prices or an export constraint given the similar production patterns and part of the energy needs to be curtailed.

The wind output shows a dip on the 2nd of July, due to either negative prices or an export constraint. The pattern of the WLF can be clearly seen for both solar farms and the wind farm.

The base case AC output of the south and east-west oriented farm and the output of the wind turbine based on July 2019 can be found in Figure A.3.

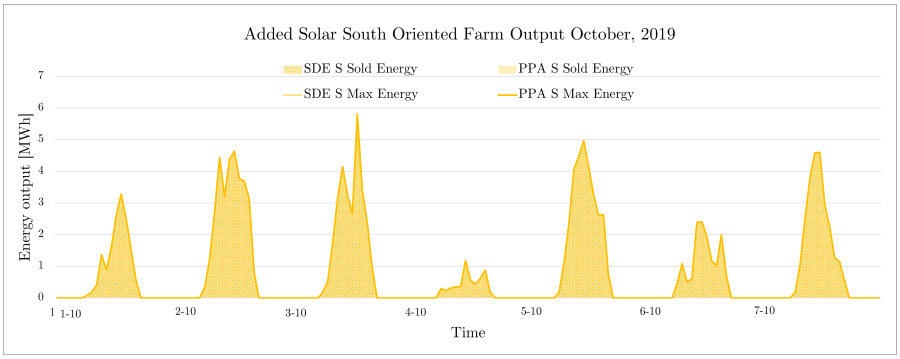

(a) AC output of added solar farm oriented to the south for the SDE++ and PPA/ME scenarios, leading to DC/AC ratios of 2.0 and 1.6 respectively.

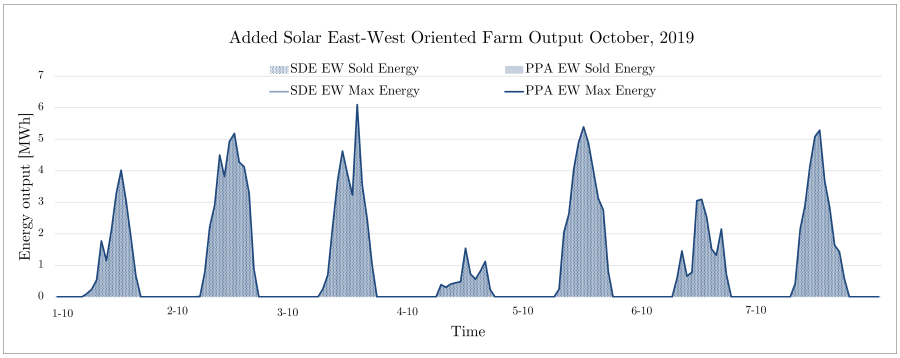

(b) AC output of added solar farm oriented to the east and west for the SDE++ and PPA/ME scenarios, leading to DC/AC ratios of 2.0 and 1.6 respectively.

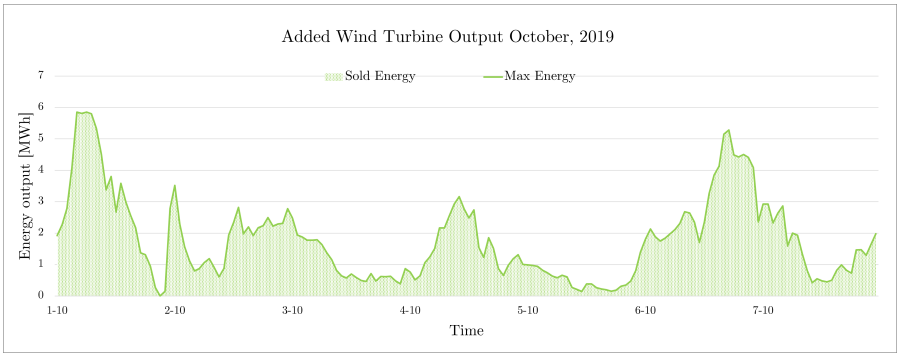

(c) Output of added wind farm

Figure A.3: AC output of added solar farms for both east-west and south oriented farms and output of the added wind turbine based on October 2019 data.

In October, the difference between the different DC/AC ratios is not visible again and the farms sized based on SDE++ and PPA can export the same amount of energy.

The maximum produced of the east-west farms is slightly higher south oriented farms, due to the larger installed capacity, but the difference is less big than in July.

The pattern of the WLF can be clearly seen for both solar farms and the wind farm.

B

Battery Behaviour

This appendix shows the behaviour of the hybrid farm including a battery and the battery SoC for different battery configurations. The impact of a 0.5 MW / 1 MWh battery and a 0.5 MW / 2 MWh battery are shown in Figure B.1 and Figure B.2.

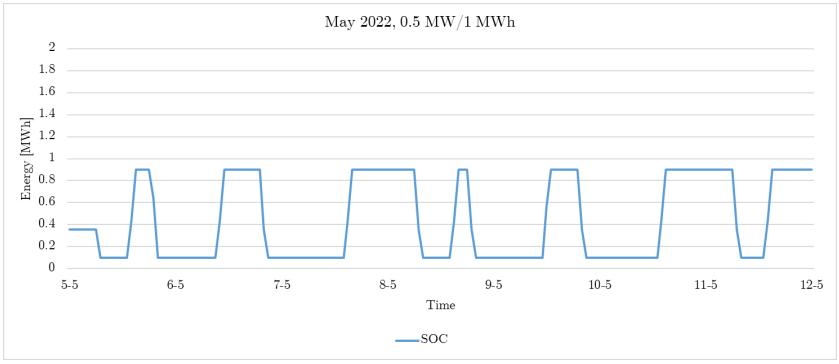

(a) SoC behaviour of one week in May for a 0.5 MW / 1 MWh battery

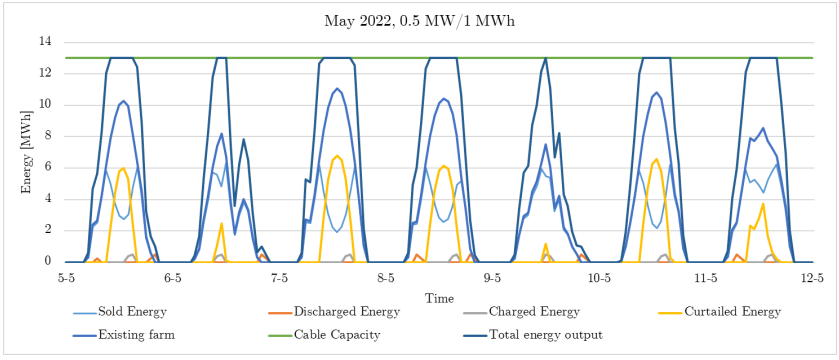

(b) Hybrid system results for one week in May including a 0.5 MW / 1 MWh battery

Figure B.1: Results including a 0.5 MW / 1 MWh battery

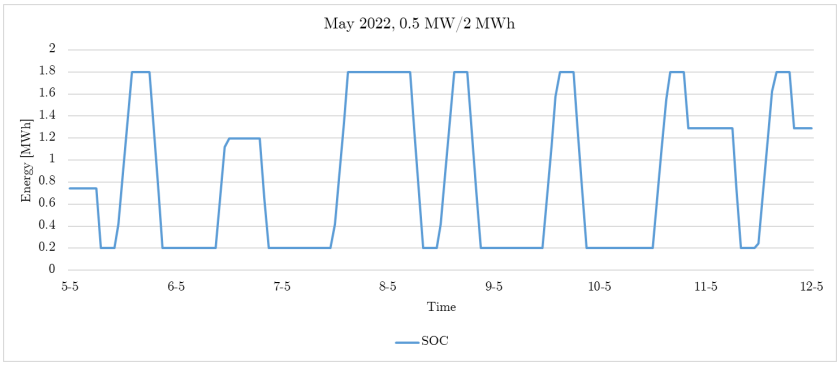

(a) SoC behaviour of one week in May for a 0.5 MW / 2 MWh battery

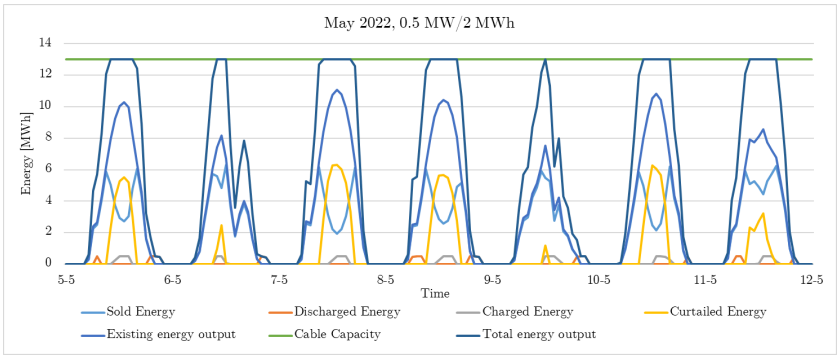

(b) Hybrid system results for one week in May including a 0.5 MW / 2 MWh battery

Figure B.2: Results including a 0.5 MW / 2 MWh battery

Doubling the size of the systems considered before leads to results as shown in Figure B.3 and Figure B.4 for the 1 MW / 4 MWh and 2 MW / 4 MWh battery configuration respectively.

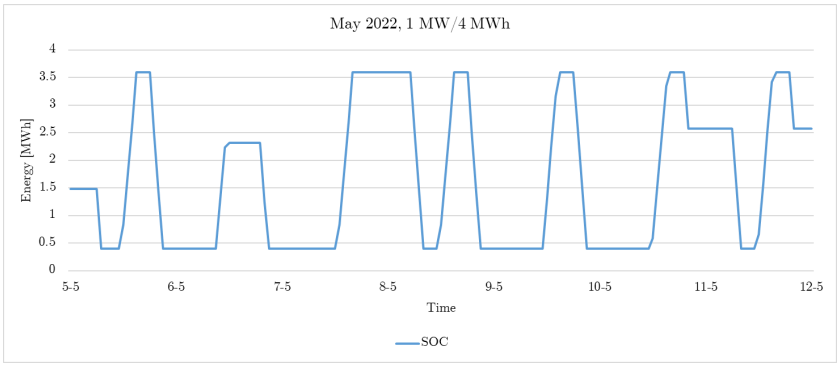

(a) SoC behaviour of one week in May for a 1 MW / 4 MWh battery

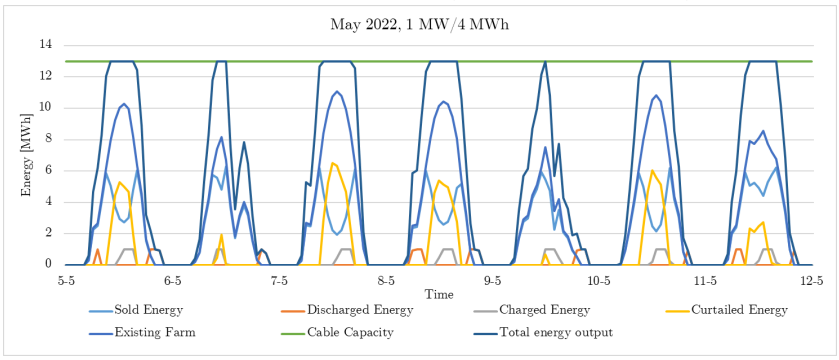

(b) Hybrid system results for one week in May including a 1 MW / 4 MWh battery

Figure B.3: Results including a 1 MW / 4 MWh battery

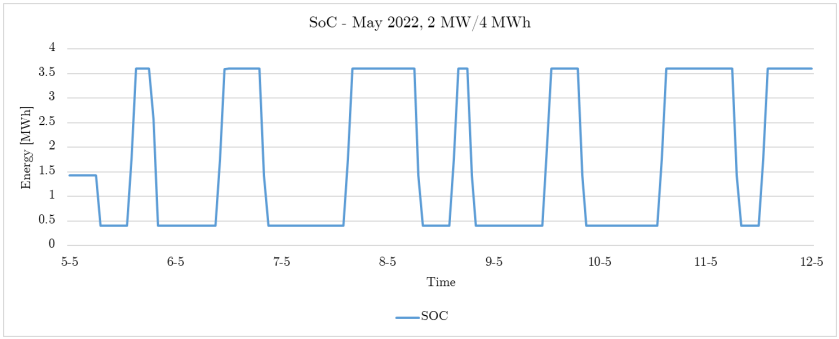

(a) SoC behaviour of one week in May for a 2 MW / 4 MWh battery

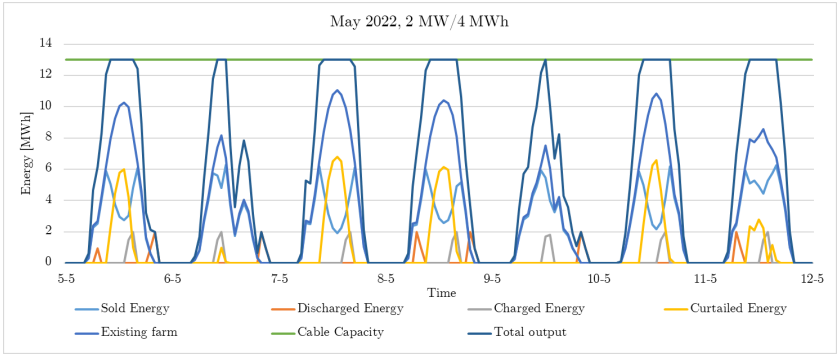

(b) Hybrid system results for one week in May including a 2 MW / 4 MWh battery

Figure B.4: Results including a 2 MW / 4 MWh battery

The last figure, Figure B.5, shows the results for a 3 MW / 12 MWh configuration.

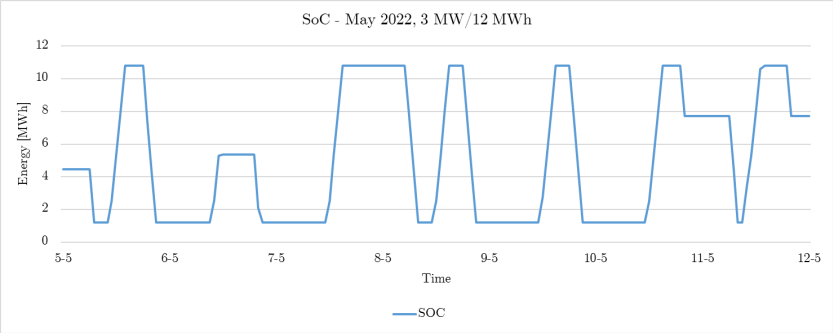

(a) SoC behaviour of one week in May for a 3 MW / 12 MWh battery

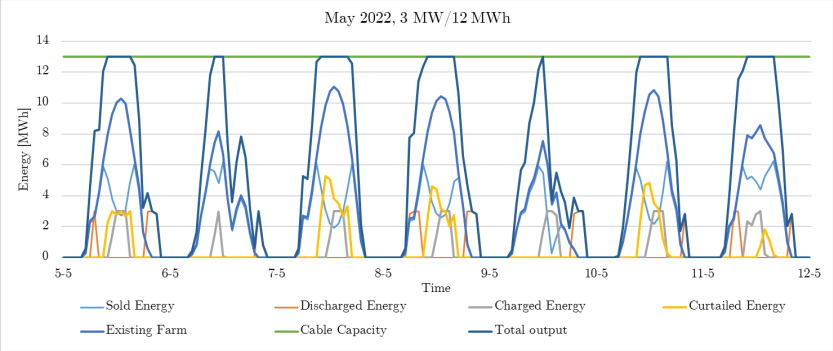

(b) Hybrid system results for one week in May including a 3 MW / 12 MWh battery

Figure B.5: Results including a 3 MW / 12 MWh battery